OBESITY ALTERS GLOBAL RESPONSE TO ISCHEMIA AND GLP-1 AGONISM

Daniel Jay Sassoon

Submitted to the faculty of the University Graduate School
in partial fulfillment of the requirements
for the degree
Doctor of Philosophy
in the Department of Cellular and Integrative Physiology,
Indiana University

August 2016

Accepted by the Graduate Faculty, Indiana University, in partial fulfillment of the requirements for the degree of Doctor of Philosophy.

Doctoral Committee

_____

Johnathan D. Tune, Ph.D., Chair

_____

Michael Sturek, Ph.D

Doctoral Committee

_____

Kieren J. Mather, M.D.

_____

B. Paul Herring, Ph.D.

May 13, 2016

_____

Jeffrey S. Elmendorf, Ph.D.

Acknowledgements

The author extends his warm thanks to Johnathan Tune PhD, and co-mentor Kieren Mather MD. The work presented herein was conceived and made possible with their support, mentorship, and expertise. Also, the author is grateful for the guidance provided by his thesis committee members including Paul Herring PhD, Michael Sturek PhD, and Jeffrey Elmendorf PhD. Additionally the author thanks Adam Goodwill PhD, Jillian Noblet PhD, Jeanette McClintick PhD, Abass Conteh, and Josh Sturek for all of their help and support in generating the data presented within this document. The author also extend thanks to the IU Medical Scientist Training Program, Indiana Clinical and Translational Science Institute for the opportunities to develop with expert physicians, educators, and scientists.

This work was supported by a National Institutes of Health grant (HL117620 J. Tune and K. Mather, PI), Heart Association (13POST1681001813 A. Goodwill, PI), the NIH National Center for Advancing Translational Sciences, Clinical and Translational Sciences Award TL1 TR000162 (A. Shekhar, PI). The author also thanks Jeanette McClintick and the Center for Molecular Genomics at Indiana University School of Medicine for performing miR microarrays, as well as Arpad Somogyi and the Proteomics Core at The Ohio State University for performing protein extraction and mass spectrometry.

Daniel Jay Sassoon

Obesity Alters Global Response to Ischemia and GLP-1 Agonism

Glucagon-like peptide 1 (GLP-1) receptor agonists are a class of incretin based therapeutics which aid in blood glucose management in Type II diabetes mellitus (T2DM). Recent studies have demonstrated direct cardiovascular benefits conferred by these agents including protection in ischemia and heart failure. Despite these observations, human clinical trials fail to support improvements in cardiovascular outcomes independent of glucose lowering effects in the T2DM populations. Prior data from our lab demonstrate that obesity impairs GLP-1 associated increases in myocardial glucose uptake. However, the reasons for this impairment/resistance to cardiac effects of GLP-1 in the setting of obesity remain ill defined. This investigation tested the hypothesis that underlying differences in the cardiac proteome and microRNA (miR) transcriptome could contribute to distinct cardiac responses to ischemia and activation of GLP-1 signaling in the setting of obesity.

To identify whether obesity modulated cardiac functional responses to GLP-1 related drugs, we first examined the effects of obesity on cardiac function, miR transcriptome, and proteome in response to short duration ischemia-reperfusion (I/R). We observed divergent physiologic responses (e.g. increased diastolic volume and systolic pressure in lean, decreased diastolic volumes in obese) to regional I/R in obese vs lean hearts that were associated with significant molecular changes as detected by protein mass spectrometry and miR microarray. Molecular

changes were related to myocardial calcium handling (SERCA2a, histidine-rich Ca^{2+} binding protein), myocardial structure and function (titin), and miRs relating to cardiac metabolism, hypertrophy, and cell death, including miR-15, miR-30, miR-199a, miR-214. Importantly, these effects were modified differently by GLP-1 agonism in lean vs obese swine.

Additional studies investigated the functional effects of 30 days of treatment with the GLP-1 analogue liraglutide on a model of slowly-developing, unrelieved coronary ischemia. Liraglutide failed to reduce infarct size or collagen deposition. However, analysis of left ventricular pressure-volume relationships support that liraglutide improved diastolic relaxation/filling, load-dependent indices of cardiac function, and cardiac efficiency in response to sympathetic stimulation in obese swine. Taken together, these findings support that miR and proteomic differences underlie distinct changes in functional cardiac responses to I/R and pharmacologic activation of GLP-1 signaling in the setting of obesity.

Johnathan D. Tune, Ph.D., Chair

Table of Contents

List of Tables

List of Figures

List of Abbreviations

anti-miR – anti-microRNA (aka antigomiR)

BMI – body mass index

CAD – coronary artery disease

CVD – cardiovascular disease

dP/dT – change in pressure of time – a measure of load dependent cardiac contractile function

EF – ejection fraction

EX-4 – exendin-4

GLP-1 – Glucagon Like Peptide-1

GLP1R – Glucagon Like Peptide-1 Receptor

LAD – left anterior descending artery

LV – left ventricle of the heart

LVEDP – left ventricular end diastolic pressure

LVEDV – left ventricular end diastolic volume

LVESP – left ventricular end systolic pressure

LVESV – left ventricular end systolic volume

MetS – metabolic syndrome

miR – microRNA

MS/MS – tandem mass spectrometry

ObM – Obesity and/or Metabolic Disease

P38 – P38 MAP Kinase

PVA – pressure volume area

RAAS – Renin-Angiotensin-Aldosterone System

SERCA2A – sarcoplasmic/endoplasmic reticulum Calcium exchanger 2a

SV – stroke volume

T2DM – Type II Diabetes Mellitus

UTR – 3'-Untranslated Region

MPTP – mitochondrial permeability transition pore

Chapter 1: Introduction to Obesity

An Overview of Diet Induced Obesity and Metabolic Disease in the United States: Causes and Epidemiology

Obesity is reaching epidemic proportions in the United States affecting more than one-third of adults and approximately 20% of youth[1]. This simple fact is quite concerning as obesity is a powerful risk factor for Type-2 Diabetes Mellitus (T2DM) and numerous cardiovascular related diseases[2-4]. The rate of growth of this epidemic is fueled on a national level by countless cultural, social, and economic pressures that promote increasingly sedentary lifestyles and consumption of readily available calorie dense foods[5]. A patient meets the criteria for being overweight or obese if they have body mass index (BMI = mass in kilograms/[patient height in meters]^2) above 30. Despite the many limitations of using BMI as a defining characteristic of obesity, it still proves to be a useful metric for predicting cardiovascular and diabetes related morbidity and mortality[6]. It is important to understand increased risks associated with obesity as it predisposes patients to all manner of negative outcomes that can seriously impact patients and families, as well as significantly increase the burden (both patient load and financial) of health care providers, government programs and insurers. Figure 1 allows for visualization of the overlap of prevalence of obesity with two of its most significant sequelae, Type II diabetes mellitus, and cardiovascular disease death.

Type II diabetes mellitus (T2DM) is one common and significant disease on the continuum of metabolic disease that often begins with obesity[7] (Figure 2Figure 2). T2DM is also increasing in prevalence, occurring in over 8% of adults in the US

as of 2010 and projected to increase to 33% by the year 2050[4]. According to the Center for Disease Control between 2003 and 2006 American adults with T2DM experienced 1.7 times higher rates of cardiovascular disease (CVD) related death, and had hospitalizations rates that were 1.8 times higher for heart attack and 1.5 times higher for stroke than adults without diagnosed T2DM[4]. Worsening of the obesity and T2DM epidemics, create an ever growing need to counter the CVD associated with these impaired metabolic states. The importance of elucidating the effects of metabolic disease on CVD are dire as CVD kills more people than any other cause in the western world. In addition to having profound medical implications, the 2014 CDC National Diabetes Report estimated that the total cost of diabetes in the US was 245 billion dollars in 2012[4]. Improved prevention and treatment of obesity, T2DM and their cardiovascular sequelae would greatly reduce national morbidity and mortality, not to mention significant cost to our overburdened health care system.

Obesity and Diabetes Worsen Cardiovascular Disease Morbidity and mortality

Obesity and its associated metabolic derangements (ObM) are known to increase prevalence, severity and death due to cardiovascular disease outcomes[8-13] (see Figure 3). Excess fat stores across the whole body produce many changes in normal physiology (Figure 4). These perturbations are evidenced by the common clinical findings (each of which are independent risk factors for cardiovascular events) in patients on the ObM spectrum, including: hypertension[14], dyslipidemia, glucose intolerance, insulin resistance, elevated inflammation

biomarkers, and a variety of ECG changes (Table 1)[15, 16]. As metabolic/physiologic derangements progress, alterations in substrate utilization (decreased glucose metabolism and increased free fatty acid metabolism), inflammation, fibrosis[17] and cell death contribute to impairments of cardiac function are believed to contribute to the interrelation of obesity, T2DM, cardiac dysfunction and worsened outcomes of CVD[16]. These outcomes include increased risk and severity of myocardial infarction, arrhythmias, heart failure, and sudden cardiac death[2, 8-12, 18-20]. Despite the well-defined clinical observations, more investigation is needed to improve understanding of the processes mechanisms underlying this exacerbation of CVD. Because several physiologic parameters are altered (Figure 5, Figure 6), many molecular pathways are implicated in driving cardiac physiology away from normal phenotype.

Obesity Alters Normal Cardiac Physiology: Mechanisms of Obesity-Associated Cardiac Dysfunction

There are many components of normal physiology that are known to be perturbed in the setting of obesity. As stated previously, the focus of this document is limited primarily to adult obesity and metabolic disease. For a discussion of childhood obesity and cardiovascular disease, please read the review by Tracey Bridger M.D [21]. The following section will provide an overview of the effects of ObM on hyperdynamic circulation, adrenergics, the Renin-Angiotensin-Aldosterone System (RAAS), cardiac function, and vascular function. While not discussed in this document, other important factors are implicated in obese effects on cardiovascular physiology (hypertrophy/fibrosis[17, 22-25], lipotoxicity[26],

metabolism[27]/autophagy[28]/mitochondrial function[29], epigenetics[30], inflammation[31], sleep apnea/hypoxia[29]) and participate in driving all of the disease processes that are discussed in more detial[32].

Associations of RAAS, a Hyperdynamic Circulatory State, and Hypertension with Aberrant Vascular and Cardiac Morphology and Function in ObM

Significant accumulations in body fat depots (Figure 4) contribute to altered neuro-endocrine-immune cross talk, thereby producing a multi-system disease state[15]. ObM coincides with blood volume and endocrine changes leading to the activation of the RAAS and closely associated neural and endocrine changes contribute to increased sympathetic tone (see subsection called 'Systemic Adrenergic Overdrive Potentiates Cardiovascular damage')[15]. Chronic angiotensin II signaling has a multitude of effects. Importantly, it produces increases in vasoconstriction[33-36] that contribute to the production of a hyperdynamic circulatory state (discussed in the following paragraph). Angiotensin II is also known to induce inflammation, vascular and cardiac remodeling, thrombosis, and plaque rupture[37].

Early/uncomplicated obesity is associated with the development of a "hyperdynamic" circulatory state in which blood pressure, central blood volume, cardiac output and tissue metabolic demand are significantly elevated relative to normal [31, 38, 39]. Normally, increases in central blood volume should be associated with greater cardiac output. However, ObM associated impairments in peripheral vascular function (increased resistance driven in part by RAAS discussed above) drives significant elevations in blood pressure[40]. Hypertension amplifies deraignment independent of obesity, producing autonomic[41]/endocrine[42] changes

and vascular damage[43], promoting atherosclerosis[34, 35], the morphologic/functional changes of the heart[43-45], and damage to other organs including neural and endocrine tissues[15, 31]. Thus, obesity and hypertension result in redundant and combinatorial systemic detriment[40].

In order to adapt to the systemic changes the heart undergoes morphological changes including increased left ventricular diameters and mass, cardiac hypertrophy (eccentric and concentric)[46, 47]. Morphology changes coincide with cardiac functional changes including reduced diastolic, and occasionally systolic function, have been observed in obese human subjects[25, 48, 49]. Over time, further declines in function predispose patients to myocardial infarction due to atherosclerosis/Coronary Artery Disease (CAD), and congestive heart failure (Figure 5)[50-52].

Systemic Adrenergic Overdrive Potentiates Cardiovascular damage

The historic scientific literature relating to the effect of obesity on the autonomic nervous system is worthy of attention as it suggests a multifaceted role implicating inappropriate autonomic nervous system activity as both a cause and effect of obesity, and concurrently provides an example of how advancements in technology can change generally accepted beliefs in biological science.

Works describing the relationship between neural/hormonal perturbations and obesity can be traced back to the work of Babinski in 1900 and Frohlich 1901 [53]. The following seven decades provided additional case studies associating development of obesity with pre-existing “hypothalamic impairment”[53]. These observations, when paired with advances in the understanding of endocrine

functions and metabolism of lipids set the framework for the studies by Young, Landsberg, and Bray in the 1970's and 1980's. In 1977 Young and Landsberg provided the first observations that altering feeding patterns could alter catecholamine turnover in rat hearts. Bray's scholarly works pushed the field of study forward, integrating of much of the historic data and proposing mechanisms for further study[53-55]. However, studies on humans were lacking.

Work from the Pfeifer group in 1988 provided the first characterization of autonomic function in several organ systems of 56 "healthy" humans (25-36 year old males) across a spectrum of body compositions (as measured by body fat percentage 2-46%)[56]. They found organ dependent changes in autonomic indices dependent on body fat percent. In the heart they found weak correlations of body fat percent with heart rate (r=0.3) and r-r interval (r= -0.3 after propranolol) which they interpreted as a decrease in overall autonomic activity in the heart. Through the 1980s and early 1990s, physiologists ascribed to the belief that reductions sympathetic tone was mediating obese changes[55, 57]. In 1992 a review by Young et al. demonstrated that literature was highly variable relating to measurements of plasma and urine catecholamine measurements in relation to body weight[58]. This variability arose from the use of indirect and insensitive measures of sympathetic activity through use of plasma and urine norepinephrine concentrations[59] which could be overcome by use of microneurographic techniques[60]. In 1994, a study by Scherrer et al. provided strong evidence that, despite variable plasma norepinephrine concentrations in lean and obese humans, obesity (BMI >27) was associated with nearly twofold higher rates of sympathetic discharge to skeletal

muscle compared to lean subjects[61]. This hyperactivity in sympathetic nerve activation was reproduced by Grassi et al. in 1995[62]. Nearly ten years later, ObM related sympathetic predominance in the heart began to dominate relevant literature[63-65].

Contrary to the early studies, it is now widely accepted that persons ObM exhibit heightened sympathetic tone systemically and in the heart. As discussed previously, multiple concurrently and interrelatedly changing factors contribute to change in autonomic stimulation and are thought to mutually impact a variety of systemic and cardiovascular systems contributing to disease progression[66-69]. Further research is needed to understand the clinical implications of non-diabetic obesity with respect to modulating development of cardiovascular disease and response to therapeutic interventions.

Ischemic Damage in the Obese, Non-Diabetic Heart is Understudied

Over time, these underlying changes in physiology are thought to contribute to augmented cardiac filling pressures, impairment of contractile function, left ventricular hypertrophy, left ventricular diastolic dysfunction, and diminished β-adrenoceptor responsiveness (despite heightened sympathetic neural tone)[41, 63, 67]. These changes may ultimately drive the development of the obesity cardiomyopathy [16, 46]. In contrast to the extensive research in diabetic hearts, where we know diabetic individuals experience worsened outcomes to acute myocardial infarction[70-72], coronary angioplasty [70] and coronary artery bypass grafting[73-75], relatively little is known about the effects of (non-diabetic) obesity on susceptibility of the heart to ischemic damage. Experimental studies have

documented both impairment[76] and improvement[77-79] of functional recovery and infarct size development in response to ischemia-reperfusion injury in animal models of obesity[79]. Additional basic and clinical studies are needed to better understand the effects of obesity on cardiac function, on ischemia susceptibility, and altered pharmacologic responses.

Cardiac Response to Ischemia

As obligate aerobes, human cells are fundamentally incompatible with ischemia. Cessation of blood flow prevents delivery of nutrients and oxygen, while preventing the removal of cellular waste products. The mechanisms through which this leads to cell death begin in the mitochondria[80, 81]. As oxygen is unavailable, oxidative phosphorylation cannot proceed. Hydrogen ions accumulate in the inner mitochondrial matrix depolarizing the mitochondrial membrane. ATP depletion occurs as the cell relies on anaerobic glycolysis. Eventually ATP drops to a concentration in which the F1/F0 ATPase running in reverse (consuming ATP instead of producing it). Improper maintenance of cellular ion pump function (H+, Na+, Ca2+)[80-82]. Improper ion gradients conclude with the elevation of cytoplasmic calcium, and eventual cell death[83, 84]. As in every other cell, in the cardiomyocytes (and other muscle cells) the lack of ATP necessary for proper ion pump function produces breakdown of normal calcium handling, however due to dependence of contractile function on calcium handling, ischemia has significant effects on cardiac rhythmicity and function.

Minimizing damage in tissue with ischemia is dependent on expedient restoration of blood flow. The shorter the duration of ischemia the less damage will

occur[83]. Unfortunately, damage associated with ischemic events is not limited to injury resulting from ischemia. When blood flow is restored to an ischemic tissue a seemingly paradoxical form of damage occurs called “reperfusion injury.” Reperfusion injury is mediated by biochemical pathways that result in arrhythmias, myocardial stunning, and microvascular obstruction[85]. These pathways (including oxidative stress[86], intracellular calcium overload[87, 88], mitochondrial permeability transition pore (MPTP) function[89-92], and inflammation[93-96]), will not be discussed in detail, however citations for further reading are supplied.

The mechanism of ischemic cell death and subsequent infarction development significantly overlap with cellular processes modified in obesity[97]. For example, changes in calcium handling[98, 99], glucose metabolism, oxidative phosphorylation, mitochondrial function, etc. are associated with ObM and would pre-exist an ischemic event [29, 31, 32]. This may have significant advantageous or deleterious implications for cell death. However, the impact of these ObM associated changes in underlying cellular physiology are sparsely investigated and poorly understood.

Treatment of ObM and CVD

Many therapeutic classes are used in the treatment of ObM and are often used as combination therapies to simultaneously target several mechanisms of disease[100, 101]. However, the incretin therapeutics, are of particular interest as evidence demonstrates its effectiveness in lowering blood glucose, and cardioprotective effects in ischemia and heart failure[102]. These injectable peptides work to increase the availability and/or signaling capacity of Glucagon-like Peptide

1 (GLP-1). The drug class has garnered much attention as it holds potential to disrupt both ObM and CVD, thereby significantly reducing two of the top sources of morbidity and mortality in the United States.

GLP-1 Overview of Endogenous Action and Implementation as a T2DM Therapeutic

Glucagon-like peptide-1 (GLP-1), is endogenously produced in intestinal L-cells, and released in response to nutrient delivery to the small intestine. GLP-1 is a physiologically important hormone involved in glucose homeostasis by stimulating insulin and inhibiting glucagon secretion [103-105]. GLP-1 action is thought to exert its effect predominantly by binding of full-length GLP-1 (i.e. GLP-1 (7-36)) to its canonical receptor GLP-1R [106]. As a result, GLP-1 (7-36) gained interest as a potential therapeutic for patients with impaired glucose tolerance [107, 108]. In the circulation, the ubiquitously expressed protease - dipeptidyl-peptidase IV (DPP-4) - rapidly cleaves (in minutes) circulating GLP-1 (7-36) to GLP-1 (9-36) [109]. The GLP-1 cleavage products likely do not activate the GLP-1R and is inactive as an insulinotropic agent (though this is debated) [110]. Analogues of GLP-1 resistant to DPP-4 cleavage (e.g. exendin-4, exenatide, liraglutide) have been developed and are used successfully for blood glucose management [108].

Early studies suggested that GLP-1 had cardiovascular effects as evidenced by increased arterial pressure in mice and cows[111-113]. Further investigation revealed that GLP-1 modulates myocardial substrate selection and that GLP-1-based agents (GLP-1 fragments, GLP-1 mimetics, DPP-4 inhibitors) reduce myocardial ischemia/reperfusion injury and decrease severity of other

cardiac disease (see Figure 7) [110, 114-120]. Notably, these protective effects were found to be independent of the glucoregulatory actions of GLP-1 and GLP-1 mimetics [110].

The use of incretins in prediabetic and type II diabetic patients in the management of their disease increased in part due to the reported cardioprotective benefits. However, postmarketing surveillance soon revealed that while GLP-1 drugs were not associated with increased risk of CVD[121], there appeared to be no reduction of CVD independent of blood glucose lowering effects[122]. Further findings revealed model-dependent discrepancies in GLP-1 benefit conferred by GLP-1 mimetics[102]. Many molecular studies have attempted to identify specific pathways responsible for mediating the cardiac effects of GLP1[102]. However, these studies reveal inconsistencies and are largely limited to investigations of promiscuous pathways (P38 MAPK, PKA, RTK etc.)[102]. A perfect illustration is that dependent on species (though intra-species expression differences are also reported), experimental design and other factors (e.g. historic lack of anti-body specificity), there even disagreements relating even to the cardiac localization of the classic GLP-1 receptor[102]. In fact, there is evidence suggesting that there are unknown receptors, independent of the known GLP-1 receptor[102, 123]. Additionally, few studies have explored how GLP-1 treatment alters factors impacting protein expression including transcription factor expression, epigenetics, and microRNAs. Despite all of the molecular inconsistencies surrounding the cardiac GLP-1 receptor(s) and its action, one important and addressable gap exists - much of the research demonstrating cardioprotective effects was generated in organisms that

lacked the common underlying disease phenotypes in patients receiving GLP-1 therapeutics, namely obesity and metabolic disease.

Work in our laboratory lead by Dr. Steven Moberly, provided the seminal observation that T2DM in obese humans impairs the GLP-1 mediated increases in glucose uptake that were observed in their lean counterparts (see Figure 8)[124]. Other laboratories have found additional evidence supporting obesity induced differences in cardio-metabolic response to GLP-1 mimetics[124-126]. However, studies investigating whether this differential response 1) extends to cardiac function, and 2) contributes to differential cardioprotective potential of GLP-1 drugs in CVD in obese vs. lean humans are lacking.

GLP-1 Effects on Cardiac Function

The current body of literature evaluating GLP-1 effects on cardiac function support that GLP-1 action is likely related to increases in diastolic filling (i.e. Frank-Starling effect) rather than to increases in inotropy/contractility[127-129]. Interestingly, the results of these studies suggest that the cardiac effects of GLP-1 present in the setting of underlying stress/disease (e.g. myocardial ischemia, or heart failure).

Human studies evaluating the cardiac functional effects of incretin drugs have used load-dependent techniques. As a result, statements relating GLP-1 related effects on cardiac contractility/function made by the authors of these papers must be adequately interpreted as volume dependent actions of GLP-1. When added to background therapy for 72 hours in patients with acute myocardial infarction with ejection fraction (EF) <40%, GLP-1 significantly improved ejection fraction and wall motion [116]. In patients with class III/IV heart failure, improvements

in ejection fraction were reported with longer courses of therapy (5 weeks), but effects on ejection fraction were not observed in otherwise healthy control subjects [130]. In a human model of acute ischemic dysfunction resulting from a 1 minute coronary occlusion, Read et al. examined effects of GLP-1 therapies using real time pressure-volume analyses and demonstrated that GLP-1 improved LV systolic (EF, SV, dP/dt; where dP/dt is a load dependent measure) and diastolic function (tau) during a 30 minute reperfusion period [131]. GLP-1 infusion also increased load-dependent measures of contractility (+dP/dt) and improved relaxation (tau) and cardiac function (EF and SV) [131].However, this study fell short of directly assessing end systolic pressure volume relationships, which would have provided load independent measures of cardiac contractility/function.

While there is evidence supporting the ability of GLP-1 to enhance cardiac performance, in the setting of both ischemia and heart failure, the existing body of literature (due to use of load-dependent measures) is not able to explain the physiologic mechanisms underlying effects of GLP-1. Lastly, inconsistencies in data resulting from species and metabolic differences further complicate our understanding. Elucidation of GLP-1 physiology and molecular action in obesity is needed to ensure patients receiving GLP-1 based therapies obtain cardioprotective benefits. Thus, systematic study and complete evaluation of the effects of obesity on GLP-1 based therapies will allow us to use them more effectively.

Discovery of Mechanisms relating ObM to CVD and GLP-1 Effect

Mass Spectrometry History

Mass spectrometry is a technique which allows for identification of molecules based on mass to charge ratios. The technology leading to mass spectrometry arose from early experiments on anode ray tubes by Eugen Goldstein in 1886. Experiments by Wilhelm Wien found that strong electric or magnetic fields could deflect these rays of positively charged ions. In 1899 Wien constructed a device with parallel electric and magnetic fields that could separate the rays according to their charge-to-mass ratio discovering that different gasses had different charge to mass ratios. This work was expanded on by J.J Thomson who produced a mass spectrograph. In 1908 Wien used this technology and discovered that atoms of a single element could have different masses, what we now know of as isotopes. From 1918-1922 accuracy and resolution of mass spectrometers was improved by Arthur Dempster and F.W Aston. Increasingly complex mass spectrographs with ion traps developed by Hans Dehmelt and Wolfgang Paul in the 1950s allowed for the eventual application of mass spectrometry to amino acids by Carl-Ove Andersson in 1958. However, analysis of peptides was still not feasible due to the large relative mass and complixity of the biomolecules. In 1968 Keith R. Jennings pioneered work that created collision-induced dissociation which would lead to the tandem mass spectrometry techniques still used in peptide analysis to this day. In the late 1980s Joh Bennett Fenn, Koichi Tanka, Franz Hillenkamp and Michael Karas made major advancements in the ionization of biological macromolecules (including proteins)

yielding an early version of tandem mass spectrometry (MS/MS) techniques. Innovation has continued in the field, allowing complex proteins and their post-translational modifications to be analyzed with increasing sensitivity. Many variations of protein mass spectrometry exist, each utilizing a different combination of separation techniques (HPLC, electrophoresis, etc.), dissociation and ionization methods, and mass analyzers to accomplish varying goals[132-135].

Mass spectrometry techniques allow for quantification of protein (see the review by Rodriguez et al.[136] for additional information regarding label-free quantification methodology), sequencing of proteins, and evaluation of post-translational modifications[134-143]. Mass spectrometry techniques have revolutionized exploration of protein biology by both providing anti-body independent quantification to analyze both targeted proteins (hypothesis driven) and whole proteomes (discovery). However, this level of detail comes at a significant financial cost and requires specialized skillsets and machinery. Additionally, proteomic analysis using these techniques are limited by several factors that can produce altered findings including: method of protein purification, difficulties detecting low abundance proteins (signal to noise), choice of label-free quantification methodology, and known protein database used for interpreting spectral results. Despite these limitations, protein mass spectrometry is a powerful tool for antibody independent, unbiased discovery of molecular changes associated with pathology and pharmacology[144].

Whole proteome analyses have previously been utilized to demonstrate obesity-specific changes in abundance and phosphorylation of proteins related to

ion transport, mitochondrial metabolism, antioxidant function and cardiac contractile function [132, 145-148]. Missing are studies exploring obesity-specific proteomic changes in response to cardiac I/R (though studies exist for I/R only[149-152]).

MicroRNAs in the Obese Heart

The manuscripts describing the first known microRNA (miR) were published in 1993 by collaborating groups of researchers at Harvard University. Ambros, Lee, and Feinbaum found that the *lin*-4 gene did not produce a protein, but instead produced a pair of small, non-coding RNAs. Together with the Ruvkun lab, also at Harvard, they observed that the smaller of the two transcripts, only 22 nucleotides long, was complementary to multiple sites in the 3'-untranslated region (UTR) of the *lin*-14 transcript and related to its posttranscriptional regulation[153]. Since these first observations, a large body of literature has emerged relating to this ancient family of small ribonucleoic acids. In mammalian cells they primarily function as small post-transcriptional inhibitors of gene regulation by binding to complementary regions in the UTR of other RNA messages. MiR binding leads to the degradation and or sequestration of mRNA transcripts (for more information on the biogenesis and action of miRs please see the following reviews[154, 155]).

Many miRs have predicted binding sites in the UTR of well over a thousand genes found within the human genome[156]. The ability for changes in miR abundance to impact multiple processes within a cell contribute to their power as regulators of cellular physiology. Since their discovery, screening for miRs using microarrays and RNA sequencing has produced observations linking changes in

miR expression to a variety of pathologic responses ranging from cancers/genetic diseases[157], ischemic response[158-160], cardiovascular[161] and metabolic disease[162-169]. Importantly, it soon became apparent that modulating miR levels could alter the course of various pathophysiologies[170, 171]. In response, several techniques arose that facilitate modulation of miRs using both viral vectors (allows for up and downregulation) and direct suppression using anti-miRs (aka stabilized antigomirs, which allow reduction of miR levels in a method similar to RNA interference)[170, 172].

These technologies have been applied in a number of cardiac studies and have found differential regulation of key miRs in various heart diseases, and that both reduction and increases in severity of pathologies are possible by altering levels of individual miRs (see Table 2 as well as the very exhaustive review by Bostjancic and Glavac[160] for more details). While these studies illustrate the context specific involvement of miRs in physiology and disease, many of these studies reveal weaknesses that appear to be pervasive in miR research, including: the use of models lacking underlying disease phenotypes, single miR-single target assumptions, and limitation to rodent models (likely due to cost of miR modulation). The result is a body of literature with contradictory findings (dependent on species/model, experimental design - temporal factors impacting tissue sampling and degree of disease progression). Some groups have begun to fill this gap in knowledge with human studies that have provided a much more complex picture of miR biology than previously imagined (and still not properly acknowledged or appreciated by the majority of researchers within the miR field). Human studies have provided the valuable observations that in addition to underlying disease

state, many common therapeutics can change the expression of various miRs[173]. Therapeutic modulation of miR expression is pathologic states has also been recorded in mice[174]. This observation has significant implications for the attempted application of miR modulation to clinical medicine. This is especially important with regards to the medication dependent clinical management of cardiovascular disease and ObM (where patients can easily be taking several prescribed medications). Further studies assessing the impact of underlying obesity on responses to pathology and therapeutics are needed to provide more clinically relevant contexts for miR research.

Summary and Specific Aims

While ample clinical data supports the greater risk of development and severity of cardiovascular disease due to obesity, associated changes in cardiac responses to pathologic and pharmacologic stimuli are poorly understood with regards to both physiology/function and molecular expression. Prior work in our lab has revealed that ObM modulates cardiac metabolism in response to GLP-1 in humans[124], but little is known about whether those effects extend to cardiac function. Several fundamental questions arise 1) does ObM alter cardiac functional response to ischemia/reperfusion, 2) does obesity alter cardiac functional responses to GLP-1 mimetics (exendin-4) at baseline and in response to I/R, 3) does obesity modify cardiac microRNA and protein expression to GLP-1 mimetics and in the setting of I/R, 4) does treatment with GLP-1 mimetics reduce infarct resulting from unrelieved LAD ischemia in obese swine 5) does GLP-1 produce cardiac functional differences in the obese ischemic heart.

Increasingly sensitive screening tools have created new opportunities to characterize the complex interplay of cellular factors that underlie changes in complex disease phenomena. Accordingly, the goal of this work is to elucidate whether obesity alters cardiac function, injury and molecular responses to GLP-1 therapeutics in the setting of ischemia (Figure 9). We hypothesize that obesity will alter cardiac functional responses to GLP-1 and I/R, and furthermore, that underlying these differences are associated changes in miR and protein expression.

Aim 1. Determine the effects of obesity on the cardiac functional response to ischemia/reperfusion and/or glucagon like peptide-1 (GLP-1) receptor activation, and screen for underlying microRNA and protein changes. To investigate this aim, lean and obese Ossabaw swine were given 24 hours of intra-venous saline or exendin-4 (30 fmol/kg/min), a GLP-1 receptor agonist. An open chest (thoracotomy) model was used to investigate cardiac function at baseline and during acute ischemia-reperfusion. Myocardial biopsies were taken at the conclusion of the open chest procedure from both normally perfused and ischemia-reperfusion territory of the left ventricle. Protein and total RNA were isolated from the samples and used for molecular screens using mass spectrometry and miR microarray.

Aim 2. Investigate the potential for GLP-1R activation to influence cardiac function at rest and in response to β1-adrenergic receptor (β1ADR) stimulation in an obese swine model of ischemic heart disease. To test this, ameroid constrictors were placed on the left anterior descending (LAD) artery of

obese Ossabaw swine to produce a slowly developing (over the course 2 weeks), complete/unrelieved coronary occlusion. Following ~30 days of treatment with either saline, or the GLP-1 mimetic liraglutide (0.015 mg/kg/day), an open-chest procedure was performed in which we assessed whether liraglutide augments sympathetic mediated increases in cardiac contractility and improve efficiency of obese hearts following complete coronary occlusion and regional myocardial infarction. Furthermore, *ex vivo* investigations elucidate the impact of liraglutide treatment on infarct development, β1ADR expression, and titin in the infarcted and normally perfused myocardium.

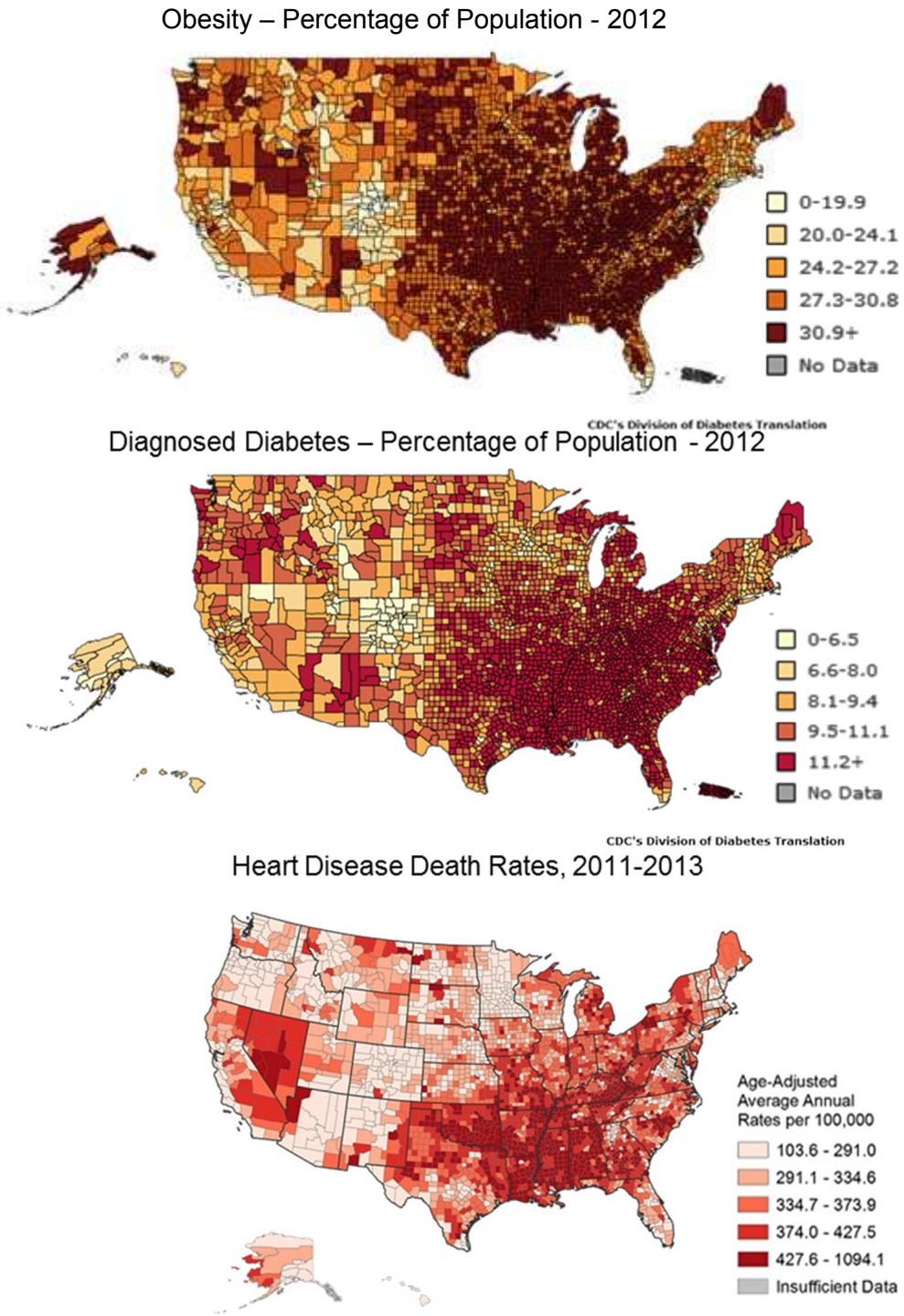

Figure 1. Percentage of Populations of obesity[175] are mirrored by diagnoses of T2DM in the united states. Additionally these metabolic diseases correspond to an increased rate of death from cardiovascular disease [175]

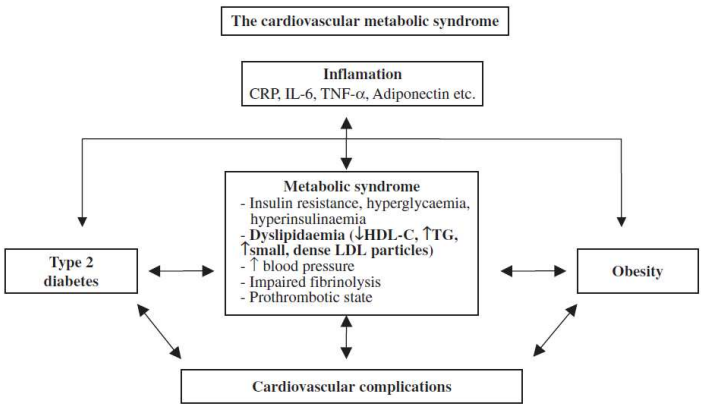

Figure 2. Factors promoting cardiovascular disease risk. Many factors contribute to, and are interrelated in, worsening cardiovascular disease risk and outcomes. Adapted from Rana, J.S 2007[176]

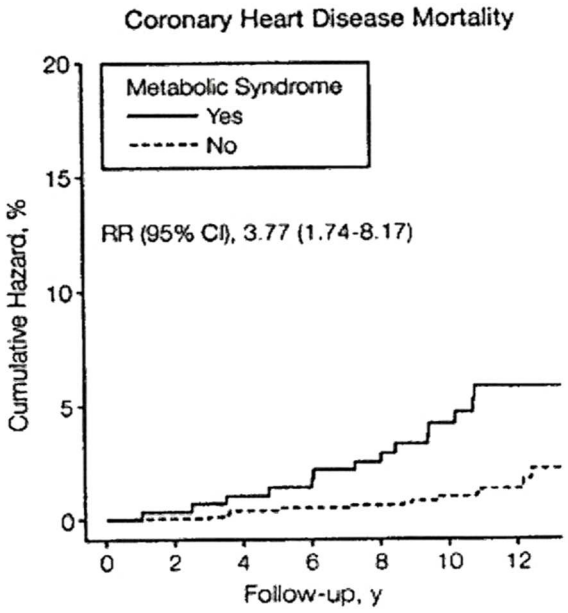

Figure 3. ObM increases likelihood of death due to cardiovascular disease[13]

Obesity associated ECG Changes
↑ Heart rate
↑ PR interval
↑ QRS interval
↑ or ↓ QRS voltage
↑ QT_c interval
↑ QT dispersion
↑ SAECG (late potentials)
ST-T abnormalities
ST depression
Left-axis deviation
Flattening of the T wave (inferolateral leads)
Left atrial abnormalities
False-positive criteria for inferior myocardial infarction

Table 1. ECG Changes associated with obesity. These changes suggest changes to cardiac morphology and electrical system. Modified from Porrier, P., et al [31]

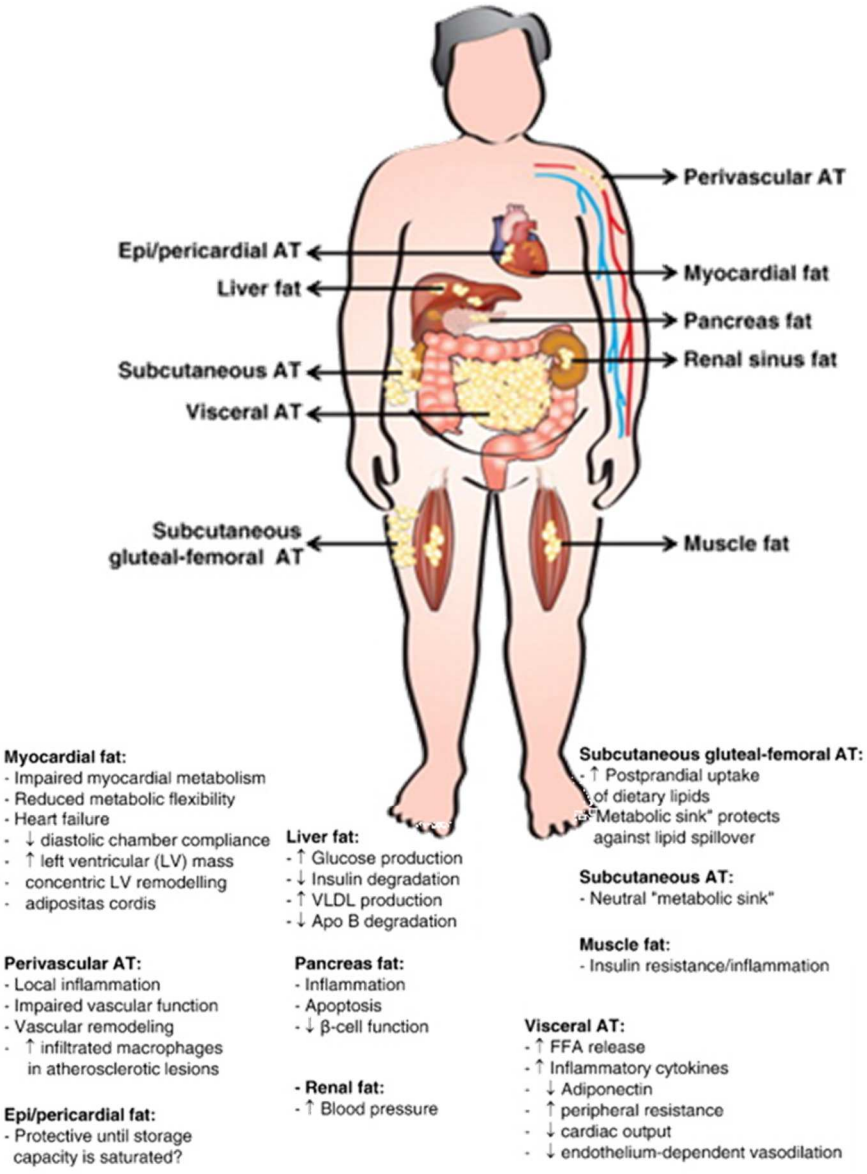

Figure 4. Abnormalities increasing risk of cardiovascular disease among overweight/obese individuals with excess visceral adipose tissue/ectopic fat. Abbreviations: Apo: apolipoprotein; FFA: free fatty acids; AT: adipose tissue. Modified from Bastien et al.[15]

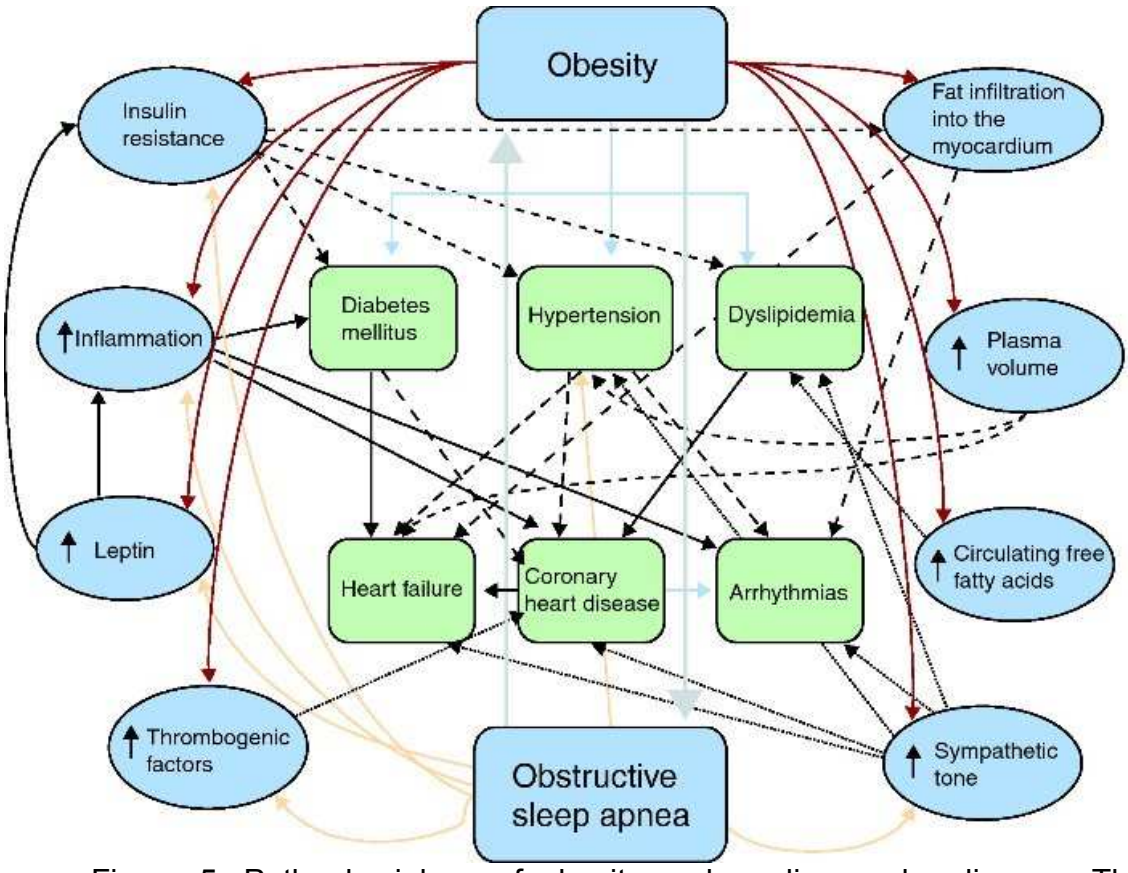

Figure 5. Pathophysiology of obesity and cardiovascular disease. The different physiopathological mechanisms by which obesity is associated with cardiovascular disease are complex and are not limited to factors such as diabetes mellitus type 2, hypertension or dyslipidemia. Other factors with an indirect interaction have been described, such as subclinical inflammation, neurohormonal activation with increased sympathetic tone, elevated leptin and insulin concentrations, obstructive sleep apnea, increased free fatty acid turnover and intramyocardial and subepicardial fat deposition. From Lopez-Jimenez et al. 2011[52]

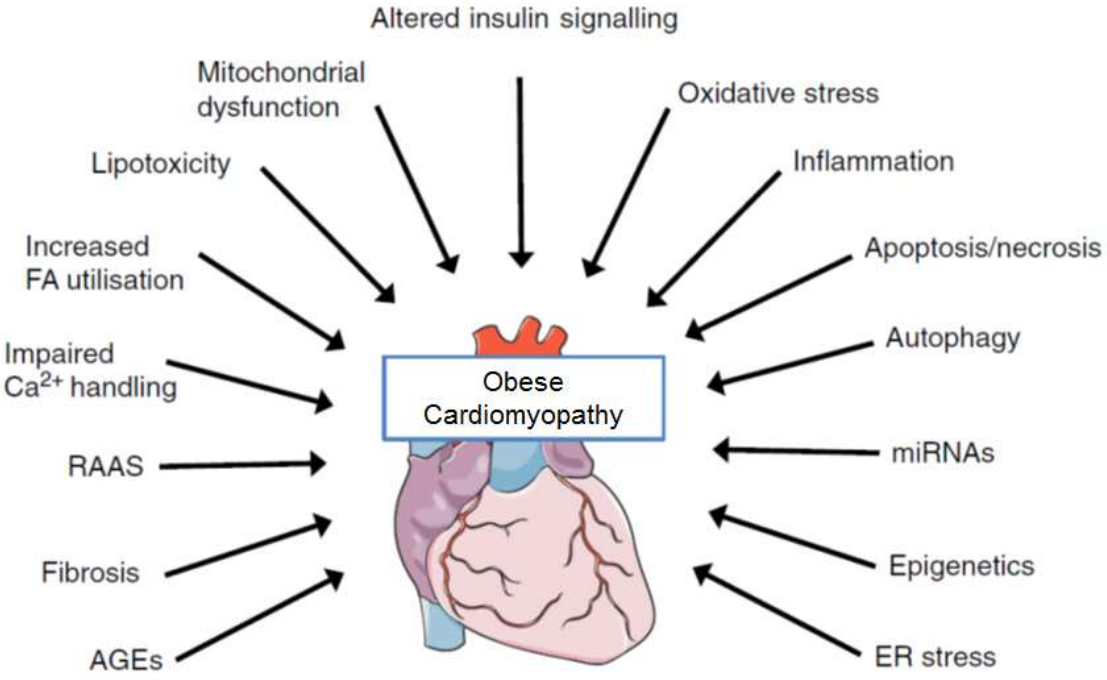

Figure 6. Molecular processes modulated by ObM. Image modified from Bugger et al. 2014[30]

miRNA	Indication	Therapeutic Effect of miR suppression	Organism	Ref #
miR-15 family	Post-MI remodeling	Reduces infarct size by increasing the number of viable myocytes after ischemic injury, resulting in improved cardiac function	mouse	177
miR-15 family	Cardiac Regeneration	Increases the number of mitotic cardiomyocytes	neonatal-mouse	178
miR-19 family	Cardiomyocyte hypertrophy	Decreases markers of hypertrophic signaling	neonatal rat cardiomyocytes	179
miR-21	Cardiac Fibrosis	Inhibits and reverses cardiac fibrosis, leading to enhanced cardiac function in response to pressure overload	mouse	180
miR - 23 and 27	retinal angiogenesis	Represses neovascularization in the choroid in response to laser injury	mouse	181
miR 24	post-MI remodeling	Reduces infarct size by increasing capillary density, resulting in improved cardiac function after MI	zebrafish embryos	182
miR-33	atherosclerosis	Increases plasma HDL in mice	mouse	183, 184
miR-33	atherosclerosis	Increases plasma HDL and decreases VLDL in non-human primates on a high-fat diet	African green monkeys	185
miR-29	aneurysms	Increases collagen expression, resulting in a significant reduction in vascular dilation and aneurysm progression	mouse	186, 187
miR-92a	neoangiogenesis	Enhances blood vessel growth and functional improvement of damaged tissue in models of hindlimb ischemia and MI	mouse	188
miR-92a	Ischemia Reperfusion Injury	Reduction in infarct size and post-ischemic loss of function (improved EF and LVEDP)	swine	189

miR-145	pulmonary hypertension	Reduces systolic right ventricular pressure during pulmonary hypertension	mouse	[190]
miR-155	viral myocarditis	Lowers myocardial damage and increases survival in response to viral myocarditis	mouse	[191]
miR-199a	Hypoxia preconditioning	Induces hypoxia preconditioning	neonatal rat cardiomyocytes	[192]
miR-199b	cardiac hypertrophy	Inhibits cardiomyocyte hypertrophy and fibrosis, resulting in improved cardiac function in different models of heart disease	mouse	[193]
miR-208a	pathological cardiac remodeling	Blocks cardiac remodeling and improves cardiac function and survival in hypertension-induced heart failure	Dahl salt-sensitive rats	[194]
miR-208a	metabolic disease	Reduces weight gain and improves glucose handling and plasma lipid levels in response to a high-fat diet	high fat fed mouse model	[195]
miR-320	post-MI remodelling	Reduces infarct size in response to ischaemic injury	mouse	[196]

Table 2. Therapeutic Targeting of cardiovascular miRNAs: Preclinical rodent and large animal studies have shown that antimiR-mediated inhibition of specific miRNAs has therapeutic potential in different aspects of cardiovascular disease. HDL, high-density lipoprotein; MI, myocardial infarction; miRNA, microRNA; VLDL, very-low-density lipoprotein. Modified from van Rooij et al. 2012 [197]

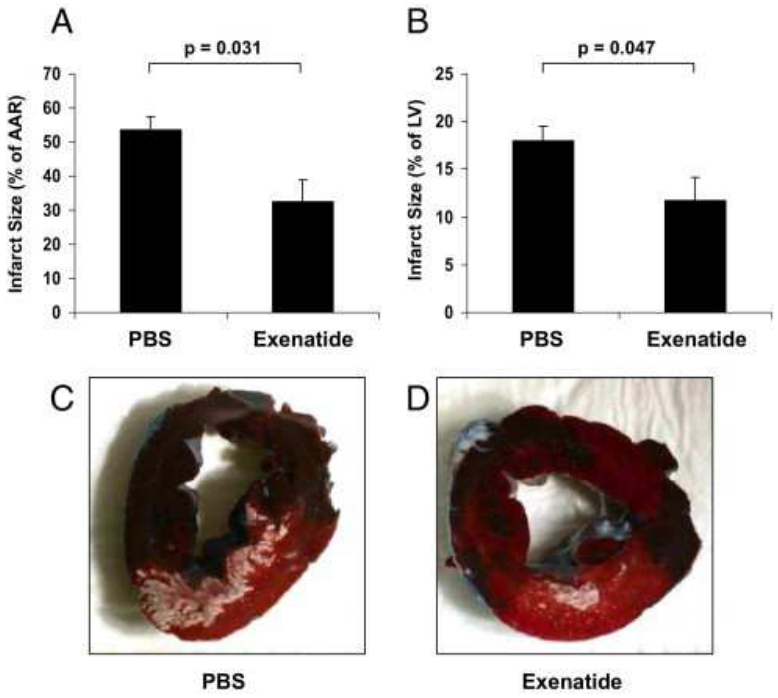

Figure 7. Myocardial infarct size quantification as a percentage of the area at risk (AAR) (A) and as a percentage of the total left ventricle (B). Phosphate-buffered saline (PBS) n = 9; exenatide n = 9. Representative pictures after Evans Blue (Sigma-Aldrich) and triphenyltetrazolium chloride staining are shown in C and D. Blue indicates non-threatened myocardium, red indicates the non-infarcted area within the area at risk, and white indicates myocardial infarction. From Timmers et al. JACC 2008[120]

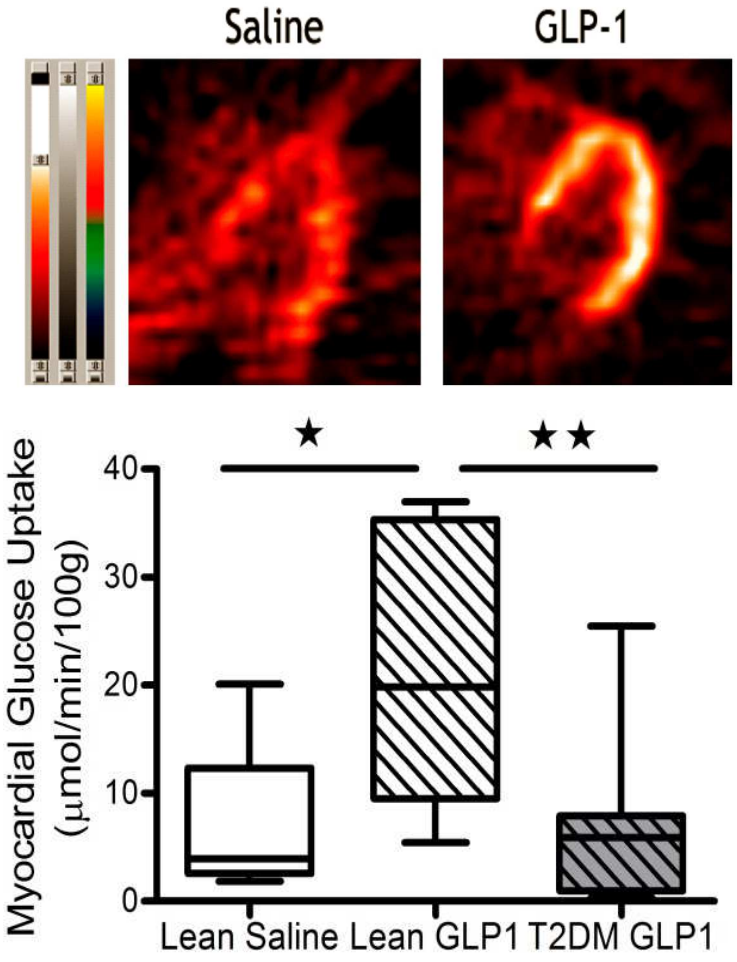

Figure 8. Representative PET image demonstrating the effect of GLP-1 on myocardial glucose uptake in lean human volunteers. Below are quantifications of PET measures showing that GLP-1 increased myocardial glucose uptake in the lean heart but did not affect glucose uptake in obese T2DM humans.

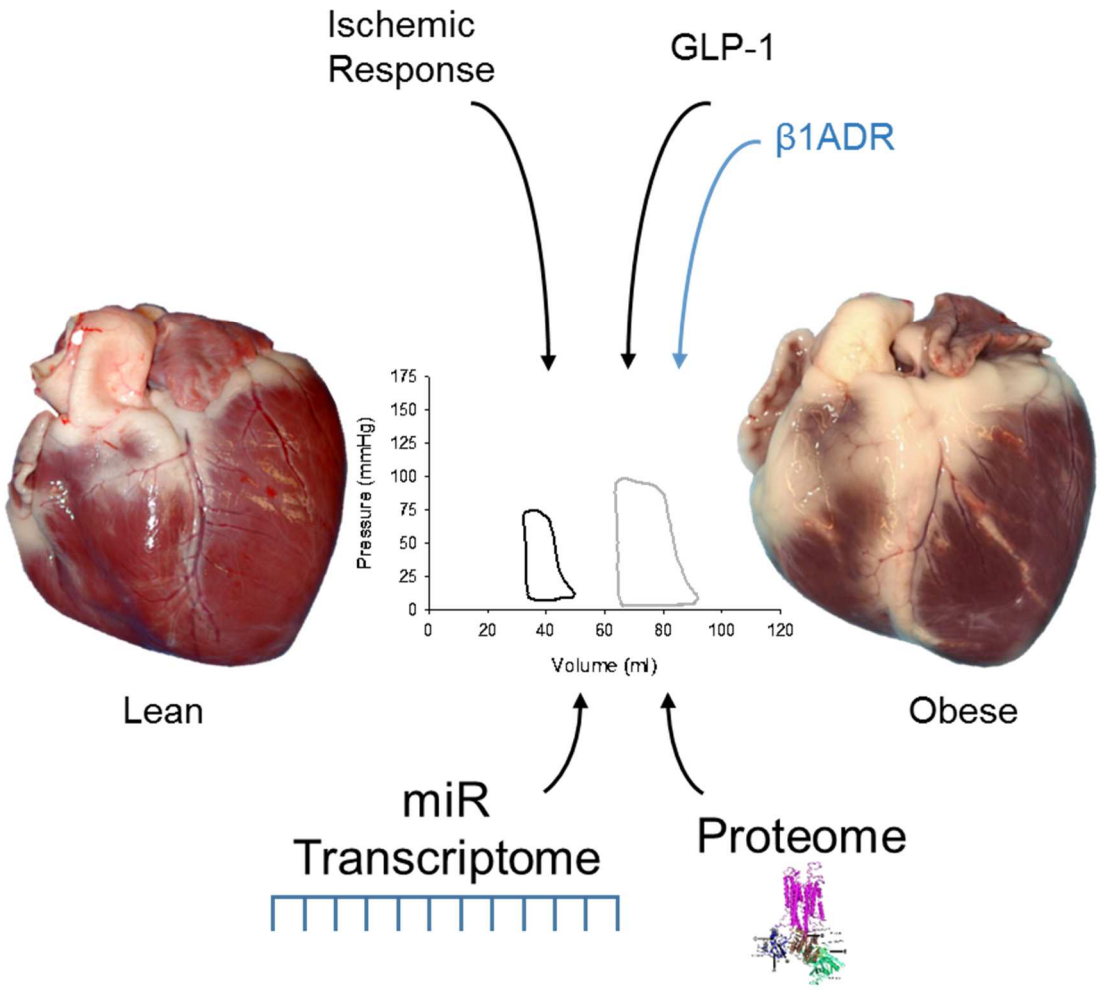

Figure 9. This figure illustrates the contributing factors in our attempt to define whether cardiac functional and molecular effects of GLP-1 are different in lean vs obese swine. Blue text denotes that dobutamine response and β1ADR were only assessed in aim 2/chapter2.

Chapter 2: Original Research - Obesity Alters Cardiac Response to Ischemia-Reperfusion with and without the GLP-1 mimetic, Exendin-4

Introduction

Obesity is a complex disease state that is accompanied by a number of cardiac disease risk factors including hypertension and metabolic dysregulation (glucose intolerance, insulin resistance, dyslipidemia)[198] that are associated with pathologic changes in the heart (ventricular hypertrophy, heart failure)[22, 24, 25, 49] and in the vasculature (atherosclerosis, microvascular dysfunction)[67, 199, 200]. In prospective clinical studies, overweight or obese individuals have increased rates of cardiovascular diseases [16, 46, 201], contributing to a 2-3 fold increase in overall mortality relative to normal weight individuals[15, 31, 201-204]. In addition to a direct link with occlusive vascular disease, obesity is strongly associated with impairment of systolic and diastolic function and the development of cardiac fibrosis (i.e. obesity cardiomyopathy) [16, 46]. Together these changes contribute to an obesity-related increased incidence of heart failure and associated morbidity and mortality [46, 205].

To date studies have investigated a broad set of potential contributors to this impaired function, such as alterations in β-adrenoceptor signaling, oxidative stress, lipotoxicity, epigenetic changes, and autophagy responses[30], but the adverse effects of obesity on cardiac function remain incompletely understood. The recent discovery of the important regulatory effects of small non-coding ribonucleic acid sequences referred to as microRNAs (miRs)[206] presents novel opportunities for discovery in this area. Limited prior investigations suggest that obesity induces alterations in specific cardiac miRs (miR-34b, miR-34c, miR-199b,

miR-210, miR-650, and miR-223) in association with altered metabolism, hypertrophy and heart failure[207]. Improvements or exacerbations of various cardiovascular disease states have been described following experimental alterations of miRs using gene therapy or pharmacologic inhibitors of miRs (antimiR)[197], demonstrating the functional relevance of these molecules. Objectively, very little is known about the nature and contributions of miRs to cardiovascular disease in the obese heart.

Regulatory changes ultimately exert effects by changes in the amount and/or activation of cellular proteins. In parallel with advances in techniques for miR profiling, tools for the evaluation of whole-proteome have been developed. Such techniques have been used to demonstrate obesity-specific changes in abundance and phosphorylation of proteins related to ion transport, mitochondrial metabolism, antioxidant function and cardiac contractile function [145-148]. Missing are studies exploring obesity-specific proteomic changes in response to cardiac ischemia and with reperfusion following relief of ischemia, and no published work has concurrently evaluated the changes in miRs and the proteome. Evaluating these changes in parallel under an experimental paradigm designed to produce an informative physiological context can produce novel observations of previously unknown factors and pathways associated with obesity-specific alterations in cardiac function and ischemic responses.

Recent work from our laboratory and others indicates that obesity impairs the effects of glucagon like peptide-1 (GLP-1) to modify the cardio-metabolic response to exercise and to regional myocardial ischemia [124-126]. The underlying

mechanisms remain largely unexplained. Here we have evaluated effects of obesity/metabolic syndrome on the cardiac functional response to ischemia/reperfusion injury with and without prior exposure to GLP-1 receptor activation. We tested the hypothesis that these responses differ in obese animals, and that these differences are associated with obesity-specific alterations in the cardiac proteome and microRNA (miR) transcriptome. We observed distinct alterations of functional responses (*in vivo*) accompanied by obesity-related differences in myocardial protein and miR expression profiles, including changes in previously unknown factors that could contribute to the development of obesity cardiomyopathy.

Methods

Animal Models and Surgical Preparation. This protocol and use of animals were approved by the Indiana University School of Medicine Institutional Animal Care and Use Committee and were in accordance with the Guide for the Care and Use of Laboratory Animals (NIH Pub. No. 85-23, Revised 1996). Male Ossabaw swine were placed on a normal (lean; n = 10) or modified obesogenic diet (obese; n = 9) for 6 months beginning at 6 months of age as previously described [208]. These group sizes are historically sufficient to demonstrate important physiologic differences between animals. Briefly, lean control swine were fed ~2,200 kcal/day of standard chow (5L80, Purina Test Diet, Richmond, IN, USA) containing 18% kcal from protein, 71% kcal from complex carbohydrates, and 11% kcal from fat. Obese swine were fed an excess ~8,000 kcal/day high fat/fructose, obesogenic diet containing 17 % kcal from protein, 20% kcal from

complex carbohydrates, 20% kcal from fructose, and 43% kcal from fat (mixture of lard, hydrogenated soybean oil, and hydrogenated coconut oil), and supplemented with 2.0% cholesterol and 0.7% sodium cholate by weight.

Following 6 months of their respective diets, animals were anesthetized with isofluorane for placement of a jugular venous catheter. The degradation-resistant GLP-1 analogue Exendin-4 (30 fmol/kg/min; lean; n= 5, obese; n= 5) or an equivalent volume of saline (lean; n= 5, obese; n= 4) was then infused systemically through the jugular venous catheter for 24 hours via an elastomeric balloon (MILA International Inc, Erlanger, Kentucky; 2 mL/hr). Immediately following this 24 hour infusion, swine were anesthetized with telazol (5 mg/kg, sc), ketamine (3 mg/kg, sc), and xylazine (2.2mg/kg, sc) cocktail IM and anesthesia maintained with morphine (3 mg/kg) and α-chloralose (100 mg/kg, i.v). The exendin-4 or saline infusion continued throughout the remaining period of the experimental protocol. Depth of anesthesia was monitored by observing continuous measurements of arterial blood pressure and heart rate as well as regular (15 minute intervals) reflex tests (corneal, jaw, limb withdrawal), beginning after induction of anesthesia and continuing throughout the experimental protocol. Prophylactic supplementation with chloralose was performed every 1.5 hour to maintain a level, stage 3 plane of anesthesia. The right femoral artery and vein were isolated and cannulated to allow measurement of systemic arterial pressure and venous access, respectively. Next, the heart was exposed by a left lateral thoracotomy. The left circumflex artery was isolated for placement of a perivascular flow probe and a snare occluder. A catheter was then placed in the great cardiac vein to enable sampling of coronary

venous blood from the area supplied by the left circumflex artery. A Sci-Sense pressure/volume admittance catheter (Transonic Technologies, London Ontario, Canada) was then placed directly into the left ventricle via an apical transmural stab and secured with a purse-string suture. The pressure-volume system requires input of an estimated stroke volume. This estimate was based on manufacturer's recommendation of 0.9μL/g of body weight and produced baseline cardiac performance values consistent with those established in swine using other measurement modalities. Heparin was administered intravenously at a bolus dose of 500 U/kg to prevent clotting. All data were recorded using IOX acquisition software (EMKA Technologies, Falls Church VA. USA).

Experimental Protocol. Following surgical instrumentation, swine were allowed to recover for ~20 min. Hemodynamic parameters (blood pressure, heart rate, coronary blood flow, left ventricular volume and pressure) were continuously monitored throughout the experimental protocol. Baseline arterial and coronary venous blood samples were obtained at the end of the stabilization period. Next the left circumflex artery was transiently occluded for 30 min with a reversible snare occluder. The snare was then released to allow reperfusion of the circumflex perfusion territory. Hemodynamic parameters were recorded and blood samples were obtained at the end of 30 min of coronary occlusion, and then at 60 min intervals following release of the occlusion (i.e. following coronary reperfusion). At the end of the experimental protocol, while still anesthetized, animals were euthanized by fibrillation (by application of a 9 volt battery placed near the apex in the heart) with subsequent rapid excision of the heart. The heart was reverse

perfused with cold calcium free Krebs solution and transmural left ventricular biopsies were flash frozen in liquid nitrogen for protein mass spectrometry. The biopsies were taken from both the left anterior descending coronary artery perfused region (i.e. normal, non-ischemic territory) and left circumflex coronary artery perfused region (i.e. ischemia-reperfusion territory) taking care to avoid visible vasculature.

Metabolic analysis and troponin measurements. An Instrumentation Laboratories automatic blood gas analyzer (GEM Premier 3000) and CO-oximeter (682) system was used to measure arterial and venous pH, PCO_2, PO_2, hematocrit, hemoglobin, oxygen saturation, and oxygen content. Baseline blood samples were also analyzed commercially (Antech Diagnostics; Fishers, Indiana) for measurements of insulin, triglycerides and cholesterol. Mass of left circumflex perfusion territory was estimated to be 20% of total heart weight, which approximates the “area at risk” in this study. Troponin measures were made using a i-STAT1, model 300-G (Abbott, Illinois, USA), using systemic blood samples taken at baseline prior to coronary occlusion, and 120 min following release of the occlusion.

RNA isolation, quantification and micro-RNA array. Total RNA from myocardial core biopsies was isolated using PureLink RNA Micro Kit (Life Technologies) according to the manufacturer’s instructions. Total RNA was eluted from the column in RNase-free water and stored at -80°C. The Agilent 2100 Bioanalyzer Small RNA kit was used by the Center for Genetics in Indiana University School of Medicine to assess quantity and quality of miRNA.

To perform the arrays, total RNA samples were labeled using the Genisphere FlashTag HSR kit. The labeled samples were individually hybridized to Affymetrix GeneChip miRNA 3.0 arrays. They were stained and washed using the standard miRNA protocol. Affymetrix GeneChip Command Console Software (AGCC) was used to scan the arrays and generate CEL files. CEL files were imported into Partek Genomics Suite (Partek, Inc., St. Louis, Mo). RMA (robust multi-array average) signals were generated for all probe sets using the RMA background correction, quantile normalization and summarization by Median Polish[209]. Summarized signals for each probe set were $\log_2$ transformed. These log-transformed signals were used for Principal Components Analysis, hierarchical clustering and signal histograms to determine if there were any outlier arrays. No outliers were detected in this analysis. Untransformed RMA signals were used for fold change calculations. Contrasts were calculated as required. Fold changes were calculated using the untransformed RMA signals. Probe sets with $\log_2$ expression levels < 1.0 were considered very close to background. Probe sets with average expression levels < 1.0 were removed before the False Discovery Rate (FDR) was calculated using the Storey method[210]. Fold change of miRs whose expression was significantly different ($P < 0.05$) from lean saline-treated normally perfused controls were used to generate heat maps using the NCI CIMminer tool (http://discover.nci.nih.gov/cimminer). Euclidean distance and average linkage were used to create heat maps. To produce similar scales for both heat maps minimum (min) and maximum (max) fold change was added to each heat map.

Proteome Analysis. Myocardial biopsies were transported to the Ohio State University Proteomics Core. Protein was extracted from transmural myocardial biopsies from perfused and ischemia-reperfusion regions, prepared for capillary-LC-nanospray-MS/MS and subsequent label free quantitation. Proteomic quantifications were performed in accordance with previous studies [211, 212] In brief mass spectrometry methodology is detailed online at the following web address: http://link.springer.com/article/10.1007%2Fs00395-016-0563-4. In brief, protein quantification and identification was accomplished using the NCBInr Other Mammalia Database (version 20150104, 1,412,788 sequences). A decoy database was also searched to determine the false discovery rate (FDR) and peptides were filtered according to the FDR. The significance threshold was set at $P < 0.05$. Percolator score was used to further validate the search results and the actual FDR was less than 1% after using percolator scores. Label-free quantitation was performed using the spectral count approach, in which the relative protein quantitation is measured by comparing the number of MS/MS spectra identified from the same protein in each of the multiple LC/MSMS datasets. Scaffold was used for quantitation analysis. The protein filter was set at 99% to ensure the false discovery rate is less than 1% and the peptide filter was set at 95%.

Proteome and miR Analysis via Ingenuity Pathway Analysis. Ingenuity Pathway Analysis (IPA) (a Qiagen® product) was used to assist with interpretation and target discovery of proteome and microarray data. As IPA does not query porcine databases, all array and proteomics results were converted to the nearest bovine (protein) or human or mouse (miR) homologs. The proteomics data set was

used in conjunction with the miR data set for the miR Target Finder Feature. Proteins and miR thresholds for inclusion in IPA analyses were set for $P<0.05$.

Microarray and Proteomic Database Locations. MiR microarray results were uploaded to GEO (accession GSE77378). Complete microarray and proteomics results are also provided online via springer publishing group (doi: 10.1007/s00395-016-0563-4).

Statistical Analyses. Data were analyzed using the SigmaPlot statistical package (version 11 Systat Software Inc, San Jose, CA) and SPSS (version 22 IBM, Chicago, IL). Data are presented as mean ± standard error. Comparisons were assessed by two-way repeated measures ANOVA; (Factor A = treatment (saline/exendin-4); Factor B = condition (baseline/occlusion/reperfusion 60 min/ reperfusion 120 min)). When significance was established with ANOVA, Student-Newman-Keuls posthoc testing was performed to identify pairwise differences between groups and conditions. For Table 3 and Table 5A comparisons were assessed by one way ANOVA. The troponin data (Table 4) were significantly right-skewed, particularly for the reperfusion values; therefore the effect of reperfusion was assessed using the Wilcoxon signed rank test, and to evaluate effects of obesity and treatment on this response generalized linear mixed modeling was applied in parallel to the ANOVA as above, specifying a gamma distribution without assumptions of equal error distributions between groups in order to correctly model this data distribution. Statistical significance was declared when $p<0.05$. Statistical comparisons of proteomic results were performed on proteins which met Scaffold false discovery rate (FDR) criterion by Student's t-test. In accordance with our

discovery-based approach, proteins and miRs with $P < 0.05$ after passing this FDR threshold were considered significantly different between conditions. Proteins with average spectral counts of zero for a group were not statistically analyzed.

Results

Phenotypic characteristics and hemodynamics. Phenotypic characteristics of swine at baseline on the day of the physiologic studies following diet ± exendin-4 treatment, are presented in Table 3**.** The excess calorie high fat/fructose obesogenic diet significantly increased body weight (~39%; P = 0.006) and cholesterol (525%; P = 0.005) relative to the lean-control diet. Obese animals were significantly hyperglycemic and hyperinsulinemic, fulfilling criteria for the metabolic syndrome. Exendin-4 for 24 hours did not produce any statistically significant changes in the metabolic characteristics of lean or obese swine at baseline, including no detectable reduction in glycemia.

The ischemia/reperfusion protocol produced marked elevations in troponin I (Table 4). The reperfusion data were markedly skewed necessitating nonparametric analytic approaches as described in the Methods. The effect of reperfusion to increase troponin (P = 0.0002) did not differ between lean and obese animals (P = 0.09). Exendin-4 reduced troponin values overall (P = 0.004) but the effect to reduce reperfusion-induced increase in troponin did not achieve significance (P = 0.09), and this effect did not differ between lean and obese animals (P = 0.85). Ischemia/reperfusion produced sequential reductions in mean blood pressure in lean (P < 0.001) and obese (P = 0.005) swine (Table 5 and Table 6). Administration of exendin-4 increased mean blood pressure ~30% in lean

swine at baseline and during ischemia/reperfusion (P = 0.06; Table 5), while exendin-4 had no effect on blood pressure in obese swine (P = 0.61; Table 6). Heart rate was elevated at baseline in exendin-4 treated lean swine relative to lean controls (~30%), and decreased in both treatment groups during ischemia/reperfusion (P = 0.02;Table 5). Exendin-4 had no effect on heart rate in obese swine. These data are also presented in a format that allows direct comparison of hemodynamics and cardiovascular function in lean versus obese animals in Table 7 (saline-control) and Table 8 (exendin-4).

Cardiac function. In lean swine, ischemia/reperfusion caused progressive reductions in end-diastolic volume (P = 0.002), stroke volume (P < 0.001), cardiac output (P = 0.003) and ejection fraction (P < 0.001) (Table 5). Under baseline conditions, exendin-4 administration reduced ejection fraction ~35% (P = 0.03) in lean swine, likely related to the ~30% increase in resting heart rate in exendin-4 vs. control-saline treated swine (Table 5). While ejection fraction declined with ischemia/reperfusion in obese control and exendin-4 treated swine, end-diastolic volume, stroke volume, and cardiac output were not significantly altered by ischemia/reperfusion and/or exendin-4 in obese swine (Table 6). Of note, however, ejection fraction and cardiac output (untreated only) were higher during ischemia/reperfusion in obese vs. lean swine (Table 7 and Table 8).

Left ventricular pressure volume loops representative of average group responses for lean and obese swine are presented in Figure 10. In response to ischemia/reperfusion, lean swine exhibited reductions in end-diastolic volume, systolic pressure development, and stroke volume, evident by comparing

pressure-volume relationships for saline-treated lean swine at baseline (Figure 10A) and following reperfusion (Figure 10B). In contrast, obese swine maintained pressure development and stroke volume during ischemia/reperfusion via a relative right-ward shift (increase in end-diastolic volume) of the pressure-volume relationship, observed by comparing saline-treated obese swine at baseline (Figure 10C) and following reperfusion (Figure 10D). In lean swine under baseline conditions, exendin-4 treatment increased systolic pressure development and decreased stroke volume (~35%) with essentially no change in diastolic filling (Figure 10A). However, the ~30 mmHg increase in systolic pressure in exendin-4 treated lean swine following ischemia/reperfusion was associated with an ~25% increase in end-diastolic volume relative to control (Figure 10B). In obese swine, exendin-4 had relatively little effect on the pressure-volume relationship at baseline (Figure 10C), but produced a marked left-ward shift of the loop (decrease in end-diastolic volume with similar pressure development) following ischemia/reperfusion (Figure 10D). Overall the effect of exendin-4 was to mitigate the response to ischemia/reperfusion, although these were directionally opposite in lean versus obese swine.

The relationship between stroke volume and end-diastolic volume (i.e. Frank-Starling relationship as an index of cardiac contractility) revealed a markedly lower slope in obese compared to lean swine under saline-treated control conditions (Figure 11; $P < 0.001$). Exendin-4 treatment significantly reduced stroke volume at a given end-diastolic volume in lean animals (Figure 11A), changing the intercept ($P < 0.001$) but not the slope ($P = 0.21$) of the relationship. Exendin-4

shifted the slope ($P < 0.001$) of this relationship in obese animals (Figure 11B); however, the final slopes were not different between lean and obese exendin-4 treated swine.

Protein and miR Expression Patterns. We performed capillary-lc ms/ms proteomic and miR microarray analyses on myocardial biopsies from the ischemic and non-ischemic zones from the same lean and obese swine ± exendin-4 treatment utilized for the *in vivo* studies described above. A complete list of all 678 quantified proteins, and their differences by physiologic and treatment states, is provided in at http://link.springer.com/article/10.1007%2Fs00395-016-0563-4. Among all the conditions we observed significant changes in expression of 218 proteins. These proteins were overall related to cell structure, contractile apparatus and calcium handling proteins, cellular metabolism and mitochondrial function. Figure 12 illustrates the changes in proteins related to cardiac function and calcium handling. An important novel observation is that obesity was associated with increases in multiple isoforms of the myocardial “molecular-spring” and signaling integrator protein, titin (Figure 12A). The abundance of titin was further elevated following ischemia/reperfusion in hearts from obese but not lean swine. Exendin-4 decreased the abundance of titin in lean and obese swine, in both normally perfused ($P = 0.02$ for lean, and $P < 0.001$ for obese) and ischemic ($P = 0.01$ for lean, $P < 0.001$ for obese) tissues. In addition, the abundance of the sarcoplasmic reticulum ATPase SERCA2A was augmented in hearts from obese but not lean swine following ischemia/reperfusion (Figure 12C). This increase in SERCA2A abundance was mitigated by exendin-4. Obesity also altered expression of other

Ca^{2+} binding proteins including calsequestrin-2 (Figure 12B), S100A1 (Figure 12D), and histidine rich calcium binding protein (Figure 12E). Differences in expression of Protein Kinase A, a key signaling protein in cardiomyocyte contractility, were also noted across diet and treatment conditions (Figure 12F).

Bioinformatics analysis of changes in protein expression using Ingenuity Pathway Analysis (IPA) software identified a number of effects of obesity and exendin-4 treatment on proteins related to cell death and survival (Table 10). Selected cell death and apoptosis related proteins are presented in Figure 13 (pro-apoptotic A-D, anti-apoptotic E,F). Individual proteins were identified to exhibit altered amounts related to ischemia (Figure 13A and Figure 13E) or exendin-4 treatment (Figure 13B, C, D and F). However, no differences in overall expression patterns of these proteins were attributable to obesity and no systematic effect of exendin-4 was evident.

A listing of all miRs detected by microarray, and their differences in expression in each sample group, are provided online (http://link.springer.com/article/10.1007%2Fs00395-016-0563-4). The heat maps shown in Figure 14 and Figure 15 illustrate that several groups of miRs are concordantly altered by obesity, ischemia/reperfusion and exendin-4 treatment (regions marked A-D on Figure 14 and A-I on Figure 15). For example, miRs 378,423-3p, 133a-5p, 361-3p, and 423-5p (Group A in Figure 14) were all down-regulated by ischemia/reperfusion in lean control swine whereas a different group of miRs (miRs 652, 143-5p, 17-3p, 26a, 24, 214, 140-star, 143-3p, 199a, and 152) were down-regulated by ischemia/reperfusion in obese swine (Group D,).

Interestingly, exendin-4 treatment prevented the downregulation of Group A miRs in lean swine during ischemia/reperfusion and resulted in altered expression of a distinct group of miRs (Group D, Figure 14). Obesity alone resulted in decreased expression of miRs 378, 130b, 1307, 331-5p, 2320, 129a, 30b-3p, 30e-3p (Group B, Figure 15) and upregulation of miRs 497, 494, 30c, 105-1, 331-3p. Interestingly some of the miRs downregulated in obese hearts (Group B, Figure 15) were also downregulated by ischemia/reperfusion in the lean swine (e.g. Group A, Figure 14, miR 378, and 133a-59). Exendin-4 prevented the alterations observed in obese swine (Groups A and B, Figure 15), and resulted in upregulation of miRs 491, and 146a (Group E, Figure 15) which were unchanged in all other comparisons. Obese exendin-4 treated hearts during ischemia/reperfusion had the greatest number of miR changes, with 26 of the 36 total unique to the comparison. In particular, miRs decreased in group H (Figure 15) (miRs 140, 122,424-star, 345-3p, 15a, 324, let 7 a/f/g/i, 362, 151-5p/3p, 16, 126, 106a, 425-5p, 365-3p, 181-5p, 221, 28-3p, and 199a-3p). The functional or regulatory significance of these differences is not currently known, but can be inferred from bioinformatics analyses that apply known associations between miR species and specific categories of biological function. Therefore the differentially expressed groups of miRs were evaluated using IPA software for analysis of predicted molecular and cellular function (Table 9 and Table 11). The most discernable finding of this analysis was that significantly more miRs were altered in obese relative to lean swine and that IPA identified numerous potential links of these miRs to known pathways of injury and disease (Table 9 and Table 11)

To determine if any of the observed changes in miR expression could account for alterations in protein expression that we identified from our proteomic analysis we used the Target Finder feature within IPA software. A summary of these results and other is presented in Table 11. Eleven miRs were identified for which the change in their expression inversely correlated with expression of their predicted target proteins. These proteins were not readily categorized into a single functional group although they are important metabolic, structural and signaling molecules.

Discussion

Experiments in this study were designed to explore obesity-associated differences in myocardial function in response to ischemia/reperfusion, and how these responses are modified by pharmacologic treatment (i.e. with the GLP-1 agonist exendin-4). Admittance pressure volume catheter technology, the gold standard measure for cardiac function [213, 214], was used in *in-vivo* experiments to provide highly-sensitive, real time measures of cardiac pressures and volumes. We found that obese and lean swine produced divergent physiologic responses to ischemia/reperfusion, and that the effects of exendin-4 treatment on ischemia/reperfusion were dramatically different between lean and obese swine. We performed unbiased analyses of changes in protein and miR expression associated with these differing responses as a platform for discovery of novel underlying molecular changes that could contribute to the observed physiologic effects and differences between groups. The distinctive *in vivo* responses to ischemia/reperfusion and exendin-4 were associated with informative and

interestingly different expression profiles of proteins and miRs, including in factors known to be associated with regulation of cardiac function (validating the approach) but also including factors not previously known to play a regulatory or functional role in relation to obesity.

Obesity and cardiac function in response to ischemia/reperfusion. We found that obesity is associated with a number of important functional differences in the regulation of cardiac contractile function and systemic hemodynamics. In particular, under normal baseline conditions obesity tended to produce a leftward shift of the left ventricular pressure-volume relationship relative to lean swine (Figure 10). Such reductions in end-diastolic filling volumes with similar systolic pressure generation have been previously observed in animal models[215] and in obese humans[216]. These changes are likely attributable to augmented sympathetic tone, which is well documented in the setting of obesity [41, 67, 217]. While the difference in the pressure-volume relationship between the lean and obese swine was relatively modest at baseline, more distinct effects were noted following ischemia/reperfusion. These differences were not likely attributable to differing infarct size, as the ischemia/reperfusion-induced increase in troponin did not differ between lean and obese animals (Table 4). Our data demonstrate that regional ischemia/reperfusion produced marked reductions in indices of global contractile function in lean swine, namely significant reductions in arterial pressure, ejection fraction (Table 5), and end-diastolic volume (Figures 10 and 11). Thus, lean swine exhibited post-ischemic contractile dysfunction consistent with myocardial stunning [218]. In contrast, indices of cardiac function (stroke volume, cardiac output,

ejection fraction) were relatively maintained throughout ischemia/reperfusion in obese swine and thus, were significantly higher in obese vs. lean swine (Table 5). This preservation of ventricular stroke volume and pressure generation is contrary to the presence of an obesity cardiomyopathy phenotype which one might predict to observe in these animals *a priori* [16, 198]. However, further inspection of these data suggests that the relative preservation of ventricular function in our model of early obesity was accompanied by a rightward shift in the pressure-volume relationship (Figure 10); i.e. obese hearts can invoke a Frank-Starling mechanism (increase end-diastolic filling volume) to maintain cardiac output in response to an ischemia/reperfusion insult (Figures 10 and 11). While the lack of post-ischemic contractile dysfunction in obese hearts seems unexpected, it is important to recognize that the slope of the relationship between stroke volume and end-diastolic volume was significantly lower in obese relative to lean swine (Figure 11); furthermore, such increases in blood pressure, stroke volume, and ejection fraction would act to augment myocardial energy demand, ventricular wall stretch, and exacerbate underlying ischemic injury over time [218]. Prior echocardiographic studies in humans are in accordance with these findings and suggest that the cardiac effects of obesity occur over a continuum and are directly dependent on the degree and duration of obesity and the degree of underlying metabolic risk factors [26, 67, 200].

Effects of exendin-4 on cardiac responses to ischemia/reperfusion. The current study is the first to describe the functional consequences of altered GLP-1 responses relative to cardiovascular effects of regional

ischemia/reperfusion in a large animal model of obesity. There is considerable experimental evidence supporting beneficial cardiovascular effects of treatment with GLP-1 based therapies. In animal models, GLP-1 therapeutics have been associated with increased cardioprotective capacity related to myocardial substrate selection, heart rate effects, blood pressure effects, reduction in myocardial infarct size, and improved cardiac function[125]. In contrast, large clinical trials of GLP-1 based therapies in humans with obesity and type 2 diabetes have failed to show the expected cardiovascular benefits to date [219, 220]. Recent work from our laboratory suggests that cardiometabolic effects of GLP-1 are impaired in the setting of obesity, raising the possibility of "cardiovascular GLP-1 resistance" in the population being treated with these agents [124, 126, 129]. Our data demonstrate that the obese state produced divergent GLP-1 therapeutic responses to ischemia/reperfusion. Obese treated swine maintained pressure like their untreated counterparts, and did so despite marked reductions in end-diastolic volume; i.e. increases in cardiac contractility. Lean treated swine responded to ischemia/reperfusion with increases in pressure generation and end-diastolic volume (Figure 10)Error! Reference source not found., despite overall reductions in stroke volume at a given ventricular filling volume (Figure 11).These observations contribute to the growing body of experimental and clinical literature supporting marked differences in cardiovascular responses to GLP-1 therapeutics in the setting of obesity [124, 126, 219, 221].

Proteomic and miR expression profile in obese hearts. To explore potential molecular changes that could contribute to the differential cardiac

phenotype of obese hearts, we performed proteomics and miR microarray analyses on myocardial biopsies from the lean and obese swine following completion of the *in vivo* ischemia/reperfusion protocols, sampling tissue from ischemic and non-ischemic zones. In parallel with our physiological analyses, protein and miR expression analyses revealed obesity-related differences, and differences in changes with exendin-4 treatment, in protein and miR expression. Of particular note we observed increased abundance of titin in the myocardium of obese swine under control conditions, which was mitigated with GLP-1 therapy. The giant protein titin plays multiple roles within the cardiomyocyte including providing structure in the sarcomere (binding myosin to the z-disk); contributing significantly to the passive and restoring force of the cardiac sarcomere; fine-tuning myocardial stiffness (via differential splicing of titin transcripts as well as titin phosphorylation); and mediating hypertrophic signaling [222, 223]. It is known that modulating titin (via altering the predominant isoform or the phosphorylation status) is associated with cardiac pathophysiology [224], but little prior work has evaluated the role of titin in obesity-associated cardiomyopathy. Hamdani et al. found altered phosphorylation status of titin of in the setting of metabolic risk [225, 226]. Also, therapeutics that increase GLP-1 signaling have been associated with alterations in titin phosphorylation status[226]. Our observations suggest a need for further studies to elucidate isoform switching and phosphorylation status of titin in the setting of obesity, exendin-4 treatment, and ischemia/reperfusion response.

The proteomic data confirm obesity-associated differences in calcium handling molecules predicted by prior work (e.g. SERCA2A [98, 99, 227, 228],

calsequestrin [229]). Importantly these data also highlight the involvement of calcium handling proteins not previously associated with obesity-related cardiac dysfunction (e.g. histidine-rich calcium binding protein). GLP-1 mimetics have been found to differently modulate calcium handling in vascular smooth muscle of swine depending on obesity [230], but, until now, have not been associated with direct changes in the level of calcium handling proteins in myocardium. Modulation of calcium handling and titin protein abundance has profound implications for signaling (whether by calcium as a second messenger, or titin hypertrophic signaling e.g. via NFAT [223]), cardiac stiffness, and cardiac contractility. Taken together, it appears that significant insights into the cardiac effects of obesity can be gained from more in depth investigation of these proteins, including for example splice variants of titin (e.g. N2B, N2Ba, FCT)[231], phosphorylation of specific titin residues[225, 232], down-stream NFAT signaling[233-235] and the interplay with altered calcium handling[224, 236]. [226]. These discoveries underscore the value of the proteomic approach as we have applied it, in the context of a specific set of studies that produce physiologically relevant states.

MicroRNAs are recognized for their widespread regulatory roles (which are predominantly inhibitory). These ancient systems influence multiple pathways concurrently, allowing for coordinated alterations in multiple components of cellular physiology in response to stimuli. Microarray results demonstrate that global miR regulation is different in obese hearts in response to ischemia/reperfusion and drug intervention with exendin-4. Studies investigating miR expression changes in pathology or therapeutic treatment in the setting of underlying metabolic

abnormalities are lacking. In this study, we observed different patterns of miR expression between lean and obese animals, and with ischemia/reperfusion injury with and without exendin-4 treatment. Further, the expression patterns associated with combinations of these conditions were themselves different from the effects of the individual factors (Figure 14 and Figure 15), and therefore not predictable based on knowledge of the effects of individual factors. We see important contributions in particular from a relatively small set of miRs (let 7 family, 10a, 15, 30 family,199 family, and 214), some of which have been previously associated with heart disease. In mice, ischemia was found to upregulate miR 15 family members[177, 237, 238], miR 30 family members[239], and miR 214[240]. In contrast to our observations, in that study ischemia/reperfusion did not alter expression of any of these miRs in lean hearts. In our data in obese swine, these miRs were significantly downregulated during ischemia/reperfusion (while miR-30c was upregulated in obese normally perfused myocardium compared to lean). A prior observation of diminished expression of miR-199a in early ischemia in isolated porcine cardiomyocytes[192] is also consistent with our observed tissue level changes, perhaps acting via increases in cardiac Hif-1α expression. Previous studies have demonstrated that GLP-1 mimetics induce miR expression changes in various non-cardiac tissues [174, 241]. However, our study is the first to demonstrate GLP-1-induced miR expression changes in myocardium, and that those effects differ considerably depending on obesity status. Furthermore, miR expression response to ischemia/reperfusion is both GLP-1 and obesity dependent. These changes in miRs thus mimic the different physiological changes and responses to

ischemia/reperfusion that occur in response to exendin-4 in lean and obese swine, suggesting that they may be contributing to the pathophysiological changes. Growing evidence suggests that GLP-1 receptor activation alters DNA transcription in addition to the expected direct signaling effects [174, 241], suggesting the potential for a relatively unexplored mechanism through which GLP-1 may impart direct and/or indirect effects. Further investigation into the mechanisms of GLP-1 mimetic-induced transcriptome changes are needed. IPA software was used to generate literature associated predictions of processes effected by changed proteins and miRs (Table 9, Table 10 and Table 11) and provide some context in which experimental validation of the effects of these miRs, or miR groups, might be further explored. Again, the value of these observations is primarily related to the experimental paradigm under which the tissues were collected, which provides a physiological context to allow interpretation of the differences observed.

***Limitations*.** Owing to the resource-intensive nature of these studies and some animal loss during the ischemia/reperfusion event, sample sizes were relatively low in this study. Nevertheless, we noted statistically significant group- and treatment-related differences in key physiologic end points which were consistent with recent data from our laboratory [124, 125, 129] and directly associated with marked differences in the cardiac proteome and miR transcriptome between lean and obese swine both at baseline and in response to ischemic injury. These observations therefore are not compromised on statistical power overall.

Unusually for this model, the group of animals fed the obesogenic diet were also hyperglycemic, hyperinsulinemic, and hypertriglyceridemic, and furthermore they failed to lower glucose values with the 24 hour exposure to exendin-4. Our current data do not allow post-hoc analyses that separate obesity from obesity plus dysglycemia/metabolic syndrome. These factors may have contributed to the observed differences between groups, however, this does not detract from the observations of significant group differences associated with a high-fat, obesogenic diet. Although our experimental protocol included progressive reductions in venous return using a central venous balloon for gold-standard assessments of contractility (i.e. end-systolic pressure volume relationship (ESPVR)), we were unable to acquire adequate reductions in end-diastolic volume in a sufficient number of animals for adequate statistical analysis of cardiac contractility per se.

The molecular observations we present are associative, rather than representing direct experimental manipulations of these systems to evaluate causality. This does not diminish the overall power of our hypothesis-free approach as a discovery platform, because we were able to make novel and unexpected observations, and in particular make observations about the highly integrated and multi-factorial changes in these systems in response to clearly described experimentally induced physiologic circumstances (in the same animals). These observations provide novel and valuable insights into the functioning of these systems in ischemia, and provide the first ever description of these changes in response to GLP-1 agonist treatment.

Conclusions and Implications. Taken together, these observations validate this discovery approach and reveal novel associations that suggest previously undiscovered mechanisms contributing to the effects of obesity on the heart and contributing to the actions of GLP-1 following ischemia/reperfusion. Further experimental studies will be needed to understand the causal relationships between transcriptome and proteome changes such as those we have observed and the associated changes in myocardial function.

Chapter 2: Tables and Figures

Phenotypic characteristics of lean and obese swine

	Lean Saline n=5	Lean Exendin-4 n=5	Obese Saline n=4	Obese Exendin-4 n=5
Body Weight (kg)	75 ± 6	67 ± 8	104 ± 6*	106 ± 4*
Heart Weight (g)	212 ± 16	194 ± 18	247 ± 9	224 ± 11
Glucose (mmol/L)	8.6 ± 2.3	6.8 ± 1.8	13.3 ± 1.1	14.1 ± 1.9*
Insulin (pmol/L)	73 ± 13	52 ± 11	111 ± 57	129 ± 35
Triglycerides (mmol/L)	0.6 ± 0.1	0.5 ± 0.1	1.0 ± 0.4	0.9 ± 0.1
Total cholesterol (mmol/L)	1.6 ± 0.4	1.4 ± 0.4	10.0 ± 3.3*	10.1 ± 2.0*

Table 3. Phenotypic characteristics of lean and obese swine. Measurements were performed before at baseline after 24 hours Exendin-4 or saline infusion. Values are mean ± SE. * $P \leq 0.05$ vs. lean same treatment. Measurements were performed after 24 hours Exendin-4 or saline infusion.

	Lean		Obese	
	Saline	Exendin-4	Saline	Exendin-4
Baseline	0.30 [0.18 – 0.67]	0.37 [0.15 – 0.57]	0.35 [0.03 – 0.66]	0.10 [0.04 – 0.3
Reperfusion	0.88 [0.39 – 17.53]	0.55 [0.28 – 0.93]	5.05 [0.27 – 15.22]	0.84 [0.41 – 4.3(

Table 4. Troponin measures were acquired at the end of each experimental time point. Due to the use of non-parametric statistics, values are expressed as median [range]. Reperfusion values were significantly increased compared to baseline (P = 0.0002). Exendin-4 significantly reduced the troponin values overall (P = 0.004), although the effect of exendin-4 to reduce the reperfusion-induced increase in troponin did not achieve significance (P = 0.09). Obese animals were not statistically different in these effects (P = 0.85 overall; P = 0.09 comparing reperfusion-induced increase between groups).

	Saline	Exendin-4	Condition	Treatment	Interaction
Mean Blood Pressure (mmHg)					
Baseline	101 ± 21	131 ± 5			
Occlusion	89 ± 23	127 ± 6†	*P* < 0.001	P = 0.06	*P* = 0.89
Reperfusion 60 min	75 ± 11	108 ± 8			
Reperfusion 120 min	63 ± 11*	91 ± 6*			
Heart Rate (beats/min)					
Baseline	87 ± 20	113 ± 4			
Occlusion	72 ± 8	68 ± 12	*P* = 0.02	*P* = 0.96	*P* = 0.67
Reperfusion 60 min	83 ± 13	84 ± 8			
Reperfusion 120 min	85 ± 14	80 ± 7			
End Diastolic Volume (ml)					
Baseline	83 ± 15	82 ± 7			
Occlusion	60 ± 8*	77 ± 7	*P* = 0.002	*P* = 0.34	*P* = 0.42
Reperfusion 60 min	58 ± 7*	65 ± 6			
Reperfusion 120 min	49 ± 8*	64 ± 6			
Stroke Volume (ml)					
Baseline	41 ± 10	26 ± 5			
Occlusion	18 ± 7*	21 ± 4	*P* < 0.001	P = 0.727	*P* = 0.13
Reperfusion 60 min	12 ± 4*	14 ± 3			
Reperfusion 120 min	11 ± 3*	13 ± 4			
Cardiac Output (L/min)					
Baseline	2.2± 0.5	1.7 ± 0.5			
Occlusion	1.2± 0.4*	1.3 ± 0.2	*P* = 0.003	*P* = 0.97	*P* = 0.52
Reperfusion 60 min	0.9± 0.2*	1.1 ± 0.2			
Reperfusion 120 min	0.9± 0.2*	1.0 ± 0.3			
Ejection Fraction (%)					
Baseline	47 ± 6	31 ± 4†			
Occlusion	27 ± 8*	26 ± 3	*P* < 0.001	*P* = 0.40	*P* = 0.04
Reperfusion 60 min	20 ± 5*	20 ± 3*			
Reperfusion 120 min	21 ± 4*	20 ± 4*			

Table 5. Hemodynamics and cardiovascular measurements of lean swine. Values are mean ± SE for lean (n = 4) and lean + exendin-4 (n = 5) swine. By two way repeated measures ANOVA: * = P < 0.05 vs. Baseline, same treatment; † = P < 0.05 vs. lean control, same condition. Condition denotes effect of sequential ischemia/reperfusion (baseline/occlusion/reperfusion periods), evaluated as a repeated measure comparison of the 4 experimental stages; Interaction tests whether this ischemia/reperfusion effect differs by treatment.

	Saline	Exendin-4	Condition	Treatment	Interaction
Mean Blood Pressure (mmHg)					
Baseline	99 ± 10	89 ± 5			
Occlusion	91 ± 8	86 ± 4	*P* = 0.005	*P* = 0.61	*P* = 0.45
Reperfusion 60 min	85 ± 11*	86 ± 4			
Reperfusion 120 min	83 ± 8*	77 ± 6			
Heart Rate (beats/min)					
Baseline	83 ± 8	74 ± 12			
Occlusion	90 ± 11	68 ± 8	*P* = 0.80	*P* = 0.35	*P* = 0.28
Reperfusion 60 min	87 ± 11	75 ± 11			
Reperfusion 120 min	86 ± 7	77 ± 10			
End Diastolic Volume (ml)					
Baseline	66 ± 8	59 ± 5			
Occlusion	76 ± 10	65 ± 3	*P* = 0.68	*P* = 0.25	*P* = 0.25
Reperfusion 60 min	97 ± 32	55 ± 7			
Reperfusion 120 min	89 ± 30	48 ± 8			
Stroke Volume (ml)					
Baseline	26 ± 5	28 ± 4			
Occlusion	32 ± 3	31 ± 4	*P* = 0.30	*P* = 0.33	*P* = 0.43
Reperfusion 60 min	23 ± 8	23 ± 3			
Reperfusion 120 min	28 ± 7	17 ± 4			
Cardiac Output (L/min)					
Baseline	2.1 ± 0.4	1.9 ± 0.1			
Occlusion	2.9 ± 0.5	2.0 ± 0.2	*P* = 0.54	*P* = 0.18	*P* = 0.72
Reperfusion 60 min	2.9 ± 0.9	1.8 ± 0.5			
Reperfusion 120 min	2.4 ± 0.6	1.4 ± 0.5			
Ejection Fraction (%)					
Baseline	39 ± 5	46 ± 6			
Occlusion	42 ± 3	47 ± 6	*P* = 0.04	*P* = 0.32	*P* = 0.80
Reperfusion 60 min	36 ± 4	41 ± 1			
Reperfusion 120 min	35 ± 3	35 ± 2			

Table 6. Hemodynamics and cardiovascular measurements of obese swine. Values are mean ± SE for obese (n = 4) and obese + exendin-4 (n = 4) swine. * = $P < 0.05$ vs. Baseline, same treatment. The analytic approach is identical to that presented for Table 5.

	Lean	Obese	Diet	Condition	Interaction
Mean Blood Pressure (mmHg)					
Baseline	101 ± 21	99 ± 10	*P =0.68*	*P = 0.01*	*P* = 0.533
Occlusion	89 ± 23	91 ± 8			
Reperfusion 60 min	75 ± 11	85 ± 11			
Reperfusion 120 min	63 ± 11*	83 ± 8			
Heart Rate (beats/min)					
Baseline	87 ± 20	83 ± 8	*P* = 0.36	*P* = 0.04	*P* = 0.12
Occlusion	72 ± 8	90 ± 11			
Reperfusion 60 min	83 ± 13	87 ± 11			
Reperfusion 120 min	85 ± 14	86 ± 7			
End Diastolic Volume (ml)					
Baseline	83 ± 15	66 ± 8	*P* = 0.39	*P* = 0.82	*P* = 0.08
Occlusion	60 ± 8	76 ± 10			
Reperfusion 60 min	58 ± 7	97 ± 32			
Reperfusion 120 min	49 ± 8	89 ± 30			
Stroke Volume (ml)					
Baseline	41 ± 10	26 ± 5	*P* = 0.215	*P = 0.05*	*P* = 0.01
Occlusion	18 ± 7*	32 ± 3			
Reperfusion 60 min	12 ± 4*	23 ± 8†			
Reperfusion 120 min	11 ± 3*	28 ± 7			
Cardiac Output (L/min)					
Baseline	2.2 ± 0.5	2.1 ± 0.4	*P* = 0.05	*P* = 0.58	*P* = 0.07
Occlusion	1.2 ± 0.4	2.9 ± 0.5†			
Reperfusion 60 min	0.9 ± 0.2	2.9 ± 0.9†			
Reperfusion 120 min	0.9 ± 0.2	2.4 ± 0.6†			
Ejection Fraction (%)					
Baseline	47 ± 6	39 ± 5	*P* = 0.15	*P* < 0.001	*P* = 0.006
Occlusion	27 ± 8*	42 ± 3†			
Reperfusion 60 min	20 ± 5*	36 ± 4†			
Reperfusion 120 min	21 ± 4*	35 ± 3			

Table 7. Hemodynamics and cardiovascular measurements of saline treated swine. Values are mean ± SE for lean (n = 4) and obese (n = 4) swine. By two way repeated measures ANOVA: * = P < 0.05 vs. Baseline, same diet; † = P < 0.05 vs. lean, same condition.

	Lean	Obese	Diet	Condition	Interaction
Mean Blood Pressure (mmHg)					
Baseline	131 ± 5	89 ± 5†	*P* = 0.003	*P* < 0.001	*P* = 0.004
Occlusion	127 ± 6	86 ± 4†			
Reperfusion 60 min	108 ± 8*	86 ± 4†			
Reperfusion 120 min	91 ± 6*	77 ± 6			
Heart Rate (beats/min)					
Baseline	113 ± 4	74 ± 12	*P* = 0.89	*P* = 0.22	*P* = 0.70
Occlusion	68 ± 12	68 ± 8			
Reperfusion 60 min	84 ± 8	75 ± 11			
Reperfusion 120 min	80 ± 7	77 ± 10			
End Diastolic Volume (ml)					
Baseline	82 ± 7	59 ± 5†	*P* = 0.07	*P* = 0.01	*P* = 0.63
Occlusion	77 ± 7	65 ± 3			
Reperfusion 60 min	65 ± 6	55 ± 7			
Reperfusion 120 min	64 ± 6	48 ± 8			
Stroke Volume (ml)					
Baseline	26 ± 5	28 ± 4	*P* = 0.12	*P* = 0.01	*P* = 0.64
Occlusion	21 ± 4	31 ± 4			
Reperfusion 60 min	14 ± 3	23 ± 3			
Reperfusion 120 min	13 ± 4	17 ± 4			
Cardiac Output (L/min)					
Baseline	1.7 ± 0.5	1.9 ± 0.1	*P* = 0.20	*P* = 0.19	*P* = 0.74
Occlusion	1.3 ± 0.2	2.0 ± 0.2			
Reperfusion 60 min	1.1 ± 0.2	1.8 ± 0.5			
Reperfusion 120 min	1.0 ± 0.3	1.4 ± 0.5			
Ejection Fraction (%)					
Baseline	31 ± 4	46 ± 6†	*P* = 0.003	*P* = 0.004	*P* = 0.62
Occlusion	26 ± 3	47 ± 6†			
Reperfusion 60 min	20 ± 3	41 ± 1†			
Reperfusion 120 min	20 ± 4	35 ± 2†			

Table 8. Hemodynamics and cardiovascular measurements of EX-4 treated swine. Values are mean ± SE for lean+exendin (n = 5) and obese + exendin (n = 4) swine. *= P < 0.05 vs. Baseline, same diet; † = P < 0.05 vs. lean, same condition.

Heat Map	Effect of	Group	IPA Associations: Molecular and Cellular Function
Lean	I/R in Lean	A	cell death and survival
	EX-4 in Lean	B	cellular movement development growth and proliferation
	EX-4 and I/R in Lean	C	cell-to-cell signaling and interaction cellular development cellular growth and proliferation cell death and survival cell morphology
		D	N/A
Obese	Obesity	A	cell morphology cellular function and maintenance DNA replication/ recombination/repair cellular assembly and organization
		A + B	cell death and survival
		B	cellular compromise cell cycle cellular development cell-to-cell signaling and interaction
		C	cell cycle

	I/R and Obesity	C + D	cellular development cellular growth and proliferation
		D	cell death and survival cell-to-cell signaling and interaction small molecule biochemistry
	Ex-4 and Obesity	E	cell-to-cell signaling and interaction cellular assembly and organization cellular compromise cellular movement cell death and survival
	EX-4, I/R and Obesity	F	cell-to-cell signaling and interaction cellular assembly and organization cellular function and maintenance
		F + H	cell death and survival
		H	cell cycle cellular movement
		H + I	cellular growth and proliferation
		F + H + I	cellular development
		G	N/A

Table 9. IPA predictions of molecular and cellular functions associated with miR change

Lean Saline Normally Perfused versus	IPA Top Canonical Pathways Predicted based on Protein Changes	Unique miRs changed relative to lean saline normally perfused	IPA miR Target Finder (miR and predicted protein target/s)
Obese Saline Perfused	Oxidative Phosphorylation, Mitochondrial Dysfunction, Aspartate Biosynthesis, L-cysteine Degredation III, Glutamate Degradation II	1307, 130b, 30b, 105-1, 331-3p, 494	miR-30b--3p/VCL miR-130b/COL6A3
Lean Saline Ischemic	Oxidative Phosphorylation, Mitochondrial Dysfunction, Aspartate Biosynthesis, Methylglyoxal Degradation I, L-cysteine Degradation III	N/A	N/A
Obese Saline Ischemic	Glycolysis I, Fatty Acid B-oxidation I, Glutaryl-CoA degradation, Tryptophan Degradation III	100, 1277, 140-star, 143-3p, 143-5p, -152, 17-3p, 199a, 202, 214, 24, 26a, 652	mir-24/LRPAP1 miR-140-3p/SCP2 miR-214/(SCP2,COL6A3) miR-139-5p/PRKAR2A
Lean EX-4 Perfused	Mitochondrial Dysfunction, Oxidative Phosphorylation, GDP-mannose Biosynthesis, Calcium Transport I	10a, 133a-3p, 133b, 149, 181a, 4331, 532-3p, 574, 935	miR-10a (NDUFA4, GPI, ATP5L, NDUFB6)
Obese EX-4 Perfused	Glycolysis I, Aspartate Biosynthesis, Glutamate Degradation II, Calcium Signaling, L-cysteine Degradation I	19a, 146a, 491	miR-193-5p/PRKAR2A
Lean EX-4 Ischemic	Glycolysis I, Gluconeogenesis I, Integrin Signaling, Actin Cytoskeleton Signaling	374b-5p, 487b	N/A
Obese EX-4 Ischemic	Glycolysis I, Gluconeogenesis I, Tx.RXR Activation, GDP-mannose Biosynthesis, Ketolysis	let-7a/f/g/i, 106a, 126, 140, 151-3p, 151-5p, 15a, 16, 181d-5p, 192, 199a-3p, 206, 221, 28-3p, 324, 339-5p, 342, 345-3p, 362, 365-3p, 424-star, 425-5p	miR-345-3p/col6a3 miR-1273h-5p/GPI, miR-221-3p/GPI

Table 10. Additional IPA findings based on changes in protein and miR data sets across each comparison.

Heat Map	Effect of:	Group	IPA Associations: Downstream Effects Analysis results pertinent to cardiovascular system	Prediction based on expression change vs LSN	Prediction p-value	miR changed leading to prediction
Lean	I/R in Lean	A	Apoptosis of cardiomyocytes	decreased	3.97E-02	378a-3p
			Failure of heart	affected	5.62E-02	423-5p
	EX-4 in Lean	B	N/A			
		C	Cell Viability of Heart Cells	affected	1.04E-02	133a-5p
			Arrhythmogenesis	affected	1.45E-03	133a-5p
			Hypoplasia of heart ventricle	increased	1.56E-02	133a-5p
	EX-4 and I/R in Lean	D	Non-insulin-dependent diabetes mellitus	affected	4.77E-02	129a
Obese	Obesity	A	dilated cardiomyopathy	Increased; affected	6.93E-04	Increased 497; affected 30c
			disarray of muscle cells	increased	1.15E-03	497
			disorganization of cardiomyocytes	Increased	3.84E-04	497
			fibrosis of heart	affected	5.76E-04	497, 30c
		B	diabetes mellitus	affected	3.42E-03	129a, 130b, 378a
			inflammation of organ	affected	5.30E-03	30b-3p, 130b, 30e-3p
			non-insulin-dependent diabetes mellitus	affected	5.58E-03	129a, 130b
	I/R and Obesity	C	Differentiation of muscle cell lines	increased	8.73E-03	100
		D	Fibrosis	affected, decreased	1.41E-04	Affected 26a, 140*, 17-3p; Decreased 199a
			Hypertrophy	decreased, affected	1.82E-03	Decreased 26a, 199a; Affected 214
			Diabetes mellitus	affected	2.34E-03	24, 143-3p, 152, 17-3p
	Ex-4 and Obesity	E	Disruption of focal adhesions	increased	5.82E-04	491
	EX-4, I/R and Obesity	F	Quantity of ventricular myocytes	increased	2.91E-04	206
			Arrhythmogenesis	affected	4.85E-04	206
			Ischemia of heart	affected	4.46E-03	206
		G	N/A			
		H	Inflammation of organ	affected	1.01E-08	106a, 126, 51-3p, 425-5p, 365-3p, 221, 181d-5p, 140, 15a let-7i, 324-5p
			G1/S phase transition of fibroblast cell lines	increased	2.27E-06	106a, 15a, let-7i
			Dilated cardiomyopathy	affected	2.20E-05	Affected 106a, 199a-3p, let-7i; Decreased 15a
		I	Polymyositis	affected	5.23E-03	30e-3p
			Inflammation of Organ	affected	1.97E-02	30b-3p, 30e-3p

Table 11. IPA predictions of molecular and cellular functions associated with miR changes. P-value represents a measure of the likelihood that the association

between a set of genes in your dataset and a related function is due to random association.

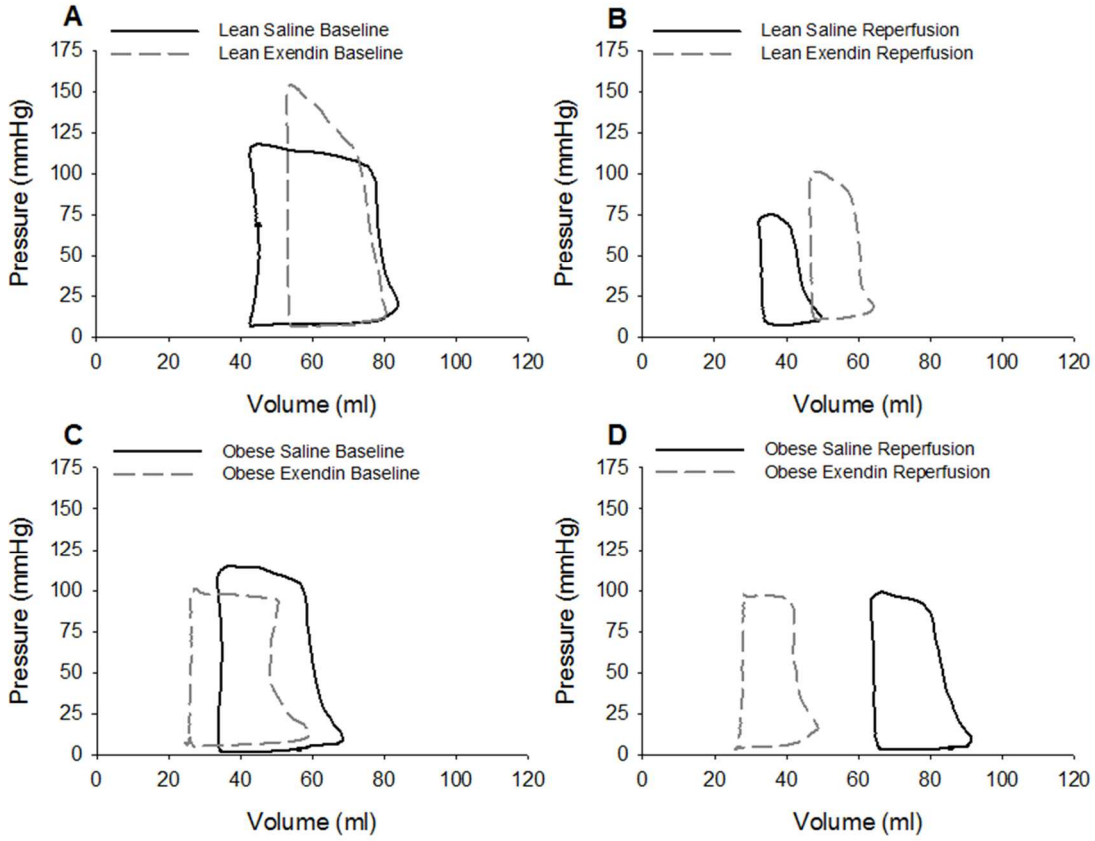

Figure 10. Representative pressure-volume loops for lean and obese swine at baseline, following ischemia-reperfusion injury, in the absence and presence of the GLP-1 receptor agonist exendin-4.

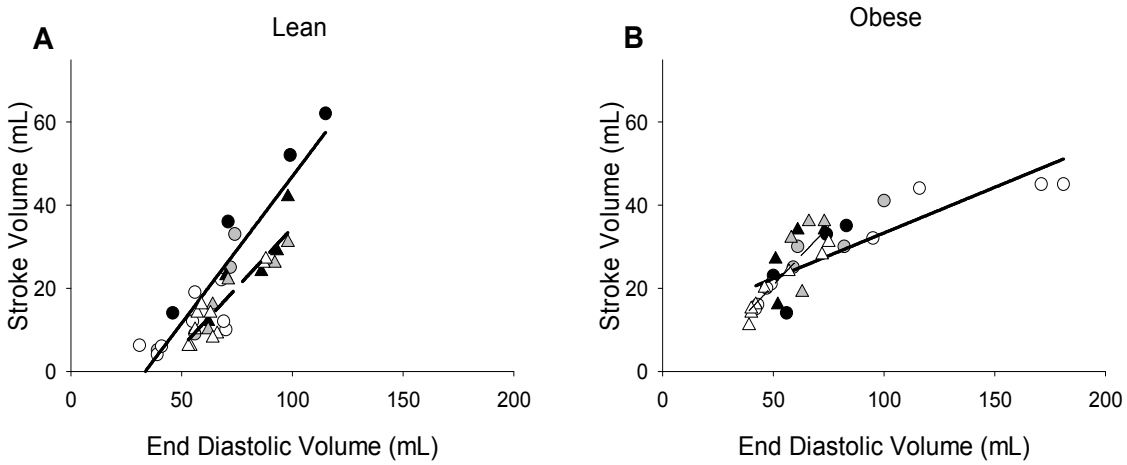

Figure 11. Effects of obesity and exendin-4 on the relationship between stroke volume and end-diastolic volume (i.e. Frank-Starling relationship). Solid lines represent best fit lines for saline (circles); dashed lines are the fit lines for exendin-4 (triangles). Filled symbols are measurements from the baseline pre-occlusion state; gray symbols are measurements during occlusion; and open symbols are measurements at 120 minutes of reperfusion. The slope of this relationship was significantly diminished in obese-control vs. lean-control swine ($P < 0.0001$). Exendin-4 treatment significantly reduced stroke volume at a given end-diastolic volume in lean animals (Panel A), changing the intercept ($P < 0.001$) but not the slope ($P = 0.21$) of the relationship. Exendin-4 shifted the slope ($P = 0.003$) of this relationship in obese animals (Panel B); however, the final slopes were not different between lean and obese exendin-4 treated swine ($P = 0.92$).

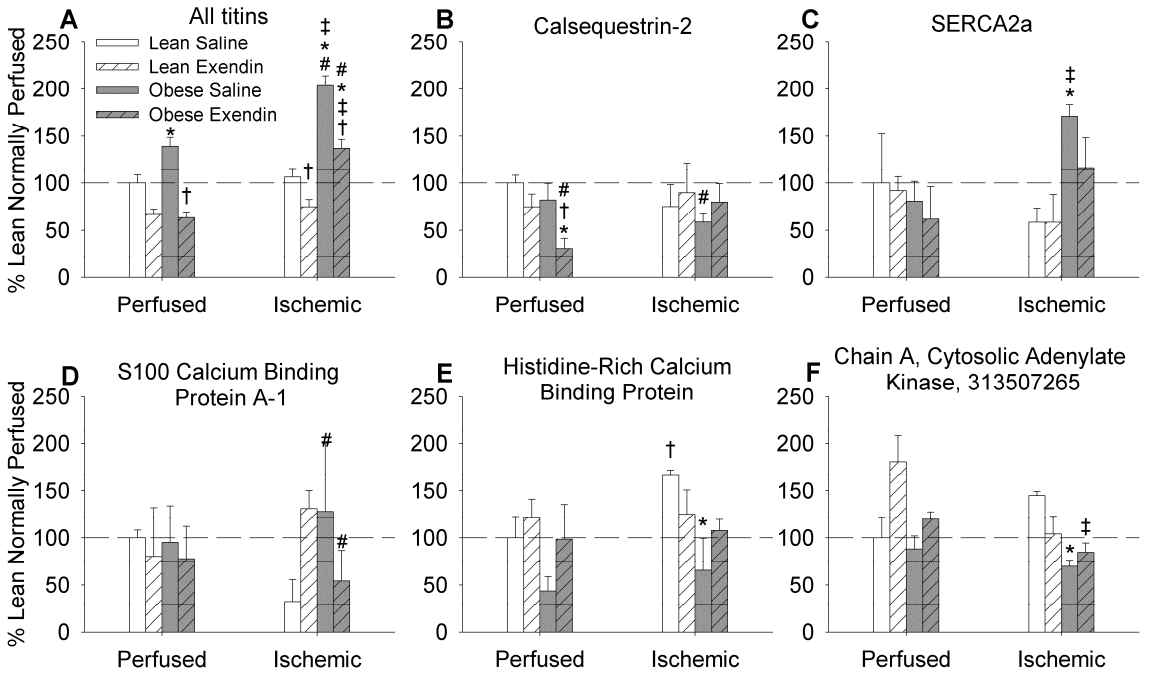

Figure 12. Effects of obesity and exendin-4 on proteins underlying myocardial function and calcium handling in normally perfused hearts and in myocardium following ischemia/reperfusion injury. Bars represent average percent relative to lean normally perfused value and error bars represent standard error. * = P<0.05 for comparison of diet within the same treatment and condition; † = P<0.05 for comparison of treatment within the same condition and diet; ‡ = P<0.05 for condition within the same diet and treatment. # = P > 0.05 for comparison relative to Lean Perfused Untreated myocardium. Panel A shows an aggregate of all titin proteins identified in mass spectrometry. Comparison for panel A by ANOVA All other comparisons by t-test. n=3 for lean perfused saline, n=4 lean perfused exendin-4, n=4 obese perfused saline, n= 4 obese perfused exendin-4, n=4 lean ischemic saline, n= 4 lean ischemic exendin-4, n=3 obese ischemic saline, n=4 obese ischemic exendin-4.

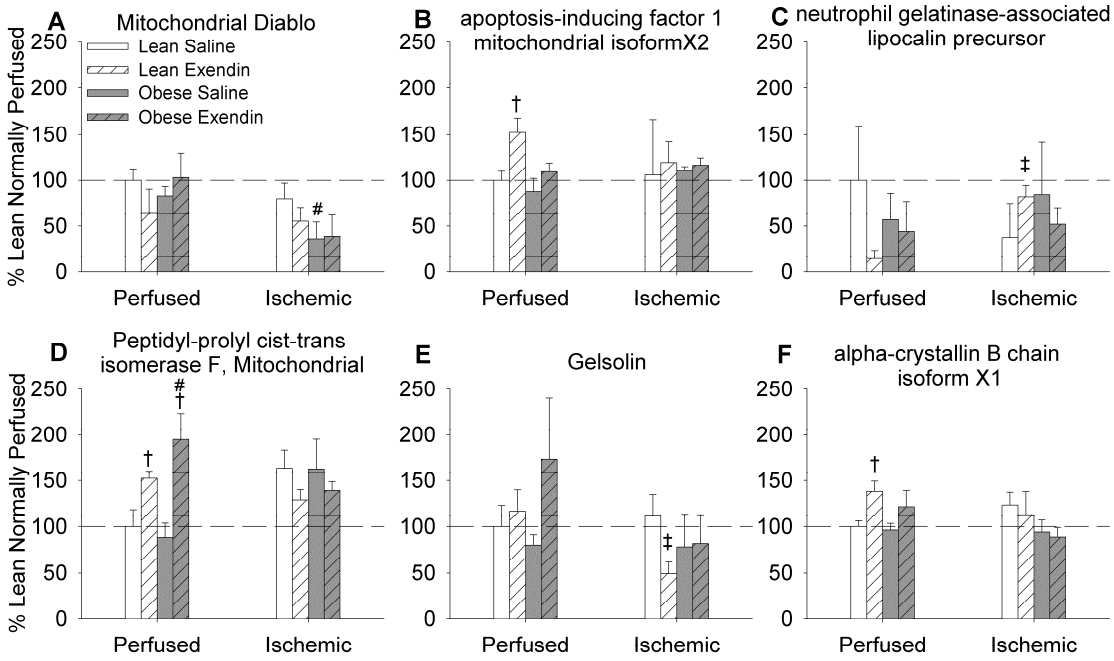

Figure 13. Effects of obesity and exendin-4 on proteins underlying cell death in normally perfused hearts and in myocardium following ischemia/reperfusion injury. Bars represent average percent relative to lean normally perfused value and error bars represent standard error. * = $P<0.05$ for comparison of diet within the same treatment and condition; † = $P<0.05$ for comparison of treatment within the same condition and diet; ‡ = $P<0.05$ for condition within the same diet and treatment. # = P > 0.05 for comparison relative to Lean Perfused Untreated myocardium All comparisons by unpaired T-test. n= 3 for lean perfused saline, n=4 lean perfused exendin-4, n=4 obese perfused saline, n= 4 obese perfused exendin-4, n=4 lean ischemic saline, n= 4 lean ischemic exendin-4, n=3 obese ischemic saline, n=4 obese ischemic exendin-4.

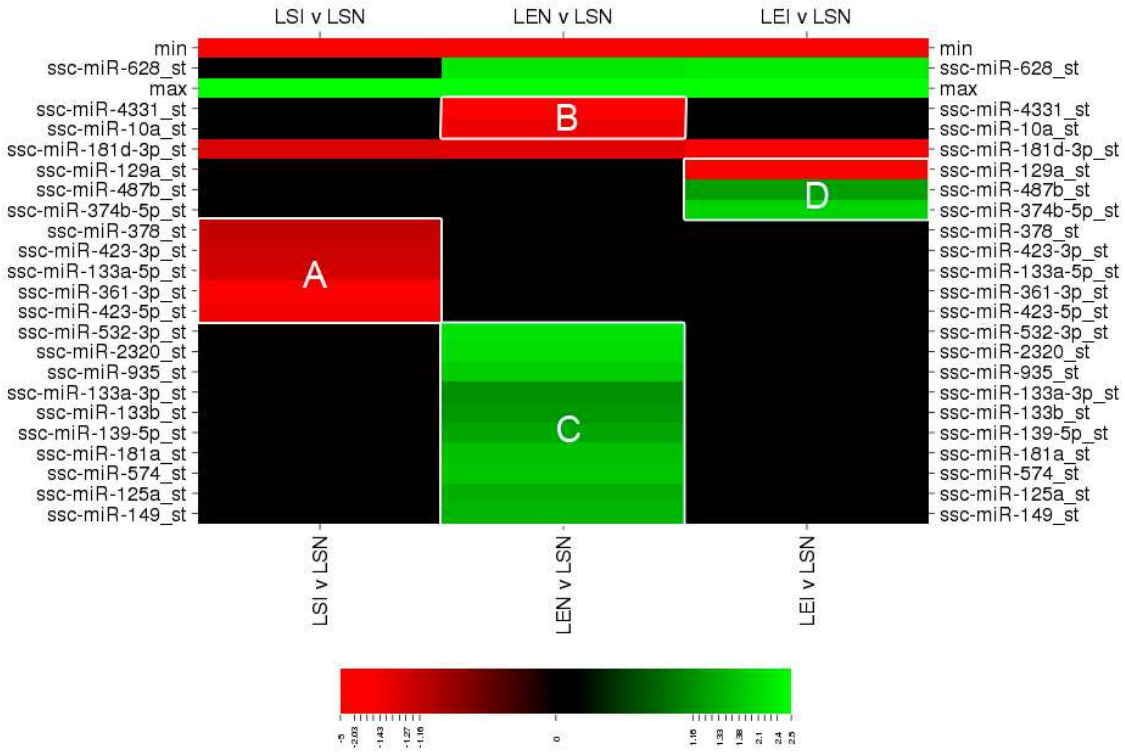

Figure 14. Heat map of miRs changed in lean left ventricular myocardium. n = 5 for all groups within comparisons. Differently regulated clusters of miRs in each comparison were ascribed to a group (indicated by letters A-D), based on common differences within comparisons. For each group the fold change and p-values were submitted to IPA for analysis of each cluster. Results of IPA analysis are presented in Table 5. Rows titled “min” and “max” were added to create similar scales for Figures 5 and 6. LSI = Lean Saline Ischemic. LEN = Lean EX-4 Normally Perfused. LEI = Lean EX-4 Ischemic. LSN = Lean Saline Normally Perfused.

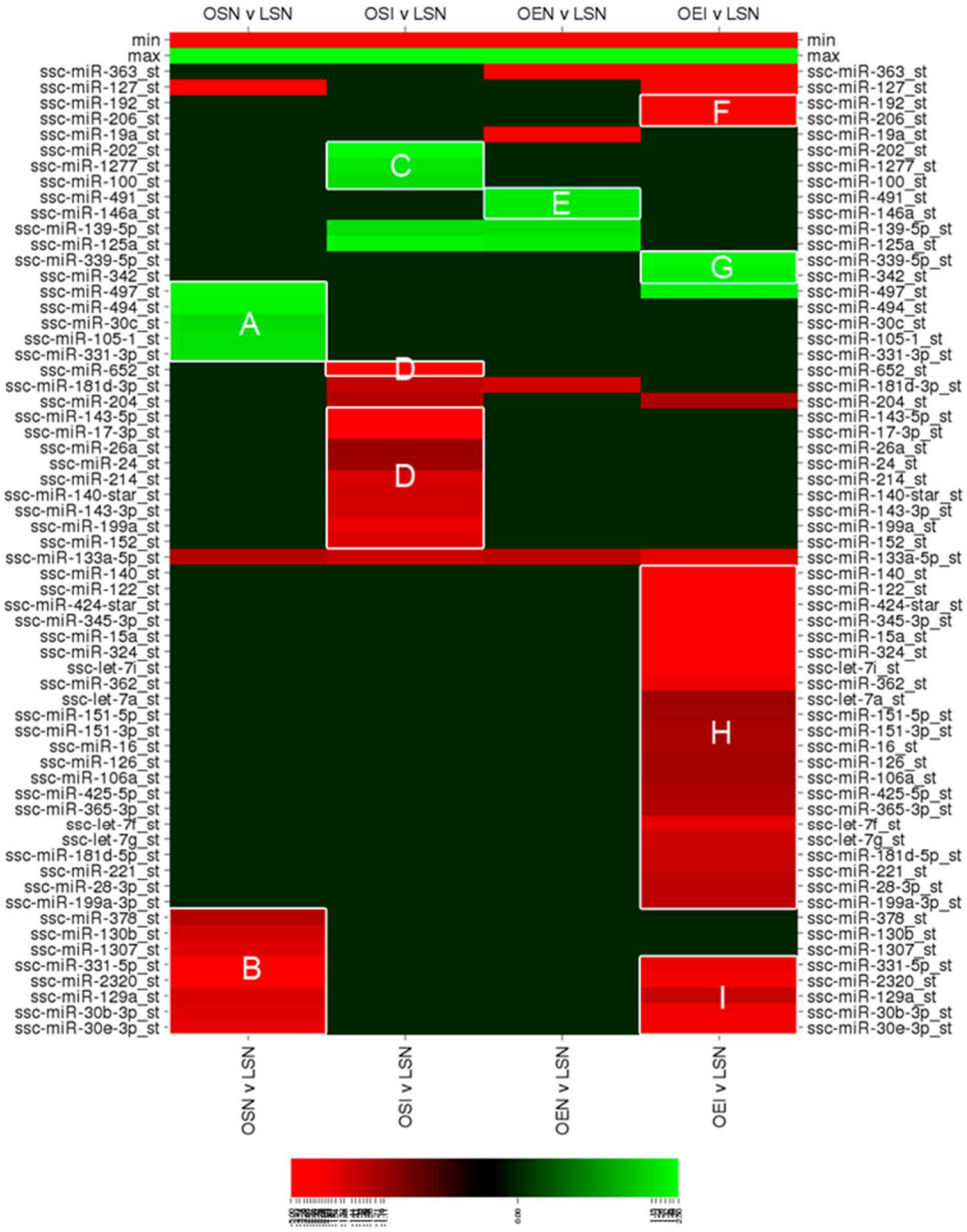

Figure 15. Heat map of miRs changed in obese left ventricular myocardium. For Lean saline perfused (n = 5). n = 4 obese saline, n = 5 obese exendin-4 ischemic and normally perfused. Differently regulated clusters of miRs in each comparison were ascribed to a group (indicated by letters A-I). For each group the fold change and p-values were submitted to IPA for analysis of each cluster. Results of IPA analysis are presented in Table 4. Rows titled “min” and “max” were

added to create similar scales for Figures 4 and 5. OSN = Obese Saline Normally Perfused. OSI = Obese Saline Ischemic. OEN = Obese EX-4 Normally Perfused. OEI = Obese exendin-4 ischemic. LSN = Lean Saline Normally Perfused

Chapter 3: Glucagon like peptide-1 receptor activation augments sympathetic mediated increases in cardiac function and improves efficiency in obese swine following myocardial infarction

Introduction

The use of glucagon like peptide-1 (GLP-1) based therapies for the treatment of type 2 diabetes mellitus has increased significantly since the initial discovery of incretin hormones in the early 1980's [102]. While these agents demonstrate unequivocal efficacy in the control of blood glucose concentration, an emerging body of evidence indicates that these compounds also have direct cardiovascular benefit, including improvements in cardiac contractile function [129] and reductions in myocardial infarct size [120]. Because obesity is associated with increased incidence and severity of negative cardiovascular outcomes [15, 51] these potential cardioprotective findings hold great therapeutic potential. However, prior studies of the cardiovascular effects of GLP-1 have largely been performed in models lacking comorbidities relevant to the at risk population.

Recent evidence supports that GLP-1 mediated increase in myocardial glucose uptake are attenuated in obese swine [124] and type 2 diabetic humans [124, 126]. Our laboratory has also recently documented distinct differences in cardiac responses to GLP-1 receptor (GLP-1R) activation in lean vs. obese swine following regional ischemia-reperfusion injury [242]. In particular, we found that the GLP-1R agonist exendin-4 augmented end-diastolic volume and systolic pressure generation in ischemic lean hearts while maintaining systolic pressure despite marked reduction in diastolic filling in obese hearts [242]. Proteomic analysis of left

ventricular myocardial biopsies demonstrated significant obesity induced differences in abundance of titin, PKA, and calcium handling proteins. Interestingly, GLP-1 based therapeutics modulated the abundance of these proteins uniquely dependent on obesity status. Such divergent effects combined with the failure of large scale clinical trials to demonstrate cardiovascular benefit of GLP-1 based therapeutics [243, 244] supports the need for a better understanding of the cardiac effects GLP-1 in the setting of obesity and metabolic dysregulation; especially in the setting of complex coronary vascular disease.

The purpose of this study was to investigate the potential for GLP-1R activation with the clinically employed agent, liraglutide, to influence cardiac function at rest and in response to β1-adrenergic receptor (β1ADR) stimulation in an obese swine model of ischemic heart disease. Based on the previous body of evidence indicating the potential for significant alterations to the cardiac proteome with GLP-1 based therapies [242], we hypothesized that chronic (~3-4 weeks) administration of the GLP-1 analogue liraglutide would demonstrate cardioprotective capacity in the ischemic hearts of obese animals through either infarct mitigation or alterations to cardiac function despite the previously documented absence of these effects in a more acute setting [124, 126, 245, 246]. Additional studies were also performed to examine the impact of liraglutide treatment on infarct development and β1ADR expression in the infarcted and normally perfused myocardium. These findings provide insight into the cardiac effects of GLP-1 related therapeutics in a relevant animal model of slowly developing, unrelieved, regional myocardial ischemia.

Materials and Methods

Surgical preparation and Experimental Protocol

All experiments involving animals were approved by an Institutional Animal Care and Use Committee and performed in accordance with the Guide for the Care and Use of Laboratory Animals (NIH Pub. No. 85-23, Revised 2011). Ossabaw Swine were placed on an obesogenic diet at approximately 6 months of age containing ~8,000 kcal/day high fat/fructose, 16 % kcal from protein, 41 % kcal from complex carbohydrates, 19 % kcal from fructose, and 43 % kcal from fat (mixture of lard, hydrogenated soybean oil, and hydrogenated coconut oil), and supplemented with 2.0 % cholesterol and 0.7 % sodium cholate by weight (KT324, Purina Test Diet, Richmond, IN, USA). At ~1 year of age, animals were randomly assigned to either saline or liraglutide treatment groups with animals weighing 60 ± 3.6 kg. At time of assignment to treatment group, animals were sedated with telazol, xylazine, and ketamine (5, 2.5, and 2.5 mg/kg, s.c.) prior to anesthesia with isoflurane (~1.5 - 3%). A brief thoracotomy procedure was performed and an ameroid constrictor (Research Instruments Southwest) placed on the proximal LAD in all animals regardless of treatment group. Animals were survived out for four weeks during which they received a step-up protocol of liraglutide (Week 1: 0.005, Week 2: 0.010, Week 3: 0.015, Week 4: 0.015 mg/kg/day; s.c.) or volume matched saline injections (Figure 16). At the end of the four-week treatment period, a terminal *in vivo* study was performed in each animal. In brief, animals were sedated again using the cocktail detailed above and anesthesia maintained with morphine (3 mg/kg, i.m.) and α-chloralose (100 mg/kg, i.v.). Catheters were

placed into the right femoral artery and vein for systemic hemodynamic measurements and administration of supplemental anesthesia, heparin and sodium bicarbonate respectively. A Fogarty balloon catheter (Edwards Lifesciences) was introduced into the left femoral vein and advanced into the inferior vena cava to allow for experimental reduction of venous return to the heart. Blood gas parameters were maintained within normal physiologic limits through periodic arterial blood gas analyses and appropriate adjustments to breathing rate and bicarbonate supplementation as necessary. A sternotomy was performed and a pressure volume admittance catheter (Transonic Systems) was introduced into the left ventricular lumen via an apical stab and affixed with a purse string suture. Animals were then subjected to sympathomimetic challenge (dobutamine 0.3-10μg/kg/min). Following the completion of *in vivo* experimental protocols, hearts were fibrillated and excised for *ex vivo* studies.

Infarct Quantification

Immediately subsequent to the acute procedure, fibrillated hearts were excised and flushed with 4°C, Ca^{2+}-free Krebs buffer (131.5 mM NaCl, 5mM KCl, 1.2 mM NaH_2PO_4, 1.2 mM $MgCl_2$, 25mM $NaHCO_3$, 10 mM glucose) via aortic cannulation. Hearts were then wrapped in plastic wrap and frozen at -20°C. The following morning, hearts were removed from the freezer and sliced into 1cm thick sections with a P-12D slicer (National Presto Industries Inc.). Sliced sections were then immersed in a 37°C, 1% w/v tetrazolium solution (0.1M NaH_2PO_4, 0.1M Na_2HPO_4, 10 g/L tetrazolium chloride, pH 7.4) for approximately 20 minutes with shaking. Slices were then transferred to a 10% buffered formalin solution for at

least 24 hours. Formalin fixed tissues were then imaged at constant focal length in a shadow free, controlled light environment (All-in-one smart photo light box; LS Pro Photo Studio) in RAW image mode with a Canon Eos Rebel SL1 (Canon) equipped with a Canon EF-S 18-55 mm lens. Infarct area (unstained) versus viable tissue (stained) was quantified on each heart slice from each animal by 2 separate investigators blinded to condition using ImageJ.

Immunohistochemistry

Biopsies from the 1cm thick heart slices were taken from both the epi- and endocardium of the ischemic and normally perfused regions of left ventricular myocardium for histological analysis. Tissues were processed into 4-5μM thick slices and stained using Masson's Trichrome as well as immunohistochemistry for CD 163 (Abcam, ab87099, Cambridge, MA), and β1ADR (Thermo Fisher, PA5-28808, Rockford, IL).

The Aperio Scan Scope CS whole slide digital imaging system (360 Park Center Drive Vista, CA 92081) was used for imaging of histology. All slides were imaged at 20X magnification. Scan times ranged from 1.50 minutes to a maximum time of 2.25 minutes. The whole images were housed and stored in eSlide Manager software system and images were shot from the whole slides. Computer-assisted morphometric analysis of digital images was performed using the included software of the Aperio Imaging system. The positive pixel algorithm (Aperio Technologies) is the only image quantitation software approved by the FDA. The positive pixel algorithm was used for immunostains and differentiates between blue and brown staining in an image. The positive pixel algorithm was modified to

distinguish between the blue and red colors characteristic of Masson's Trichrome and was used for fibrosis staining of the myocardium.

Trichrome Automatic Image Quantitation: The Positive Pixel Count Algorithm was used to quantify the amount of a specific stain present in a scanned slide image [247]. The Positive Pixel Algorithm was altered with a hue value of 0.62, hue width of 0.40, and color saturation threshold of 0.005. A spectrum of color (range of hues and saturation) and intensity (weak, positive, and strong) were masked and evaluated. The algorithm counts the number and intensity-sum in each intensity range, along with three additional quantities: average intensity, ratio of strong/total number, and average intensity of weak positive pixels. Only staining classified as "positive" or "strong positive" was used to calculate positivity; regions classified as "weak positive" were mostly cytoplasmic and background staining, and were not counted. The algorithm had a set of default input parameters when first selected; these inputs have been pre-configured for Brown color quantification in the three intensity ranges (220–175, 175–100, and 100–0). Pixels which were stained, but did not fall into the positive-color specification, were considered negative stained pixels; these pixels were counted as well, so that the fraction of positive to total stained pixels was determined. The ratio of the 'Positive' and 'Strong Positive' to the total number of pixels provided the positivity percentage for each sample. The algorithm was applied to an image by using ImageScope. This program allows for the selection of an image Region of Analysis and the specification of input parameters. After this is completed the algorithm can be applied and the results can be viewed.

Statistical Analyses

Data are presented as mean ± SEM and were analyzed using the Sigma plot statistical package (version 12 Systat Software Inc, San Jose, CA) and SPSS (version 22 IBM, Chicago IL). Comparisons were considered statistically significant when $P < 0.05$. The effect of treatment was assessed using two-way ANOVA. To establish significance of differences at baseline, parameters were additionally analyzed via t-test. When significance was established with ANOVA, Student-Newman-Keuls posthoc testing was performed to identify pairwise differences between groups. Multiple linear regression and analysis of covariance were used to compare the slopes and intercepts of the relationships between cardiac output vs. end-diastolic volume, and cardiac power vs. pressure volume area. Cardiac power was calculated as the triple product of stroke volume, aortic pressure and heart rate.

Results

Phenotypic Characteristics of Obese Swine

Body weight on the day of ameroid placement was statistically similar in saline vs liraglutide treated swine (Table 12, $P = 0.31$). Post-treatment body weight was significantly lower in the liraglutide treated group as final body weights at the time of terminal procedure were 70 ± 6 kg in saline vs. 54 ± 3 kg in liraglutide treated swine ($P = 0.02$). Ameroid closure was complete in all animals and resulted in significant infarct development in both groups. However, liraglutide therapies did not significantly impact the overall magnitude of infarction (Saline: 15.5 ± 1.9%, n

= 4 vs. Liraglutide: 13.9 ± 5.4%, n = 6; *P* = 0.81) (Figure 17). No infarction was detected in sham operated swine (*Data not shown*).

Effects of Liraglutide Treatment on hemodynamic and cardiac parameters

As chronic instrumentation was limited to ameroid placement, all physiologic data presented were obtained during a terminal procedure (Table 13). Thus, data presented hereafter provide cross-sectional analyses of saline vs. liraglutide treated swine as opposed to longitudinal studies within each animal. Mean arterial pressure was similar at baseline (*P* = 0.87), while heart rate tended to be higher in liraglutide (107 ± 9 beats/min) vs. saline-treated (77 ± 13 beats/min) (Table 13; *P* = 0.07). Additionally, key indices of cardiac function including stroke volume, ejection fraction, cardiac output, Tau½, and end-systolic elastance were unaffected by liraglutide administration under baseline conditions (Table 13). The volume axis intercept of the pressure volume relationship (V_0) was diminished ~50% in liraglutide (15 mL) vs. saline (33 ml) treated swine at rest, however this change in not achieve statistical significance (*P* = 0.09, Figure 18).

To assess whether liraglutide treatment influences cardiac responses to β1ADR activation, swine were exposed to sympathomimetic challenge via systemic administration of dobutamine (0.3-10 μg/kg/min). Systolic, diastolic, and mean arterial pressure were not significantly affected by dobutamine in saline or liraglutide treated swine (Table 13). Heart rate increased dose-dependently in response to dobutamine in both groups and was significantly higher in liraglutide treated animals (P = 0.004, Table 13). These increases in heart rate were accompanied by reductions in stroke volume and ejection fraction values (Table

13), however liraglutide reduced the degree to which in these parameters were diminished (Figure 19) resulting from enhanced diastolic function as indicated by increases in dp/dtmin and Tau (Table 13).

Both end systolic (ESV) and diastolic volumes (EDV) within the heart decreased in both groups with increasing dobutamine dosage. The relative degree of decrease was similar in both saline and liraglutide treated animals (treatment effect EDV P= 0.19, ESV P = 0.47). Pressure-volume (PV) loops in Figure 18A and B allow for visualization of end diastolic volume and end systolic volume shifts and stroke volume reductions in both groups. End diastolic volume was only significantly changed relative to baseline in saline treated animals at the highest concentration of dobutamine (P = 0.04, Table 13) and this change was not significant in the liraglutide group (P = 0.06, Table 13). Similarly, stroke volume decreased in both groups reaching significance at the 10 μg/kg/min dose (saline P = 0.005, liraglutide P = 0.022 Table 13). However, the magnitude of decrease in stroke volume over the course of the terminal procedure was reduced in liraglutide treated swine relative to saline (P=0.029, Figure 19A). Cardiac output values demonstrated a downward trend in both groups of animals with the average cardiac output across the range of sympathomimetic challenge being significantly different between treated and control animals (P = 0.02). Ejection fraction decreased in both saline and liraglutide treated swine during administration of dobutamine. Liraglutide treatment was associated with a maintenance in ejection fraction relative to saline at the highest dosage of dobutamine (P=0.006, Figure 19B).

Overall, V_0 was lower in liraglutide treated swine (P<0.001, Figure 18C) and increased with similar magnitude between groups in response to dobutamine (P=0.88, Table 14). Cardiac relaxation, both load-dependent and independent, was enhanced with liraglutide as evidenced by increasingly negative dp/dt Min and decreases in both Tau ½ and Tau $^1/_e$ (Table 13). Load-dependent measures of cardiac contraction were enhanced in both groups with dose dependent increases in dp/dt max (maximum rate of pressure change; P=0.001) as well as significantly decreased contraction time (CT) relative to baseline in liraglutide groups (Table 13). Accordingly, the mean relaxation was different between groups across the range of dobutamine challenge (dp/dt min, P < 0.001; Tau $^1/_{2,}$ P = 0.03; Tau $^1/_{e,}$ P = 0.03).

Load independent measures of cardiac contractility (end systolic elastance, aka ESPVR) were not different between both groups (Figure 18D) and did not change significantly due to liraglutide treatment during the duration of the experiment (P = 0.12, Table 14). To account for effects of body mass on cardiac output, regression analysis of cardiac index (mL/min/kg body weight) vs EDV (mL) was performed (not shown). Results of associated ANCOVA analyses (P<0.001) further support that treatment with liraglutide changes load dependent measures of cardiac function. Figure20 presents the relationship between cardiac output and EDV for both saline and liraglutide treated animals. Despite an absence of load independent effects of liraglutide on contractility, liraglutide treated animals demonstrated a significantly greater increase in cardiac output relative to EDV with dobutamine challenge.

Relationship between liraglutide therapies and cardiac efficiency at varying levels of myocardial oxygen consumption

Pressure volume area (PVA), derived from pressure volume recordings during reductions in preload (inferior vena cava occlusion), is linearly related to left ventricular myocardial oxygen consumption [248]. When cardiac power (product of stroke volume, mean aortic pressure, and heart rate) is expressed relative to PVA it produces a index of cardiac efficiency (power per unit of oxygen consumed). To assess whether liraglutide altered cardiac efficiency, we plotted cardiac power relative to PVA (Figure 21). Statistical analyses of the best fit lines support that liraglutide treatment increases power generation as myocardial oxygen consumption increases with dobutamine challenge (P=0.001 by ANCOVA) (i.e. cardiac efficiency is greater in liraglutide treated animals).

Role of alteration of LV mass and collagen deposition in physiologic outcomes of the study

Immediately following euthanasia the heart was removed from each animal and the coronary tree perfused with ice cold saline via aortic cannulation to remove residual blood. The wet weight of each heart was then recorded. Liraglutide therapy did not result in an alteration of total cardiac mass (saline 223 ± 18 vs. liraglutide 218 ± 14 g; P = 0.851) nor in heart weight/body weight ratio (saline 3.3 ± 0.4 vs. liraglutide 4.1 ± 0.2 g/kg; P = 0.396). To further establish whether any physiological findings were the result of alterations to left ventricular mass, the cross sectional thickness of the LV free wall was determined in formalin fixed slices using ImageJ at a consistent anatomical location (2 centimeters distal to the

ameroid). Left ventricular free wall thickness was not different based on treatment (saline 2.3 ± 0.1 vs. liraglutide 2.3 ± 0.1 mm; P = 0.97). Additionally, liraglutide treatment did not affect collagen deposition as there were no significant differences in Masson's Trichrome staining (treatment effect within the ischemic P = 0.62, and P = 0.60 within perfused regions).

Immunohistochemistry of Formalin Fixed Tissues

Immunohistochemistry (IHC) was performed on formalin fixed myocardium to establish whether changes in β1ADR underlie functional effects of liraglutide in response to sympathomimetic challenge. Liraglutide treatment was associated with significant reductions in β1ADR expression (Figure 22) in perfused myocardium (P = 0.017). Liraglutide treatment also diminished the ischemia induced reduction in β1ADR expression observed in saline treated myocardium (P = 0.001 for saline; P = 0.60 liraglutide).

Discussion

GLP-1 receptor activation has been implicated in cardioprotective phenomena observed in healthy animal models receiving recombinant GLP-1 based therapies. To date, little data exist to interrogate the cardioprotective potential of these therapies in the setting of complex heart disease. As GLP-1 based therapies are classically employed for the purpose of glucose regulation in a type II diabetes mellitus (T2DM) population and T2DM is positively associated with overweight/obesity, assessment of the cardiovascular effects in the setting of obesity is crucial. In this investigation we examined the effects of GLP-1 receptor activation via liraglutide on cardiac function at rest and in response to β1ADR

stimulation in an obese swine model of slowly developing ischemic heart disease using ameroid occluders. This design allows for examination of infarct limiting capacities of GLP-1 based therapies as well as cardiac performance alterations resulting from GLP-1 based therapies across a range of myocardial oxygen consumption in a gold-standard model of myocardial infarction.

Weight loss effects

Regardless of the specific drug in question, GLP-1 based therapies are consistently associated with weight loss in the clinical setting [249, 250]. At the time of study initiation, animals were statistically similar in mass and notably heavier than age matched animals employed in previous studies (Table 12)[124, 129, 251]. At the time of terminal procedure, animals that had been placed on liraglutide therapies weighed significantly less than saline treated animals. However, there was no significant or apparent weight loss in either saline or liraglutide treated animals. Rather, liraglutide therapies were associated with attenuated weight gain. Ossabaw swine typically gain between 0.06-0.10 Kg/day[252-255] when maintained on a normal laboratory diet. Swine in this study were maintained on the high fat obesogenic chow prior and subsequent to ameroid placement. Therefore, significant weight gain is expected across a 30 day period. Saline treated animals behaved consistent with this expectation and gained approximately 9kg in 30 days. By contrast, liraglutide animals gained less weight with ~1kg of weight gain across an identical period. Despite this significant difference in animal mass at the time of study, there was no difference in degree of infarction between treatment groups.

Infarct Size

This study examined GLP-1 based cardioprotection in the context of a slowly developing, unrelieved, regional myocardial ischemia. To accomplish this, an ameroid constrictor was placed around the proximal LAD during a survival procedure. Ameroid constrictors are a well-established tool in the study of coronary artery disease in swine models. *Post-mortem* analyses of ameroid closure through excision and examination under a dissecting microscope verified a 100% closure rate in all study animals; *i.e.* each animal experienced total regional ischemia of the LAD perfusion territory distal to the ameroid. The consistency of closure between both animals and groups is exemplified by the results of tetrazolium staining of the heart which demonstrated a consistent ~15% infarction of the LV (Figure 17).

The failure of chronic liraglutide therapy to mitigate the degree of myocardial infarction stands in contrast to work by Timmers *et al*. who found that administration of a comparable GLP-1 agonist, exenatide, reduced infarct size in the setting of acute ischemia reperfusion injury in otherwise healthy swine[120]. Timmers' data are further supported by clinical studies demonstrating infarct lowering capacity of exenatide in patients receiving angioplasty for the treatment of S-T elevated myocardial infarction[256-258]. How then are these disparate findings reconciled? The Timmers study examines a transient and relieved ischemia whereas this work exampins a chronic and unrelieved ischemia. One would predict, *a priori,* that there would likely be little to no effect of compound on infarct size in the setting of unrelieved ischemia owing to the absence of a reperfusion

period, the limited endogenous collateral network in swine and the limited capacity for angiogenesis in swine cardiac tissue. Despite the absence of infarct mitigation, significant improvements in cardiac function and efficiency (discussed below) were demonstrated in this study and the consistency of infarct between treatment arms minimizes the possibility that these effects are the result of changes to viable myocardial mass.

Hemodynamics

Pressor effects of GLP-1 based drugs have been reported for over 20 years. This effect is particularly pronounced in rodent models which routinely report significant increases in mean pressure as high as 20 mmHg. By contrast human studies have consistently demonstrated relatively pressor responses, reporting elevations of 2-3 mmHg or reductions < 3 mmHg in response to GLP-1 receptor agonism[259-261]. Additionally, the physiological status of study subjects significantly impacts the results or GLP-1 therapies on pressor responses. Therefore, the absence of a pressor response in this study (Table 13) is consistent with the body of literature demonstrating variable/modest effects of GLP-1 drugs on blood pressure. Moreover, the stable hemodynamic profile of treated animals in this study is consistent with work by Lovshin *et al*. who found that 3 weeks of liraglutide treatment failed to modulate blood pressure in patients with type II diabetes [262].

Whereas the results of this study, with regards to blood pressure, are confirmatory in regards to baseline measures, this study provides new insights into the ability of chronic GLP-1 therapies to modulate responsiveness to sympathetic administration of a sympathomimetic agent. Central effects of GLP-1 therapies

are well established in rodents but remain more equivocal in large animal models and humans. Previous work by our group identified no effect of hexamethonium treatment on changes to cardiac performance resulting from acute administration of GLP-1 (7-36) in the setting of myocardial ischemia [129]. These data further support an absence of sympathomimetic modulation by GLP-1 based therapies with regards to pressor responses in that systolic, diastolic and mean pressures are all consistent between treatment groups across the range of dobutamine challenge.

Cardiac Function

Similar to the pressor effects discussed above, GLP-1 mediated chronotropy (positive or negative) is highly variable in a species specific manner[125]. Anecdotally, tachycardia is most pronounced in those species which demonstrate the greatest pressor responses to GLP-1 therapies. By contrast, meta-analyses of human studies report modest GLP-1 related tachycardia with increases in heart rate of less than 2 beats per minute [249]. The results of this study are more consistent with human studies in that there is a modest increase in resting heart rate that fails to achieve statistical significance ($P = 0.205$). In response to sympathomimetic challenge, GLP-1 therapy resulted in a significantly higher heart rate across the dose response range (Table 12; $P = 0.004$) although the magnitude of change relative to baseline is consistent between groups (Table 14; $P = 0.44$). These data support a potential to modestly increase heart rate at rest although whether this is the result of actions on the nodal myocardium remains to be directly determined. To assess the potential of peripheral dilation, indirectly, peripheral

vascular resistance (calculated as MAP/CO) was calculated and found to not be different between groups minimizing the potential for peripheral dilation to be a contributor to tachycardic responses and supporting direct effects on the myocardium.

To establish the intropic potential of GLP-1 based therapies in the setting of myocardial ischemia and obesity, we performed high resolution left ventricular pressure volume analyses wherein preload was modulated by transient blockade of return through the inferior vena cava with a Fogarty balloon catheter. By determining the end systolic pressure volume points across a range of preload, we are able to assess the end systolic pressure volume relationship in a load independent manner. This serves as a gold standard measure of contractility [213]. This relationship is defined by two major characteristics. The slope of the end systolic pressure volume relationship defines the end systolic elastance (Ees) and is the classical measure of inotropy. Therefore, an increase in Ees would indicate enhanced cardiac contractility and a decrease in the slope of Ees would indicate decreased cardiac contractility. The other major parameter obtained in a preload reduction is the volume axis intercept (V_0) which is the theoretical volume at and below which the left ventricle no longer generates pressure. Based on this, changes in V_0 are often used as a measure of Starling forces in the heart as in V_0 values approaching zero, indicate force development at lower degrees of wall stretch.

In this study, liraglutide was found to lower V_0 significantly at baseline at low dobutamine concentration, indicating earlier inotropy independent (i.e. Starling)

force development at rest. This finding is consistent with previous work by our group which found improvements in left ventricular ejection fraction and GLP-1 mediated changes in cardiac function relating to diastolic filling (i.e. Frank-Starling effect Figure 20) rather than inotropy [129]. However, these observations were not made in obese hearts. Findings from this study are consistent with recent observations by Sassoon *et. al.* which demonstrate increases in inotropy of obese hearts in the setting of ischemia reperfusion[242].

Interestingly, Ees was not enhanced with dobutamine challenge in saline treated animals when examined as either an absolute change or a change relative to baseline. By notable contrast, liraglutide therapies preserved the ability of the heart to respond to adrenoreceptor activation in that there is a continuous increase in Ees across the range of dobutamine challenge both absolutely and relative to baseline. These data are further supported upon examination of the relationship between end diastolic volume and cardiac output (Starling Curve; Figure 20) which demonstrate that liraglutide treatment results in a shift of the relationship of EDV to CO such that at any given EDV, CO is greater in liraglutide treated animals relative to their saline counterparts. Classically this relationship has been used to establish whether a system is demonstrating an inotropic response. Taken together, these data support the ability of liraglutide therapy to preserve sympathetic sensitivity in the setting of myocardial ischemia and obesity. How then does this preservation occur?

Histological analyses of myocardial biopsies obtained immediately *post-mortem* provide some insight into how liraglutide therapies maintain sympathetic

responsiveness in the heart. Figure 21 depicts representative images of myocardium stained for the β-1 adrenoreceptor. Using the FDA approved algorithm (from Aperio), we were able to perform quantification on these biopsies. Relative to saline treated animals, the normally perfused myocardium of liraglutide treated animals exhibited lower levels of β-1 adrenoreceptor by approximately 50%. However, whereas the ischemic territory of saline treated animals exhibited only 10% of the staining found in the perfused territory, liraglutide treated animals demonstrated no reduction in β-1 adrenoreceptor resulting from ischemia. These data support an ability of liraglutide therapies to maintain β-1 adrenoreceptor levels despite myocardial ischemia.

Figure 18 presents representative left ventricular pressure volume loops which provide visual insight into the integrated response of the heart to liraglutide therapies in response to dobutamine challenge. At rest, all volume and pressure measures are similar between saline and liraglutide treated animals including end diastolic volume, end systolic volume, stroke volume, cardiac output and ejection fraction. Also, in addition to the previously mentioned volume independent measures, volume dependent measures of cardiac function including contraction time, relaxation time, dp/dtmax, dp/dtmin, and Tau were similar at rest. Therefore, at rest, the hearts in both treatment groups are providing similar cardiac work. Dobutamine challenge identified varied responses in a number of indices. With increasing heart rate came an accompanying and anticipated reduction in both end diastolic volume and end systolic volume in both groups. The magnitude of these reductions were similar in both groups, however, modest differences between

treatment groups do result in a significant difference in the change in stroke volume with dobutamine challenge (Table 14). Across the range of dobutamine challenge, there is a greater reduction in stroke volume of saline treated animals than is found in their liraglutide counterparts. Moreover, the relative decrease in ejection fraction found in saline treated animals (~19%) is attenuated in liraglutide treated animals (~7%). This preservation of ejection fraction in liraglutide treated animals is such that it is not significant across the range of dobutamine challenge meaning that, whereas saline treated animals demonstrate characteristics of heart failure, liraglutide treated animals are more aptly characterized as animals demonstrating heart failure with preserved ejection fraction.

While it may seem paradoxical that liraglutide treated swine had increased cardiac contractility despite lower expression of β1ADR, the combination has been previously observed as conferring benefit in other clinically relevant scenarios. Reduction in beta-adrenergic signaling, via beta blockade, is frequently used to improve cardiac function including in the setting of heart failure [263]. Reducing beta-receptor signaling disrupts the positive feeback loop (maladaptive adrenergic signaling) that pushes the heart towards hypertrophy and eventually failure [264]. Alternative mechanisms can be employed that improve cardiac mechanical work without additional demand for myocardial oxygen uptake including, altering calcium handling and contractile machinery [224], and improving nutrient utilization [214]. Prior proteomics studies performed by our laboratory [242] support that exendin-4, another GLP-1 related therapeutic, changed the expression of key calcium handling proteins, components/regulators of sarcomeric proteins, and metabolic

proteins. Further research is needed to better define the liraglutide induced alterations in calcium handling, contractile apparatus, and nutrient utilization in obesity (see next section regarding cardiac efficiency).

Cardiac Efficiency

Based on changes between groups in Starling forces at rest and inotropic responses with dobutamine challenge, the cardiac efficiency of the system could potentially be altered with liraglutide therapy. Pioneering work by Hiroki Suga has demonstrated a linear relationship between pressure volume area and myocardial oxygen consumption [248, 265]. Therefore, based on the data obtained with transient IVC occlusion in this study, we are able to assess the myocardial oxygen consumption within the heart based on the PVA. Considering that the hearts of liraglutide treated animals demonstrate force development at lower pressure when at rest, the first question with regard to efficiency is whether myocardial oxygen consumption is different between treatment groups at rest. PVA was found to be statistically similar ($P = 0.897$) indicating that myocardial oxygen consumption is similar between treatment groups. Cardiac power (work per unit time) can further be calculated as the triple product of stroke volume, aortic pressure and heart rate. As was found with PVA, cardiac power was similar between treatment groups at rest ($P = 0.084$). The relationship between cardiac power (work) and PVA (consumption) is an index of cardiac efficiency. Both groups begin at similar efficiency. However, when data for cardiac power (work per unit time) are expressed relative to PVA (Figure 22) we can see that liraglutide fundamentally increases the relationship between left ventricular power generated at any level of

oxygen consumption beyond baseline relative to saline. Therefore, although the hearts of liraglutide treated animals demonstrate similar Ees, liraglutide treatment results in a significant enhancement of cardiac efficiency under conditions of enhanced metabolic demand.

Limitations.

Owing to the resource-intensive nature of these studies and some animal loss with chronic unrelieved left ventricular ischemia/infarction, this study presents relatively small group sizes. Nevertheless, we noted statistically significant differences in key physiologic end points that were associated with marked changes in HR, SV, EF & CO relative to EDV. These observations therefore are not compromised on statistical power overall, although one could argue that the sample size raises questions of representativeness. In this regard, we did not observe individual animals to introduce significant outliers for any of the evaluated physiological parameters.

Post-euthanasia molecular analysis was limited by the need for whole, uncompromised hearts for accurate infarct measurement. Formalin fixation and staining with tetrazolium chloride prevented use of fresh tissues for gel based analysis or ELISA. Formalin fixed tissues were biopsied and used for IHC. To minimize bias inherent to histological analysis, we utilized digital pathology techniques to quantify stain.

Conclusions and Implications.

Taken together, findings from this investigation suggest that 30 day liraglutide exposure in obese swine does not reduce infarct size development in

the setting of unrelieved ischemia. As previously stated, this finding is unsurprising and the result may differ under conditions of ischemia/reperfusion. Hearts from animals receiving chronic liraglutide treatment were shown to have preserved β adrenoreceptor expression with an accompanying preservation of responsiveness to dobutamine challenge. Whereas saline treated animals were largely unresponsive to dobutamine, this was not true of liraglutide treated animals. Moreover, dobutamine challenge was associated with increasing pressure volume area in both treatment groups indicative of enhanced myocardial oxygen consumption. However, this resulted in a near zero outcome in change in cardiac power for control animals indicating that under conditions of enhanced sympathetic stress, the hearts of control animals will continue to significantly increase myocardial oxygen consumption with no benefiting increase in cardiac power. By contrast, the efficiency of liraglutide hearts across a range of dobutamine challenge is significantly enhanced owing to enhanced cardiac performance. Taken together, these data support a potential role for liraglutide therapies in maintaining sympathetic responsiveness of hearts in obese individuals with chronic ischemic heart disease.

Chapter 3 Tables and Figures

	Saline	Liraglutide	P value
Body Mass (kg) prior to ameroid placement	63 ± 11	52 ± 4	0.31
Body Mass (kg) prior to terminal study	70 ± 6	54 ± 3	0.02
Delta Body Weight (kg)	9 ± 4	1 ± 2	0.09
Heart Weight (g)	223.3 ± 17.5	218.4 ± 13.9	0.85
Heart Weight /Body Weight Ratio	0.33 ± 0.04	0.41 ± 0.02	0.09

Table 12. Phenotype characteristics of obese swine

		Dobutamine					Treatment
		Baseline	0.3	1	3	10	
Systolic Pressure	Saline	93 ± 7	96 ± 9	99 ± 8	104 ± 9	107 ± 10	P = 0.38
(mmHg)	Liraglutide	95 ± 3	95 ± 1	94 ± 1	98 ± 4	101 ± 7	
Diastolic Pressure	Saline	64 ± 6	65 ± 6	67 ± 7	67 ± 5	68 ± 6	P = 0.22
(mmHg)	Liraglutide	64 ± 4	63 ± 3	62 ± 3	63 ± 3	61 ± 4	
Mean Pressure	Saline	77 ± 6	77 ± 7	80 ± 7	81 ± 6	82 ± 7	P = 0.45
(mmHg)	Liraglutide	77 ± 3	77 ± 2	77 ± 2	78 ± 3	77 ± 4	
Heart Rate	Saline	77 ± 13	80 ± 14	89 ± 17	116 ± 22	145 ± 17*	P = 0.004
(bpm)	Liraglutide	106 ± 11	119 ± 14	122 ± 15	144 ± 13	162 ± 16	
End Diastolic	Saline	100 ± 13	88 ± 11	88 ± 16	74 ± 16	55 ± 11*	P = 0.05
Volume (mL)	Liraglutide	83 ± 8	78 ± 10	74 ± 8	61 ± 5	47 ± 4	
End Systolic	Saline	56 ± 14	57 ± 15	59 ± 16	49 ± 11	39 ± 7	P = 0.04
Volume (mL)	Liraglutide	46 ± 5	45 ± 5	43 ± 4	38 ± 4	31 ± 4	
SV	Saline	44 ± 4	30 ± 4	29 ± 3	25 ± 7	16 ± 5*	P = 0.74
(mL)	Liraglutide	36 ± 6	33 ± 6	31 ± 6	23 ± 3	17 ± 2*	
CO	Saline	3298 ± 446	2273 ± 220	2529 ± 444	2854 ± 978	2550 ± 844	P = 0.02
(mL)	Liraglutide	4594 ± 778	3871 ± 735	3713 ± 734	3310 ± 592	3029 ± 322	
Ejection Fraction	Saline	48 ± 9	39 ± 10	38 ± 9	36 ± 8	28 ± 6	P = 0.57
%	Liraglutide	43 ± 4	42 ± 4	40 ± 4	38 ± 4	37 ± 4	
CT	Saline	53 ± 2	57 ± 4	49 ± 5	43 ± 4	43 ± 4	P = 0.34
(msec)	Liraglutide	66 ± 8	59 ± 8	55 ± 8	44 ± 4*	37 ± 2*	
RT	Saline	142 ± 16	104 ± 18*	131 ± 14	113 ± 13	96 ± 9*	P = 0.11
(msec)	Liraglutide	121 ± 5	120 ± 4	112 ± 4	97 ± 4	83 ± 6*	
dPmax	Saline	1204 ± 157	1230 ± 170	1548 ± 250	2350 ± 403*	3071 ± 574*	P = 0.40
(mmHg/sec)	Liraglutide	1599 ± 92	1535 ± 92	1577 ± 162	2271 ± 239	3105 ± 439*	
dPmin	Saline	-858 ± 66	-832 ± 138	-955 ± 193	-1126 ± 235	-1379 ± 178	P = 0.001
(mmHg/sec)	Liraglutide	-1181 ± 122	-1214 ± 111	-1215 ± 130	-1493 ± 128	-1816 ± 263*	
Tau 1/2	Saline	32 ± 2	29 ± 3	33 ± 4	30 ± 4	23 ± 2	P = 0.03
(msec)	Liraglutide	30 ± 3	29 ± 1	28 ± 1	23 ± 1†	18 ± 3*	
Tau 1/e	Saline	22 ± 2	20 ± 2	23 ± 3	22 ± 3	16 ± 2	P = 0.03
(msec)	Liraglutide	21 ± 2	20 ± 1	19 ± 1	15 ± 1†	12 ± 2*	

Table 13. Effects of liraglutide therapies on hemodynamic and cardiac parameters.

Change in:		Dobutamine					Treatment
		Baseline	0.3	1	3	10	
Δ Heart Rate (bpm)	Saline	0 ± 0	3 ± 3	12 ± 8	36 ± 14	67 ± 8	P = 0.44
	Liraglutide	0 ± 0	28 ± 25	31 ± 26	53 ± 25	48 ± 13	
Δ End Diastolic Volume (mL)	Saline	0 ± 0	-12 ± 4	-13 ± 8	-26 ± 10*	-45 ± 9*	P = 0.18
	Liraglutide	0 ± 0	-5 ± 3	-8 ± 2	-21 ± 6*	-35 ± 9*	
Δ End Systolic Volume (mL)	Saline	0 ± 0	1 ± 1	3 ± 3	-7 ± 4	-17 ± 7*	P = 0.47
	Liraglutide	0 ± 0	-2 ± 1	-3 ± 2	-8 ± 3	-15 ± 5*	
Δ SV (mL)	Saline	0 ± 0	-14 ± 4	-15 ± 6	-19 ± 10*	-28 ± 9*	P = 0.03
	Liraglutide	0 ± 0	-3 ± 2	-6 ± 2	-13 ± 4	-20 ± 5*	
Δ CO (mL)	Saline	0 ± 0	-1025 ± 313	-768 ± 253	-444 ± 685	-747 ± 801	P = 0.32
	Liraglutide	0 ± 0	-722 ± 346	-880 ± 350	-1284 ± 601	-1564 ± 594	
Δ Ejection Fraction %	Saline	0 ± 0	-9 ± 2	-10 ± 3	-12 ± 7	-19 ± 11*	P = 0.006
	Liraglutide	0 ± 0	-2 ± 1	-3 ± 2	-5 ± 2	-7 ± 2†	
Δ ESPVR (mmHg/mL)	Saline	0 ± 0	2 ± 1	6 ± 2	4 ± 2	6 ± 3	P = 0.12
	Liraglutide	0 ± 0	2 ± 1	7 ± 2	9 ± 2	18 ± 7†*	
Δ V_0 (mL)	Saline	0 ± 0	12 ± 7	16 ± 4	6 ± 9	0 ± 6	P = 0.88
	Liraglutide	0 ± 0	7 ± 3	10 ± 5	12 ± 4	8 ± 3	

Table 14. Change in Hemodynamic Parameters presented in Table 13. Significantly different changes in Stroke Volume and Ejection Fraction are depicted in Figure 19.

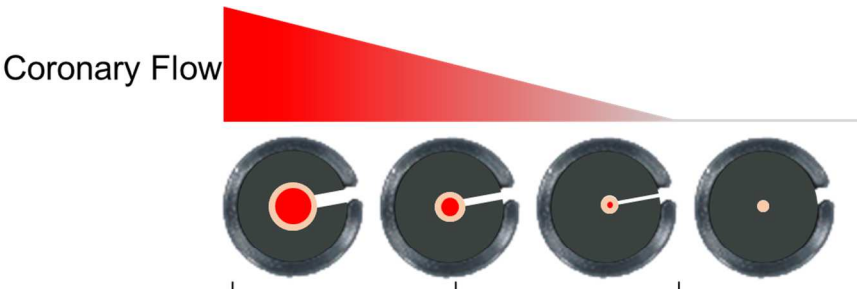

Week #	1	2	3	4
Liraglutide dose (or equivalent volume saline)	0.005 mg/kg/day	0.010 mg/kg/day	0.015 mg/kg/day	0.015 mg/kg/day

Figure 16. Illustration of approximate ameroid closure and liraglutide dosing during the duration of the experimental protocol.

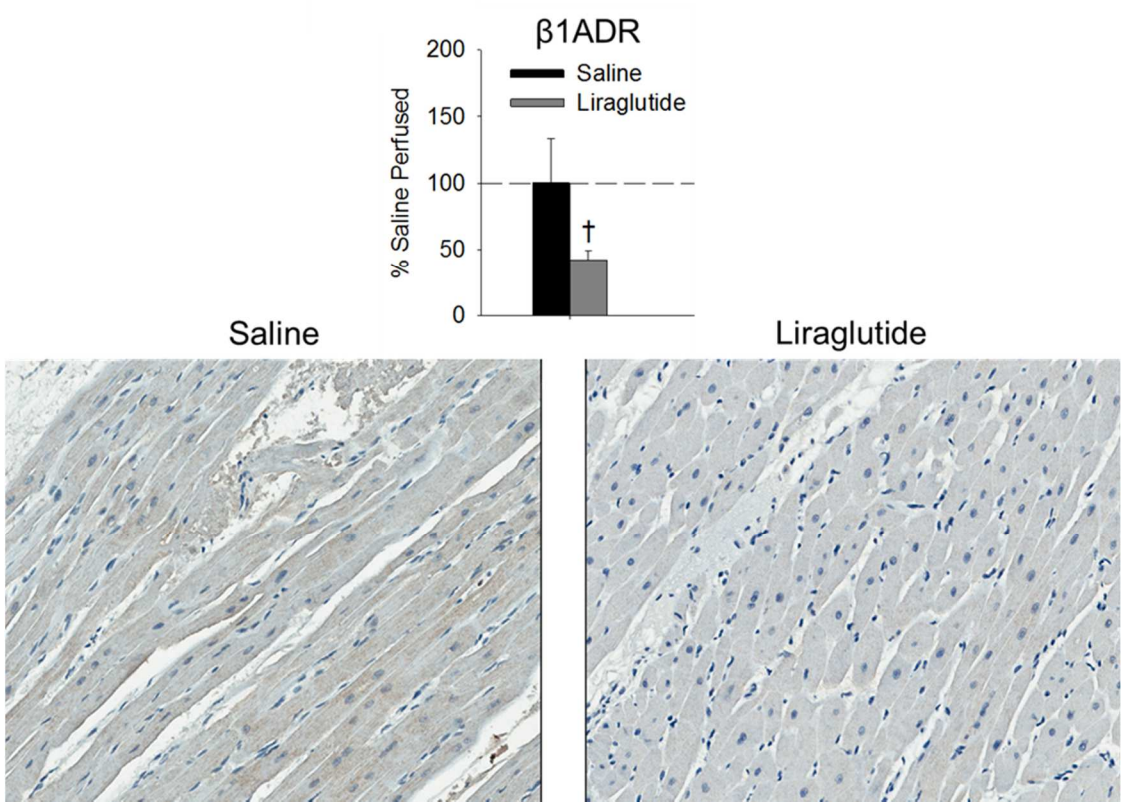

Figure 17. Representative transmural sections of left ventricle. White tissues within the myocardium were not stained, representing infarcted tissue. No difference in infarct was detected as a % of total left ventricular area.

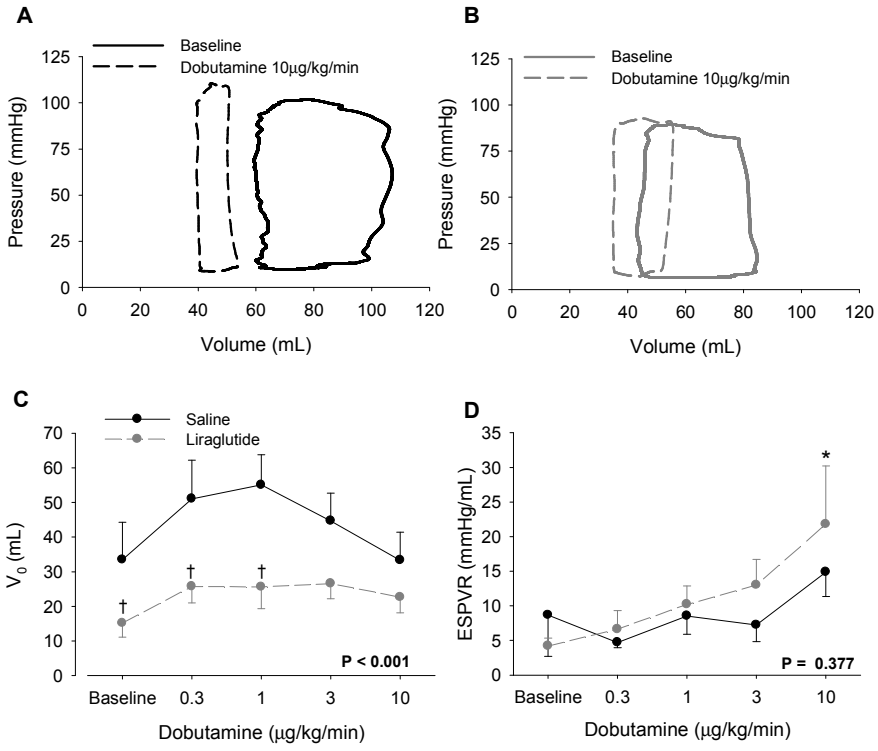

Figure 18. Panels A and B show representative PV loops from saline treated (A) and liraglutide treated (B) swine at baseline (solid) and at 10μg/kg/min dobutamine (broken). C) liraglutide treatment was associated with lower V_0 ($P < 0.001$ for treatment effect). D) Liraglutide treated swine hearts had greater contractility relative to untreated swine at the maximum dose of dobutamine, but no overall treatment effect was detected ($P = 0.377$). † = $P<0.05$ for vs tx at same time point ; * = $P<0.05$ relative to baseline same tx.

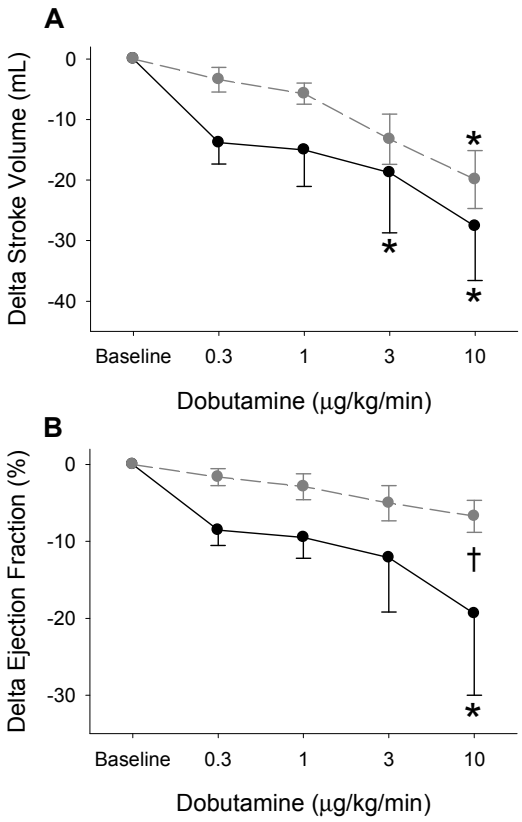

Figure 19. These graphs show change in stroke volume (A) and ejection fraction (B) over the course of the dobutamine challange. Stroke volume decreased in both groups. Dobutamine significantly reduced ejection fraction saline swine, while liraglutide diminished the reduction. * = P<0.05 dob dose relative baseline; † = P< 0.05 tx relative to saline; A. p value for tx = 0.029; B. P value for tx = 0.006.

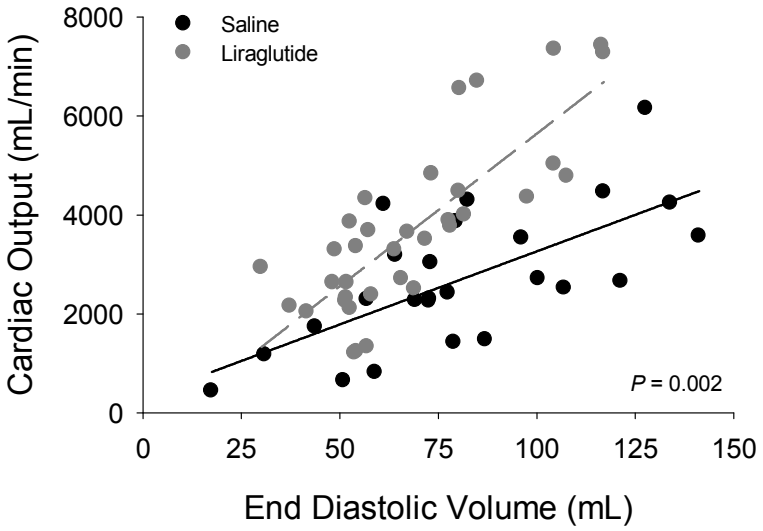

Figure 20. When data for each animal are included across all experimental time points, liraglutide was associated with greater cardiac output at a given end diastolic volume (P = 0.002 for ANCOVA tx effect).

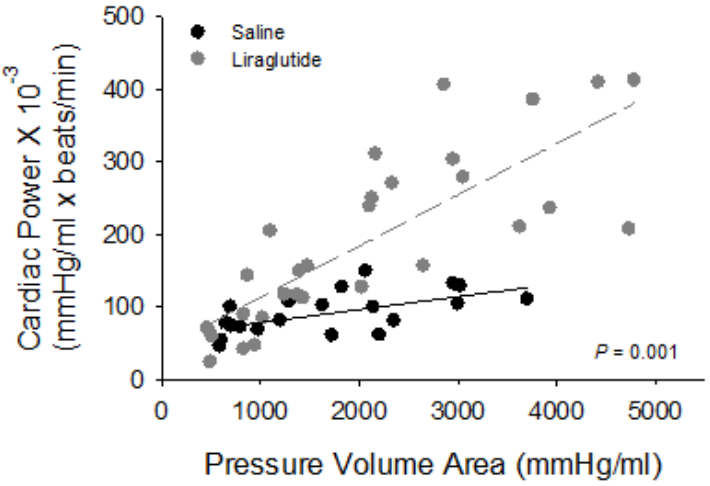

Figure 21. The slope of the relationship between cardiac power and PVA was higher in liraglutide treated swine hearts. As PVA provides an index for cardiac O_2 consumption, we see that liraglutide increased cardiac work at a given level of cardiac energetics. Thus, liraglutide increased cardiac efficiency. P value is ANCOVA tx effect. P = 0.02 for homogeneity of regressions.

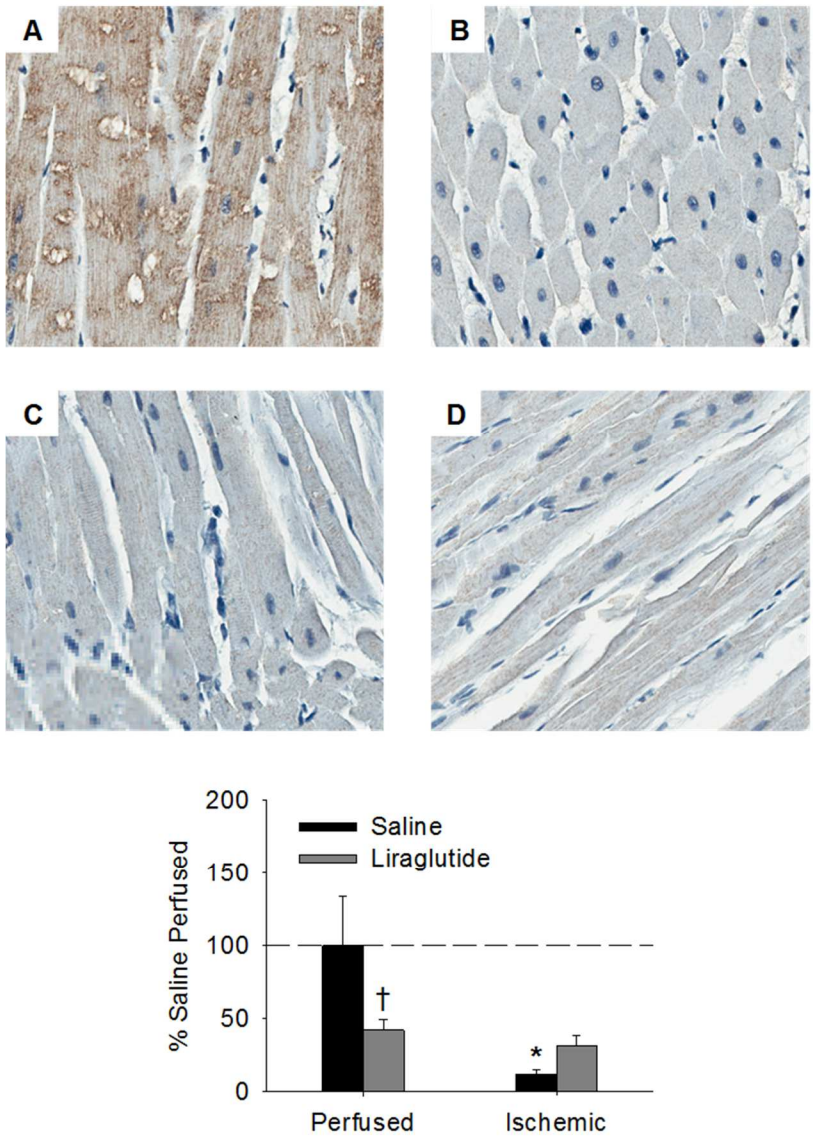

Figure 22. β1ADR expression was reduced in left ventricle of obese swine due to liraglutide and ischemia. Images A-D show representative left ventricular myocardial staining for β1ADR. A) saline treated, normally perfused, B) liraglutide treated, normally perfused, C) saline treated, ischemic, D) liraglutide treated, ischemic. † = $p<0.05$ vs. tx same condition. * = $p<0.05$ vs. condition same tx

Chapter 4: Discussion and Implications, Future Directions

Discussion and Implications

Ample clinical and epidemiological evidence supports that obesity increases the risk of development, and severity of cardiovascular disease. Additional data is emerging that supports that obesity changes cardiac responses to pathologic and pharmacologic stimuli, but they remain poorly characterized/understood with regards to both physiology and mechanism. Prior work in our lab has revealed that in humans ObM impairs cardiac metabolic responses to GLP-1[124]. Little is known about whether the discrepancy in GLP-1 effects extend to cardiac function. This work presents data that begins to address the aforementioned gaps that remain in literature: 1) does ObM alter cardiac functional response to ischemia/reperfusion, 2) are cardiac functional responses to I/R altered by GLP-1 mimetics, and are the responses similar in lean and obese animals, 3) does obesity modify cardiac microRNA and protein expression to GLP-1 mimetics and in the setting of I/R, 4) does treatment with GLP-1 mimetics reduce infarct in obese animals 5) does GLP-1 produce cardiac functional differences in the obese ischemic heart. Questions 1, 2, and 3 were assessed in aim 1 (chapter 2), while questions 4 and 5 were investigated in aim 2 (chapter 3).

Aim 1. Determine the effects of obesity on the cardiac functional response to ischemia/reperfusion and/or glucagon like peptide-1 (GLP-1) receptor activation, and screen for underlying microRNA and protein changes.

The goal of this work was to elucidate whether obesity alters cardiac function, injury and molecular responses to GLP-1 therapeutics in the setting of

ischemia. We hypothesized that obesity will alter cardiac functional responses to GLP-1 and I/R, and furthermore, that underlying these differences are associated changes in miR and protein expression.

To investigate this aim, lean and obese Ossabaw swine were given 24 hours of intra-venous saline or exendin-4 (30 fmol/kg/min), a GLP-1 receptor agonist. An open chest (thoracotomy) model was used to investigate cardiac function at baseline and during acute ischemia-reperfusion. Myocardial biopsies were taken at the conclusion of the open chest procedure from both normally perfused and ischemia-reperfusion territory of the left ventricle. Protein and total RNA were isolated from the samples and used for molecular screens using mass spectrometry and miR microarray.

1) Does ObM alter cardiac functional response to ischemia with reperfusion? Chapter 2 (Figure 10 and Figure 11) presents highly sensitive, direct measures of left ventricular pressure and volume in lean and obese swine. They illustrate that obese and lean swine respond oppositely to I/R. During reperfusion, hearts of lean swine tended to reduce cardiac filling and generate lower systolic pressures, consistent with myocardial stunning. PV loops of obese swine during I/R PV-loops show a right shift (increase in EDV) and ability to maintain LV systolic pressure.

2) Does obesity alter cardiac functional responses to GLP-1 mimetics (exendin-4) at baseline and in response to I/R? In addition to showing that obesity changes cardiac response to I/R in chapter 2, we also demonstrated that obesity alters the effect of exendin-4 on left ventricular function in the setting of I/R

(Figure 10 and Figure 11). During reperfusion, exendin-4 treatment was associated with elevated left ventricle filling volumes and pressures relative to saline treated lean swine. This suggests that exendin-4 is able to use increased diastolic filling to increase pressure via a volume-dependent (Frank-Starling) mechanism. However, during reperfusion, exendin-4 treatment drove reductions in EDV, without diminishing pressure generation (Figure 10) relative to saline treated obese swine. This supports that EX-4 increased cardiac contractility (greater pressure generation at a given EDV) compared with saline treatment in obese swine. Thus, this remarkable set of observations support distinct cardiac functional effects of exendin-4 on response to I/R dependent on obesity status.

3) **Does obesity modify cardiac microRNA and protein expression to GLP-1 mimetics and in the setting of I/R?** Molecular screens were employed to assess the overall differences in myocardial miR and protein expression as a function of obesity and, importantly, how obesity altered response to the GLP-1 mimetic exendin-4. Upon conclusion of physiological experiments, the animal was sacrificed and left ventricular myocardial biopsies were sampled from the normally perfused and I/R territories of each heart. MiR microarray and protein mass spectrometry revealed significant obesity associated alterations in expression of myocardial miR (Figure 14, Figure 15) and protein expression (Figure 12, Figure 13) were identified. Overall many more miRs were altered in the myocardium of obese groups relative to lean saline normally perfused levels. Importantly, exendin-4 had nearly exclusive effects on miR expression in obese compared to lean organisms. While no individual miR was investigated in further detail, the findings

within this work are among the first to demonstrate that miR responses to I/R are dependent on metabolic status (obesity), and treatment with therapeutics (exendin-4).

Obesity was also associated with extensive protein expression differences. Protein quantification revealed significant differences in nearly every category of myocardial cellular physiology, including: metabolism, mitochondrial function, cell structure/extracellular matrix/cell adhesion, cell proliferation/survival/death, calcium handling (Figure 12), and contractile/motor proteins. Importantly, the abundances of these proteins were differently impacted by exendin-4 in obese vs. lean hearts. While this work cannot reveal the mechanisms describing cause or consequence of these changes, novel targets emerge for further investigation. For example, myocardial titin and calcium handling proteins (Figure 12) provide possible, and relatively unexplored targets for investigation of the obesity mediated differences in cardiac pathologic and pharmacologic response.

The importance of these molecular findings should not be dismissed due to lack of causal links. The work presented in chapter 2 shows that current efforts to investigate the mechanism of GLP-1 and I/R (as well as many related diseases and therapeutics) fail to consider that obesity globally changes tissue level genetic expression/regulation in response to pathologic and pharmacologic stimuli; these molecular changes are associated with concurrent, clinically significant and fundamentally distinct cardiac functional responses.

Aim 1 Implications

The findings presented in chapter 2 (aim 1), if found to be true in humans, could have considerable implications both for future I/R and GLP-1 related basic science research, as well as clinical practice. Investigations seeking to interrogate cardiac functional responses to I/R (and related phenomena such as stunning, preconditioning, postconditioning), and search for cardioprotective therapeutics are typically performed on otherwise healthy organisms[120, 266, 267]. The data presented within chapter 2 demonstrating differential cardiac (physiologic and pharmacologic) response due to underlying metabolic disease, implies that investigators examining ischemic disease and/or GLP-1 response must take underlying metabolic status into account when proposing, designing and interpreting "translational" research. Of course, not only overweight/obese people have myocardial infarctions and CVD. This begs the question as to whether CVD should be approached as the same pathology in lean and obese humans.

The data within chapter 2 suggests that our current efforts to apply a "one size fits all" recipe for producing studies aiming to discover or assess mechanism or therapy associated with I/R and cardioprotection are likely dependent on underlying metabolic state of the model used. Similarly, differential response to I/R may suggest a clinical need for alternative post-MI treatment of lean compared with obese humans. For example, as only lean swine groups displayed functional cardiac responses suggesting myocardial stunning, are beta blockers (currently part of standard post-MI therapy[268]) of equal utility in lean and obese swine? Would beta blockers depress cardiac function further and reduce contractility leading to

impaired systemic blood delivery? Additional studies are needed to assess outcomes following the differences observed lean vs. obese swine.

Aim 2. Investigate the potential for GLP-1R activation to influence cardiac function at rest and in response to β1-adrenergic receptor (β1ADR) stimulation in an obese swine model of ischemic heart disease.

Ameroid constrictors were placed on the left anterior descending (LAD) artery of obese Ossabaw swine in a sterile, open-chest procedure. Ameroid constrictors produce a slowly developing (over the course 2 weeks), complete/unrelieved coronary occlusion. Following ~30 days of treatment with either saline, or the GLP-1 mimetic liraglutide (0.015 mg/kg/day), an open-chest procedure was performed in which we assessed whether liraglutide augments sympathetic mediated increases in cardiac contractility and improve efficiency of obese hearts following complete coronary occlusion and regional myocardial infarction. Furthermore, *ex vivo* investigations elucidate the impact of liraglutide treatment on infarct development, β1ADR expression, and titin in the infarcted and normally perfused myocardium.

4) Does treatment with GLP-1 mimetics reduce infarct resulting from unrelieved LAD ischemia in obese swine?

Ameroid constrictors were surgically implanted in obese, age-matched, ossabaw swine. Liraglutide treatment began on the day of the sterile procedure in which the ameroids were surgically implanted on the LAD. Thus, as the collagen ring in ameroid absorbed water over the course of 2 weeks both the normally perfused and ischemic territories were exposed to saline or liraglutide. Following

an additional two weeks (during which complete ameroid closure produced unrelieved ischemia of LAD perfusion territory), and a dobutamine challenge, hearts were stained for infarcted area. Figure 17 in chapter 3 illustrates the results of this experiment. Liraglutide did not reduce the volume of infarcted left ventricle compared with saline treated animals. This finding is not unexpected as the ischemia was both complete and unrelieved. Research reporting cardioprotective effects of GLP-1 mimetics often do not utilize models of unrelieved ischemia [120, 256, 257, 269-272]. However, the use of unrelieved ischemia allowed for assessment of functional effects of GLP-1 on the normally perfused myocardium.

5) Does GLP-1 produce cardiac functional differences in the obese ischemic heart? Approximately 30 days after ameroid placement pigs were anesthetized for an open-chest procedure in which cardiac function was measured at baseline and during dobutamine stress test using admittance pressure-volume catheter technology. No differences were detected in baseline function. Several important differences emerged during dobutamine dose response. Despite unchanged infarct volume of the left ventricle, liraglutide treatment increased cardiac contractility (Table 13, Figure 20), and improved diastolic function in obese swine. Additionally, Figure 21 shows that liraglutide treatment increased cardiac efficiency (more work performed at a given level PVA). As PVA is a metric of oxygen consumption[214, 273], these changes in cardiac contractility were produced independent of O_2 consumption. To probe potential involvement of inotropy mediated by adrenergic signaling, immunohistochemical analysis of β1ADR expression was performed in biopsies of both the normally perfused and infarcted

regions of the left ventricle (Figure 22). In the normally perfused territory, liraglutide was associated with a significant decrease in in staining for β1ADR. Also, a significant reduction in β1ADR staining was detected in infarcted regions of both treatment groups.

Aim 2 Implications

The findings of the experiments within chapter 2 are particularly provocative. These data are the first volume independent measures of contractile function during I/R in a large animal model of obesity receiving GLP-1 mimetics. They demonstrate that, in obese swine, liraglutide was not able to reduce infarct in unrelieved ischemia, but was able to increase efficiency of surviving myocardium under sympathomimetic stress. Interestingly, these increases in cardiac contractility seem to be independent myocardial β1ADR expression (the receptor that mediates the classic inotropic activation of sympathetic activation). These important findings contribute to the growing body of knowledge supporting that cardiovascular effects of GLP-1 require a stress (ischemia[129, 242], adrenergic challenge, etc.) to manifest.

These findings may have significant clinical implications. First, excess β1ADR signaling is a known mediator of cardiac hypertrophy and eventual heart failure[274] (hence the use of beta blockade in post MI management[268], as well as in heart failure[263]). Thus, liraglutide associated reductions in β1ADR expression in surviving myocardium may contribute to reduction in cellular signaling promoting hypertrophy, decline in cardiac function, and eventual progression towards heart failure[263, 274] as is common post-MI[275]. However, our data suggests additional

benefit conferred by liraglutide treatment in that independent of adrenergic signaling, it increased cardiac diastolic function, contractility and efficiency in the setting of pathologies associated with impaired cardiac function.

Future Directions

The results of these studies demonstrate novel effects of GLP-1 mimetics on cardiac function, gene regulation, and protein expression. The nature of these works have generated many questions (Figure 23). One pressing question that emerges when considering the differential effects of GLP-1 on lean and obese swine is whether the alterations in cardiovascular function and molecular expression observed during reperfusion confer any long term benefit or detriment to the recovering heart, as well as to the animal as a whole.

By combining elements of the protocols used in chapters 2 and 3 investigation of GLP-1 effects on load-independent cardiac function post-MI can be performed. To accomplish this, age matched lean and obese Ossabaw swine on diet for 6 months would undergo an initial sterile surgery in which implantation of catheters for aortic, jugular central line, and interventricular blood sampling cannulas, a Fogerty venous catheter placed in the IVC, as well as telemetry (Transonic) devices containing leads for admittance pressure volume catheters, coronary flow probes on the LAD and left circumflex artery, and systemic pressure would precede baseline recordings, a 30 minute left coronary artery coronary occlusion followed by subsequent closure of the surgical site and recovery.

On the day of surgery, during the 30 minute coronary occlusion, pigs would begin receiving once daily injections of either saline or liraglutide for 30 days. As

we cannot predict when a person will have a MI, this study is analogous to starting a patient on liraglutide when they show up to the hospital with a MI. Telemetry would allow for monitoring of multiple cardiac functional (including load independent cardiac contractility), hemodynamic, cardiac metabolic (via arterial vs. coronary venous plasma analysis), and circulating miR/hormone measures at various time points (even multiple times a day). The use of telemetry would also facilitate the addition of exercise or adrenergic stress tests (drug infusion via jugular central line) for intermediary functional measures during healing. Cardiac catheterization lab procedures would allow sampling of left ventricular tissue via endomyocardial biopsy. This tissue could be used for microRNA and protein analysis.

On day 30 swine would be anesthetized for terminal open chest procedure. After baseline recordings, a 30 minute circumflex coronary artery ischemic period would ensue. Following 2 hours of reperfusion, a final dobutamine challenge (as in the methods described in chapter 3). These final steps would provide slightly unrelated, but clinically relevant data, shedding light on GLP-1 mimetics' ability to improve cardiac function in patients who remain high risk individuals for additional coronary vascular disease after they have already had an MI (similar to preconditioning, though this timeline would not be considered "preconditioning" *per se*). The results and whether obesity altered the efficacy would potentially have important implications for patients at risk for CVD. Upon sacrifice, LV myocardium could also be used for additional analyses including GLP-1 receptor identification (described later), and for myocyte dispersions for calcium imaging analysis[230, 276].

The use of Ossabaw swine would be advantageous in that calcium handling and receptor differences in obese vs. lean state could be probed.

This procedure, while very complex and expensive, would provide much needed temporal understanding of functional outcomes associated with GLP-1 agonism post I/R. Periodic tissue samples would provide a much needed picture of how GLP-1 alters miR and protein regulation over time as healing occurs in the I/R region, as well as adaptation occurs in the normally perfused region.

The data in chapter 2 show that molecular response to GLP-1 in the heart appear to be highly variable and dependent on physiological/pharmacological context. Methodical studies are needed to distinguish cause from effect. As GLP-1 receptor(s) and localization are not well described, attempting to ascribe meaning (causal relationships) to single factors within the multitude of molecular changes, then decipher the effect of a single factor on gross functional outcomes within a complex/adapting system seems premature. First, there is need for more research into the binding partners of GLP-1 and related synthetic therapeutics. In order to better characterize binding partners we propose using variants of affinity chromatography to discover binding partners. First gentle cell disruption (non-denaturing and without detergent) and cellular fractionation techniques would allow separation of nuclear, mitochondrial, cytosolic and membrane bound proteins from swine myocardium. The individual fractions could then be washed over biotinylated GLP-1 (Anaspec) (ideally the same experiment would be repeated using various GLP-1 mimetics) bound to streptavidin beads, thus accomplishing a GLP-1-pulldown. After washing beads, eluting off bound proteins,

and performing mass spectrometry for protein identification, the resulting proteins identified should, in theory, be capable of binding GLP-1. This protocol would yield different results dependent on immobilization techniques and strength of binding of GLP-1 and targets. Using a variety of conditions for each cellular fraction should yield protein database with putative binding partners of GLP-1 within each fraction. An advantage to this approach is that it allows discovery of proteins that can bind GLP-1 mimetics in each fraction, thus shedding light into the hypothesized intracellular and even nuclear GLP-1 actions[277].

These findings could be confirmed biochemically using surface plasmon resonance[278]. This technique allows for immobilization of one binding partner (a recombinant version of predicted GLP-1 binding protein discovered via mass spectrometry) to a gold membrane. Lasers are reflected off of the underside of the gold foil membrane and reflect into a detector. Using microfluidics predicted GLP-1 or GLP-1 therapeutics would be washed over the membrane. As GLP-1 moves across the foil, events in which GLP-1 binds an immobilized protein produces changes in the detected laser light. The changes in detection are related to the duration of binding, thus these changes, along with using known concentrations of soluble and immobilized target, allow for determination of binding kinetics[278]. It is important to note that surface plasmon resonance has been applied to membrane bound proteins[278] and could characterize binding kinetics of various membrane bound proteins including putative membrane bound receptors.

Through the date of publication of this work, attempts to define mechanism have been convoluted by lack of a piecemeal approach in what appears to be an

abandonment of meticulous basic science methodology. Instead, attempts seem to favor uncoordinated and experimentally inconsistent approaches to find “THE” responsible factor - a sort of ‘Holy Grail’ quest. Often these studies succeed in identifying alterations in a “mechanistic component” in the search for translational end points (understandably so, as it is a near prerequisite for funding in the current climate of research). However, these findings pile up and have resulted in context-specific (often contradictory) and ultimately non-integrable body of knowledge.

It is possible that slow and steady science might “win” the translational race. Identification of GLP-1 binding proteins would provide insight into putative GLP-1 mechanisms (Figure 24). Following receptor characterization, systematic approaches could be taken to discover the mechanisms of direct cardiac effects of GLP-1s. Once the mechanism of action is characterized, hypothesis driven investigations of obesity-associated perturbations of the already known mechanism could follow.

Chapter 4 Figures

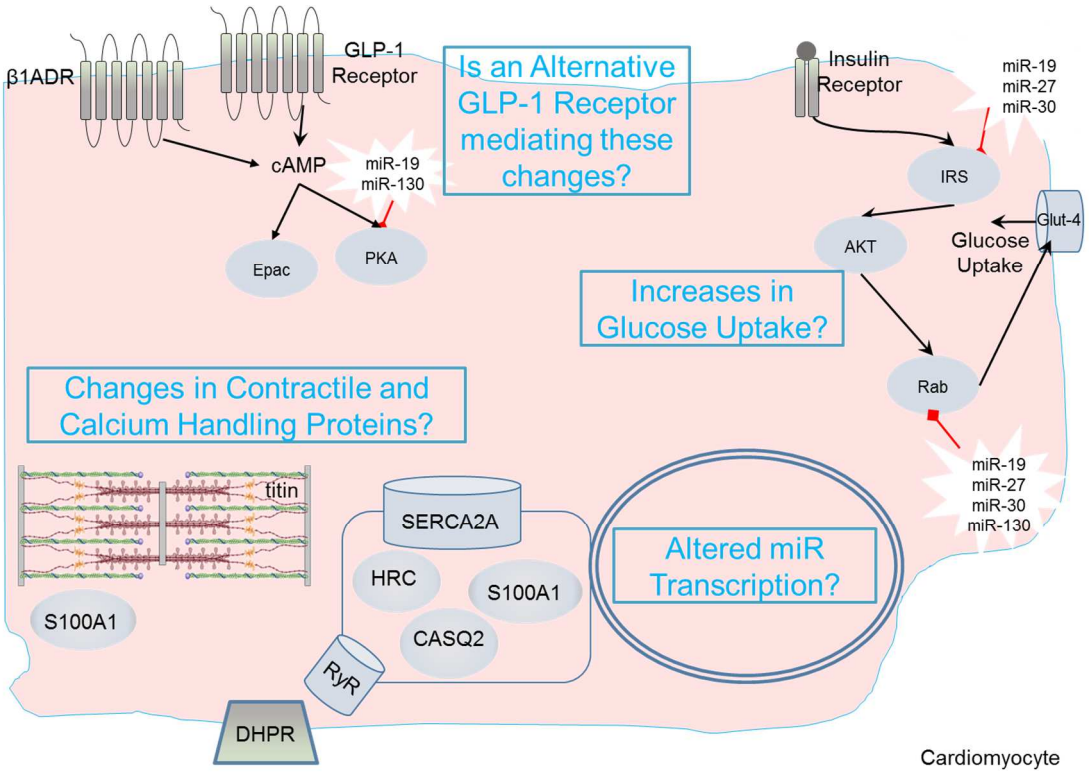

Figure 23. Many questions remain in a complex, interrelated system. Deciphering the direct cardiac effects of GLP-1 and how they are changed by obesity will take systematic and methodical approaches. Several questions are highlighted in this figure that are not classically explained by GPCR (i.e the canonical GLP-1 receptor) action. Prior investigations by Moberly et al. showed that GLP-1 can increase glucose uptake in humans and were associated with increased P38 activity. However, the end effector for this increase is still unknown. Other questions remain: how does GLP-1 alter regulation of calcium handling and contractile proteins (chapter 2 Figure 12). how does miR regulation change over time, and how do they modulate disease progression? Is a second GLP-1 receptor

mediating these changes? One key question not represented in this figure is of the utmost importance: how does obesity change this system and drug effects?

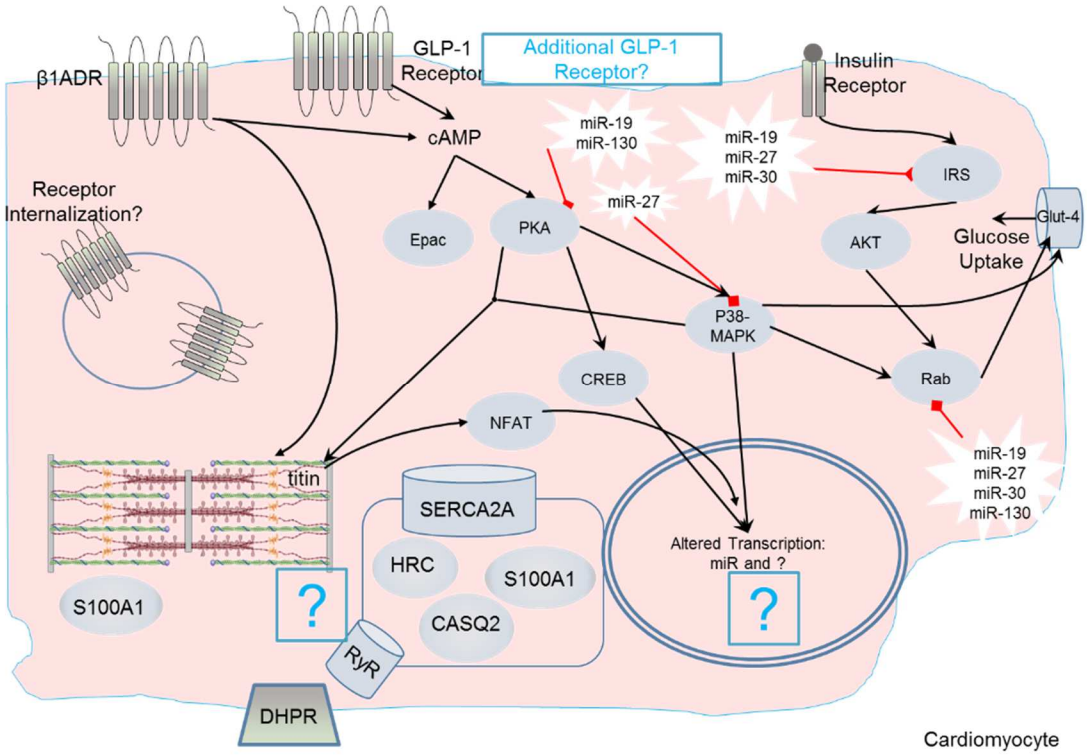

Figure 24. Many target pathways may be involved in GLP-1 effect. Characterizing the unknown “second receptor” may allow for clarification of key pathways mediating the new effects of GLP-1 highlighted by this work (changes in calcium handling proteins, miR regulation, and sarcomeric proteins).

References

1. Ogden CL, Carroll MD, Kit BK and Flegal KM. Prevalence of childhood and adult obesity in the United States, 2011-2012. *Jama*. 2014;311:806-14.
2. Haffner SM. The Metabolic Syndrome: Inflammation, Diabetes Mellitus, and Cardiovascular Disease. *The American Journal of Cardiology*. 2006;97:311.
3. Grundy SM, Brewer HB, Jr., Cleeman JI, Smith SC, Jr., Lenfant C, American Heart A, National Heart L and Blood I. Definition of Metabolic Syndrome Report of the National Heart, Lung, and Blood Institute/American Heart Association Conference on Scientific Issues Related to Definition. *Circulation*. 2004;109:433-438.
4. Report NDS. National Diabetes Statistics Report: Estimates of Diabetes and Its Burden in the United States, 2014. *PharmacoEconomics & Outcomes News*. 2014.
5. Bennett BJ ea. Nutrition and the science of disease prevention: a systems approach to support metabolic health. - PubMed - NCBI. 2016.
6. Prospective Studies C, Whitlock G, Lewington S, Sherliker P, Clarke R, Emberson J, Halsey J, Qizilbash N, Collins R and Peto R. Body-mass index and cause-specific mortality in 900 000 adults: collaborative analyses of 57 prospective studies. *Lancet*. 2009;373:1083-96.
7. Grundy SM. Metabolic syndrome: connecting and reconciling cardiovascular and diabetes worlds. *J Am Coll Cardiol*. 2006;47:1093-100.
8. Jeppesen J, Hansen TW, Rasmussen S, Ibsen H, Torp-Pedersen C and Madsbad S. Insulin Resistance, the Metabolic Syndrome, and Risk of Incident Cardiovascular Disease. *Journal of the American College of Cardiology*. 2007;49:21122119.
9. Galassi A, Reynolds K and He J. Metabolic Syndrome and Risk of Cardiovascular Disease: A Meta-Analysis. *The American journal of medicine*. 2006;119:812819.
10. Gami AS, Witt BJ, Howard DE, Erwin PJ, Gami LA, Somers VK and Montori VM. Metabolic syndrome and risk of incident cardiovascular events and death: a systematic review and meta-analysis of longitudinal studies. *J Am Coll Cardiol*. 2007;49:403-14.
11. Butler J, Rodondi N, Zhu Y, Figaro K, Fazio S, Vaughan DE, Satterfield S, Newman AB, Goodpaster B, Bauer DC, Holvoet P, Harris TB, de Rekeneire N, Rubin S, Ding J, Kritchevsky SB and Health ABCS. Metabolic Syndrome and the Risk of Cardiovascular Disease in Older Adults. *Journal of the American College of Cardiology*. 2006;47:15951602.
12. Thomsen M and Nordestgaard BG. Myocardial infarction and ischemic heart disease in overweight and obesity with and without metabolic syndrome. *JAMA internal medicine*. 2013;174:15-22.
13. Lakka HM, Laaksonen DE, Lakka TA, Niskanen LK, Kumpusalo E, Tuomilehto J and Salonen JT. The metabolic syndrome and total and cardiovascular disease mortality in middle-aged men. *Jama*. 2002;288:2709-16.

14. Belin de Chantemele EJ and Stepp DW. Influence of obesity and metabolic dysfunction on the endothelial control in the coronary circulation. *Journal of molecular and cellular cardiology*. 2012;52:840-847.
15. Bastien M, Poirier P, Lemieux I and Despres JP. Overview of epidemiology and contribution of obesity to cardiovascular disease. *Prog Cardiovasc Dis*. 2014;56:369-81.
16. Alpert MA, Lavie CJ, Agrawal H, Aggarwal KB and Kumar SA. Obesity and heart failure: epidemiology, pathophysiology, clinical manifestations, and management. *Transl Res*. 2014;164:345-56.
17. Carroll JF and Tyagi SC. Extracellular matrix remodeling in the heart of the homocysteinemic obese rabbit. *American journal of hypertension*. 2005;18:692-8.
18. Laakso M. Hyperglycemia and cardiovascular disease in type 2 diabetes. *Diabetes*. 1999.
19. Laukkanen JA, Makikallio TH, Ronkainen K, Karppi J and Kurl S. Impaired Fasting Plasma Glucose and Type 2 Diabetes Are Related to the Risk of Out-of-Hospital Sudden Cardiac Death and All-Cause Mortality. *Diabetes care*. 2012.
20. Inchiostro S, Fadini GP, de Kreutzenberg SV, Citroni N and Avogaro A. Is the Metabolic Syndrome a Cardiovascular Risk Factor Beyond Its Specific Components? *Journal of the American College of Cardiology*. 2007;49:2465.
21. Bridger T. Childhood obesity and cardiovascular disease. *Paediatr Child Health*. 2009;14:177-82.
22. Lauer MS, Anderson KM, Kannel WB and Levy D. The impact of obesity on left ventricular mass and geometry. The Framingham Heart Study. *Jama*. 1991;266:231-6.
23. Gates PE, Gentile CL, Seals DR and Christou DD. Adiposity contributes to differences in left ventricular structure and diastolic function with age in healthy men. *The Journal of clinical endocrinology and metabolism*. 2003;88:4884-90.
24. Crowley DI, Khoury PR, Urbina EM, Ippisch HM and Kimball TR. Cardiovascular impact of the pediatric obesity epidemic: higher left ventricular mass is related to higher body mass index. *J Pediatr*. 2011;158:709-714 e1.
25. Ballo P, Motto A, Mondillo S and Faraguti SA. Impact of obesity on left ventricular mass and function in subjects with chronic volume overload. *Obesity (Silver Spring)*. 2007;15:2019-26.
26. Lopaschuk GD, Ussher JR, Folmes CD, Jaswal JS and Stanley WC. Myocardial fatty acid metabolism in health and disease. *Physiol Rev*. 2010;90:207-58.
27. KE VSaB. Metabolic Flexibility and Dysfunction in Cardiovascular Cells. - PubMed - NCBI. 2016.
28. Li ZL and Lerman LO. Impaired myocardial autophagy linked to energy metabolism disorders. *Autophagy*. 2012;8:992-4.
29. Olea E, Agapito MT, Gallego-Martin T, Rocher A, Gomez-Niño A, Obeso A, Gonzalez C and Yubero S. Intermittent hypoxia and diet-induced obesity: effects on oxidative status, sympathetic tone, plasma glucose and insulin levels, and arterial pressure. 2014.
30. Bugger H and Abel ED. Molecular mechanisms of diabetic cardiomyopathy. *Diabetologia*. 2014;57:660671.

31. Poirier P, Giles TD, Bray GA, Hong Y, Stern JS, Pi-Sunyer FX, Eckel RH, American Heart A, Obesity Committee of the Council on Nutrition PA and Metabolism. Obesity and cardiovascular disease: pathophysiology, evaluation, and effect of weight loss: an update of the 1997 American Heart Association Scientific Statement on Obesity and Heart Disease from the Obesity Committee of the Council on Nutrition, Physical Activity, and Metabolism. *Circulation*. 2006;113:898-918.
32. TM LBaM. Diabetes and cardiovascular disease: Epidemiology, biological mechanisms, treatment recommendations and future research. - PubMed - NCBI. 2016.
33. Ertl G, Hu K, Bauer WR and Bauer B. The renin-angiotensin system and coronary vasomotion. *Heart*. 1996;76:45-52.
34. Magrini F, Reggiani P, Fratianni G, Morganti A and Zanchetti A. Coronary blood flow in renovascular hypertension. *Am J Med*. 1993;94:45S-48S.
35. Magrini F, Reggiani P, Paliotti R, Bonagura F, Ciulla M and Vandoni P. Coronary hemodynamics and the renin angiotensin system. *Clin Exp Hypertens*. 1993;15 Suppl 1:139-55.
36. Magrini F, Shimizu M, Roberts N, Fouad FM, Tarazi RC and Zanchetti A. Converting-enzyme inhibition and coronary blood flow. *Circulation*. 1987;75:I168-74.
37. Schindler TH, Cardenas J, Prior JO, Facta AD, Kreissl MC, Zhang XL, Sayre J, Dahlbom M, Licinio J and Schelbert HR. Relationship between increasing body weight, insulin resistance, inflammation, adipocytokine leptin, and coronary circulatory function. *J Am Coll Cardiol*. 2006;47:1188-95.
38. Barbosa JAA, Rodrigues AB, Mota CCC, Barbosa MM and Simões e Silva AC. Cardiovascular dysfunction in obesity and new diagnostic imaging techniques: the role of noninvasive image methods. *Vascular Health and Risk Management*. 2011;7:287-95.
39. Stern MP, Morales PA, Haffner SM and Valdez RA. Hyperdynamic circulation and the insulin resistance syndrome ("syndrome X"). *Hypertension*. 1992;20:802-8.
40. Reisin E and Jack AV. Obesity and hypertension: mechanisms, cardio-renal consequences, and therapeutic approaches. *Med Clin North Am*. 2009;93:733-51.
41. Huggett RJ, Burns J, Mackintosh AF and Mary DA. Sympathetic neural activation in nondiabetic metabolic syndrome and its further augmentation by hypertension. *Hypertension*. 2004;44:847-52.
42. Brilla CG. The cardiac structure-function relationship and the renin-angiotensin-aldosterone system in hypertension and heart failure. *Current opinion in cardiology*. 1994;9 Suppl 1:S2-10; discussion S10-1.
43. Viau DM, Sala-Mercado JA, Spranger MD, O'Leary DS and Levy PD. The pathophysiology of hypertensive acute heart failure. *Heart*. 2015;101:1861-7.
44. Korner PI and Jennings GL. Assessment of prevalence of left ventricular hypertrophy in hypertension. *Journal of hypertension*. 1998;16:715-23.
45. Iriarte MM, Perez Olea J, Sagastagoitia D, Molinero E and Murga N. Congestive heart failure due to hypertensive ventricular diastolic dysfunction. *Am J Cardiol*. 1995;76:43D-47D.

46. Mahajan R, Lau DH and Sanders P. Impact of obesity on cardiac metabolism, fibrosis, and function. *Trends in cardiovascular medicine*. 2015;25:119-26.
47. Antonini-Canterin F, Mateescu AD, Vriz O, La Carrubba S, Di Bello V, Carerj S, Zito C, Sparacino L, Marzano B, Usurelu C, Ticulescu R, Ginghina C, Nicolosi GL and Popescu BA. Cardiac structure and function and insulin resistance in morbidly obese patients: does superobesity play an additional role? *Cardiology*. 2014;127:144-51.
48. Russo C, Jin Z, Homma S, Rundek T, Elkind MS, Sacco RL and Di Tullio MR. Effect of obesity and overweight on left ventricular diastolic function: a community-based study in an elderly cohort. *J Am Coll Cardiol*. 2011;57:1368-74.
49. Wong CY, O'Moore-Sullivan T, Leano R, Byrne N, Beller E and Marwick TH. Alterations of left ventricular myocardial characteristics associated with obesity. *Circulation*. 2004;110:3081-7.
50. Ammar KA, Redfield MM, Mahoney DW, Johnson M, Jacobsen SJ and Rodeheffer RJ. Central obesity: association with left ventricular dysfunction and mortality in the community. *American heart journal*. 2008;156:975-81.
51. Mathew B, Francis L, Kayalar A and Cone J. Obesity: effects on cardiovascular disease and its diagnosis. *J Am Board Fam Med*. 2008;21:562-8.
52. Lopez-Jimenez F and Cortes-Bergoderi M. Update: systemic diseases and the cardiovascular system (i): obesity and the heart. *Revista espanola de cardiologia*. 2011;64:140-9.
53. Bray GA and Gallagher TF, Jr. Manifestations of hypothalamic obesity in man: a comprehensive investigation of eight patients and a reveiw of the literature. *Medicine (Baltimore)*. 1975;54:301-30.
54. Bray GA. Integration of energy intake and expenditure in animals and man: the autonomic and adrenal hypothesis. *Clin Endocrinol Metab*. 1984;13:521-46.
55. Bray GA. Autonomic and endocrine factors in the regulation of energy balance. *Fed Proc*. 1986;45:1404-10.
56. Peterson HR, Rothschild M, Weinberg CR, Fell RD, McLeish KR and Pfeifer MA. Body fat and the activity of the autonomic nervous system. *The New England journal of medicine*. 1988;318:1077-83.
57. Spraul M, Ravussin E, Fontvieille AM, Rising R, Larson DE and Anderson EA. Reduced sympathetic nervous activity. A potential mechanism predisposing to body weight gain. *The Journal of clinical investigation*. 1993;92:1730-5.
58. Young JB and Macdonald IA. Sympathoadrenal activity in human obesity: heterogeneity of findings since 1980. *International journal of obesity and related metabolic disorders : journal of the International Association for the Study of Obesity*. 1992;16:959-67.
59. Folkow B, Di Bona GF, Hjemdahl P, Toren PH and Wallin BG. Measurements of plasma norepinephrine concentrations in human primary hypertension. A word of caution on their applicability for assessing neurogenic contributions. *Hypertension*. 1983;5:399-403.
60. Mark AL, Victor RG, Nerhed C and Wallin BG. Microneurographic studies of the mechanisms of sympathetic nerve responses to static exercise in humans. *Circulation research*. 1985;57:461-9.

61. Scherrer U, Randin D, Tappy L, Vollenweider P, Jequier E and Nicod P. Body fat and sympathetic nerve activity in healthy subjects. *Circulation*. 1994;89:2634-40.
62. Grassi G, Seravalle G, Cattaneo BM, Bolla GB, Lanfranchi A, Colombo M, Giannattasio C, Brunani A, Cavagnini F and Mancia G. Sympathetic activation in obese normotensive subjects. *Hypertension*. 1995;25:560-3.
63. Grassi G, Dell'Oro R, Quarti-Trevano F, Scopelliti F, Seravalle G, Paleari F, Gamba PL and Mancia G. Neuroadrenergic and reflex abnormalities in patients with metabolic syndrome. *Diabetologia*. 2005;48:1359-65.
64. Grassi G, Seravalle G, Quarti-Trevano F, Dell'Oro R, Bolla G and Mancia G. Effects of hypertension and obesity on the sympathetic activation of heart failure patients. *Hypertension*. 2003;42:873-7.
65. Brunner EJ, Hemingway H, Walker BR, Page M, Clarke P, Juneja M, Shipley MJ, Kumari M, Andrew R, Seckl JR, Papadopoulos A, Checkley S, Rumley A, Lowe GD, Stansfeld SA and Marmot MG. Adrenocortical, autonomic, and inflammatory causes of the metabolic syndrome: nested case-control study. *Circulation*. 2002;106:2659-65.
66. Canale MP, Manca di Villahermosa S, Martino G, Rovella V, Noce A, De Lorenzo A and Di Daniele N. Obesity-related metabolic syndrome: mechanisms of sympathetic overactivity. *Int J Endocrinol*. 2013;2013:865965.
67. Knudson JD, Dincer UD, Bratz IN, Sturek M, Dick GM and Tune JD. Mechanisms of coronary dysfunction in obesity and insulin resistance. *Microcirculation*. 2007;14:317-38.
68. Thayer JF and Lane RD. The role of vagal function in the risk for cardiovascular disease and mortality. *Biol Psychol*. 2007;74:224-42.
69. Grassi G, Arenare F, Quarti-Trevano F, Seravalle G and Mancia G. Heart rate, sympathetic cardiovascular influences, and the metabolic syndrome. *Prog Cardiovasc Dis*. 2009;52:31-7.
70. Mathew V, Gersh BJ, Williams BA, Laskey WK, Willerson JT, Tilbury RT, Davis BR and Holmes DR, Jr. Outcomes in patients with diabetes mellitus undergoing percutaneous coronary intervention in the current era: a report from the Prevention of REStenosis with Tranilast and its Outcomes (PRESTO) trial. *Circulation*. 2004;109:476-80.
71. Malmberg K, Yusuf S, Gerstein HC, Brown J, Zhao F, Hunt D, Piegas L, Calvin J, Keltai M and Budaj A. Impact of diabetes on long-term prognosis in patients with unstable angina and non-Q-wave myocardial infarction: results of the OASIS (Organization to Assess Strategies for Ischemic Syndromes) Registry. *Circulation*. 2000;102:1014-9.
72. Haffner SM, Lehto S, Ronnemaa T, Pyorala K and Laakso M. Mortality from coronary heart disease in subjects with type 2 diabetes and in nondiabetic subjects with and without prior myocardial infarction. *The New England journal of medicine*. 1998;339:229-34.
73. Thourani VH, Weintraub WS, Stein B, Gebhart SS, Craver JM, Jones EL and Guyton RA. Influence of diabetes mellitus on early and late outcome after coronary artery bypass grafting. *Ann Thorac Surg*. 1999;67:1045-52.

74. Calafiore AM, Di Mauro M, Di Giammarco G, Contini M, Vitolla G, Iaco AL, Canosa C and D'Alessandro S. Effect of diabetes on early and late survival after isolated first coronary bypass surgery in multivessel disease. *The Journal of thoracic and cardiovascular surgery*. 2003;125:144-54.
75. Alserius T, Hammar N, Nordqvist T and Ivert T. Risk of death or acute myocardial infarction 10 years after coronary artery bypass surgery in relation to type of diabetes. *American heart journal*. 2006;152:599-605.
76. Akin I, Schneider H, Nienaber CA, Jung W, Lubke M, Rillig A, Ansari U, Wunderlich N and Birkemeyer R. Lack of "obesity paradox" in patients presenting with ST-segment elevation myocardial infarction including cardiogenic shock: a multicenter German network registry analysis. *BMC Cardiovasc Disord*. 2015;15:67.
77. Poncelas M, Inserte J, Vilardosa U, Rodriguez-Sinovas A, Baneras J, Simo R and Garcia-Dorado D. Obesity induced by high fat diet attenuates postinfarct myocardial remodeling and dysfunction in adult B6D2F1 mice. *Journal of molecular and cellular cardiology*. 2015;84:154-61.
78. Mourmoura E, Rigaudiere JP, Couturier K, Hininger I, Laillet B, Malpuech-Brugere C, Azarnoush K and Demaison L. Long-term abdominal adiposity activates several parameters of cardiac energy function. *J Physiol Biochem*. 2015.
79. Salie R, Huisamen B and Lochner A. High carbohydrate and high fat diets protect the heart against ischaemia/reperfusion injury. *Cardiovascular diabetology*. 2014;13:109.
80. Kalogeris T, Baines CP, Krenz M and Korthuis RJ. Cell biology of ischemia/reperfusion injury. *Int Rev Cell Mol Biol*. 2012;298:229-317.
81. Michiels C. Physiological and pathological responses to hypoxia. *Am J Pathol*. 2004;164:1875-82.
82. Frank A, Bonney M, Bonney S, Weitzel L, Koeppen M and Eckle T. Myocardial ischemia reperfusion injury: from basic science to clinical bedside. *Semin Cardiothorac Vasc Anesth*. 2012;16:123-32.
83. Yellon DM and Hausenloy DJ. Myocardial reperfusion injury. *The New England journal of medicine*. 2007;357:1121-35.
84. Shahzad T, Kasseckert SA, Iraqi W, Johnson V, Schulz R, Schluter KD, Dorr O, Parahuleva M, Hamm C, Ladilov Y and Abdallah Y. Mechanisms involved in postconditioning protection of cardiomyocytes against acute reperfusion injury. *Journal of molecular and cellular cardiology*. 2013;58:209-16.
85. Hausenloy DJ and Yellon DM. Myocardial ischemia-reperfusion injury: a neglected therapeutic target. *The Journal of clinical investigation*. 2013;123:92-100.
86. Hearse DJ and Tosaki A. Free radicals and reperfusion-induced arrhythmias: protection by spin trap agent PBN in the rat heart. *Circulation research*. 1987;60:375-83.
87. Rhodes SS, Camara AK, Heisner JS, Riess ML, Aldakkak M and Stowe DF. Reduced mitochondrial Ca2+ loading and improved functional recovery after ischemia-reperfusion injury in old vs. young guinea pig hearts. *Am J Physiol Heart Circ Physiol*. 2012;302:H855-63.

88. Arvanitis DA, Vafiadaki E, Sanoudou D and Kranias EG. Histidine-rich calcium binding protein: the new regulator of sarcoplasmic reticulum calcium cycling. *Journal of molecular and cellular cardiology*. 2011;50:43-9.
89. Qian T, Nieminen AL, Herman B and Lemasters JJ. Mitochondrial permeability transition in pH-dependent reperfusion injury to rat hepatocytes. *The American journal of physiology*. 1997;273:C1783-92.
90. Borutaite V, Jekabsone A, Morkuniene R and Brown GC. Inhibition of mitochondrial permeability transition prevents mitochondrial dysfunction, cytochrome c release and apoptosis induced by heart ischemia. *Journal of molecular and cellular cardiology*. 2003;35:357-66.
91. Lemasters JJ, Bond JM, Chacon E, Harper IS, Kaplan SH, Ohata H, Trollinger DR, Herman B and Cascio WE. The pH paradox in ischemia-reperfusion injury to cardiac myocytes. *EXS*. 1996;76:99-114.
92. Heusch G, Boengler K and Schulz R. Inhibition of mitochondrial permeability transition pore opening: the Holy Grail of cardioprotection. *Basic Res Cardiol*. 2010;105:151-4.
93. Vakeva AP, Agah A, Rollins SA, Matis LA, Li L and Stahl GL. Myocardial infarction and apoptosis after myocardial ischemia and reperfusion: role of the terminal complement components and inhibition by anti-C5 therapy. *Circulation*. 1998;97:2259-67.
94. Ma XL, Tsao PS and Lefer AM. Antibody to CD-18 exerts endothelial and cardiac protective effects in myocardial ischemia and reperfusion. *The Journal of clinical investigation*. 1991;88:1237-43.
95. Vinten-Johansen J. Involvement of neutrophils in the pathogenesis of lethal myocardial reperfusion injury. *Cardiovascular research*. 2004;61:481-97.
96. Shinde AV and Frangogiannis NG. Fibroblasts in myocardial infarction: a role in inflammation and repair. *Journal of molecular and cellular cardiology*. 2014;70:74-82.
97. Littlejohns B, Pasdois P, Duggan S, Bond AR, Heesom K, Jackson CL, Angelini GD, Halestrap AP and Suleiman MS. Hearts from mice fed a non-obesogenic high-fat diet exhibit changes in their oxidative state, calcium and mitochondria in parallel with increased susceptibility to reperfusion injury. *PloS one*. 2014;9:e100579.
98. Zhao SM, Wang YL, Guo CY, Chen JL and Wu YQ. Progressive decay of Ca2+ homeostasis in the development of diabetic cardiomyopathy. *Cardiovascular diabetology*. 2014;13:75.
99. Younce CW, Burmeister MA and Ayala JE. Exendin-4 attenuates high glucose-induced cardiomyocyte apoptosis via inhibition of endoplasmic reticulum stress and activation of SERCA2a. *American journal of physiology Cell physiology*. 2013;304:C508-18.
100. Padwal R, Majumdar SR, Johnson JA, Varney J and McAlister FA. A systematic review of drug therapy to delay or prevent type 2 diabetes. *Diabetes care*. 2005;28:736-44.
101. Gillies CL, Abrams KR, Lambert PC, Cooper NJ, Sutton AJ, Hsu RT and Khunti K. Pharmacological and lifestyle interventions to prevent or delay type 2

diabetes in people with impaired glucose tolerance: systematic review and meta-analysis. *BMJ*. 2007;334:299.
102. Poudyal H. Mechanisms for the cardiovascular effects of glucagon-like peptide-1. *Acta Physiol (Oxf)*. 2016;216:277-313.
103. Drucker DJ, Philippe J, Mojsov S, Chick WL and Habener JF. Glucagon-like peptide I stimulates insulin gene expression and increases cyclic AMP levels in a rat islet cell line. *Proc Natl Acad Sci U S A*. 1987;84:3434-3438.
104. Kreymann B, Williams G, Ghatei MA and Bloom SR. Glucagon-like peptide-1 7-36: a physiological incretin in man. *Lancet*. 1987;2:1300-1304.
105. Mojsov S, Weir GC and Habener JF. Insulinotropin: glucagon-like peptide I (7-37) co-encoded in the glucagon gene is a potent stimulator of insulin release in the perfused rat pancreas. *J Clin Invest*. 1987;79:616-619.
106. Thorens B, Porret A, Buhler L, Deng SP, Morel P and Widmann C. Cloning and functional expression of the human islet GLP-1 receptor. Demonstration that exendin-4 is an agonist and exendin-(9-39) an antagonist of the receptor. *Diabetes*. 1993;42:1678-1682.
107. Baggio LL and Drucker DJ. Biology of incretins: GLP-1 and GIP. *Gastroenterology*. 2007;132:2131-2157.
108. Ussher JR and Drucker DJ. Cardiovascular biology of the incretin system. *Endocr Rev*. 2012;33:187-215.
109. Zhu L, Tamvakopoulos C, Xie D, Dragovic J, Shen X, Fenyk-Melody JE, Schmidt K, Bagchi A, Griffin PR, Thornberry NA and Sinha RR. The role of dipeptidyl peptidase IV in the cleavage of glucagon family peptides: in vivo metabolism of pituitary adenylate cyclase activating polypeptide-(1-38). *J Biol Chem*. 2003;278:22418-22423.
110. Nikolaidis LA, Elahi D, Shen YT and Shannon RP. Active metabolite of GLP-1 mediates myocardial glucose uptake and improves left ventricular performance in conscious dogs with dilated cardiomyopathy. *Am J Physiol Heart Circ Physiol*. 2005;289:H2401-H2408.
111. Edwards CM, Edwards AV and Bloom SR. Cardiovascular and pancreatic endocrine responses to glucagon-like peptide-1(7-36) amide in the conscious calf. *Exp Physiol*. 1997;82:709-716.
112. Barragan JM, Rodriguez RE and Blazquez E. Changes in arterial blood pressure and heart rate induced by glucagon-like peptide-1-(7-36) amide in rats. *Am J Physiol*. 1994;266:E459-E466.
113. Barragan JM, Rodriguez RE, Eng J and Blazquez E. Interactions of exendin-(9-39) with the effects of glucagon-like peptide-1-(7-36) amide and of exendin-4 on arterial blood pressure and heart rate in rats. *Regul Pept*. 1996;67:63-68.
114. Ban K, Noyan-Ashraf MH, Hoefer J, Bolz SS, Drucker DJ and Husain M. Cardioprotective and vasodilatory actions of glucagon-like peptide 1 receptor are mediated through both glucagon-like peptide 1 receptor-dependent and -independent pathways. *Circulation*. 2008;117:2340-2350.
115. Bhashyam S, Fields AV, Patterson B, Testani JM, Chen L, Shen YT and Shannon RP. Glucagon-like peptide-1 increases myocardial glucose uptake via

p38alpha MAP kinase-mediated, nitric oxide-dependent mechanisms in conscious dogs with dilated cardiomyopathy. *Circ Heart Fail*. 2010;3:512-521.
116. Nikolaidis LA, Elahi D, Hentosz T, Doverspike A, Huerbin R, Zourelias L, Stolarski C, Shen YT and Shannon RP. Recombinant glucagon-like peptide-1 increases myocardial glucose uptake and improves left ventricular performance in conscious dogs with pacing-induced dilated cardiomyopathy. *Circulation*. 2004;110:955-961.
117. Zhao T, Parikh P, Bhashyam S, Bolukoglu H, Poornima I, Shen YT and Shannon RP. Direct effects of glucagon-like peptide-1 on myocardial contractility and glucose uptake in normal and postischemic isolated rat hearts. *J Pharmacol Exp Ther*. 2006;317:1106-1113.
118. Liu Q, Anderson C, Broyde A, Polizzi C, Fernandez R, Baron A and Parkes DG. Glucagon-like peptide-1 and the exenatide analogue AC3174 improve cardiac function, cardiac remodeling, and survival in rats with chronic heart failure. *Cardiovasc Diabetol*. 2010;9:76.
119. Matsubara M, Kanemoto S, Leshnower BG, Albone EF, Hinmon R, Plappert T, Gorman JH, III and Gorman RC. Single dose GLP-1-Tf ameliorates myocardial ischemia/reperfusion injury. *J Surg Res*. 2011;165:38-45.
120. Timmers L, Henriques JP, de Kleijn DP, Devries JH, Kemperman H, Steendijk P, Verlaan CW, Kerver M, Piek JJ, Doevendans PA, Pasterkamp G and Hoefer IE. Exenatide reduces infarct size and improves cardiac function in a porcine model of ischemia and reperfusion injury. *J Am Coll Cardiol*. 2009;53:501-10.
121. Filion KB, Azoulay L, Platt RW, Dahl M, Dormuth CR, Clemens KK, Hu N, Paterson JM, Targownik L, Turin TC, Udell JA, Ernst P and Investigators C. A Multicenter Observational Study of Incretin-based Drugs and Heart Failure. *The New England journal of medicine*. 2016;374:1145-54.
122. Patorno E, Everett BM, Goldfine AB, Glynn RJ, Liu J, Gopalakrishnan C and Kim SC. Comparative Cardiovascular Safety of Glucagon-Like Peptide-1 Receptor Agonists versus Other Antidiabetic Drugs in Routine Care: a Cohort Study. *Diabetes Obes Metab*. 2016.
123. Ban K, Kim KH, Cho CK, Sauve M, Diamandis EP, Backx PH, Drucker DJ and Husain M. Glucagon-like peptide (GLP)-1(9-36)amide-mediated cytoprotection is blocked by exendin(9-39) yet does not require the known GLP-1 receptor. *Endocrinology*. 2010;151:1520-31.
124. Moberly SP, Mather KJ, Berwick ZC, Owen MK, Goodwill AG, Casalini ED, Hutchins GD, Green MA, Ng Y, Considine RV, Perry KM, Chisholm RL and Tune JD. Impaired cardiometabolic responses to glucagon-like peptide 1 in obesity and type 2 diabetes mellitus. *Basic Res Cardiol*. 2013;108:365.
125. Goodwill AG, Mather KJ, Conteh AM, Sassoon DJ, Noblet JN and Tune JD. Cardiovascular and hemodynamic effects of glucagon-like peptide-1. *Rev Endocr Metab Disord*. 2014;15:209-17.
126. Gejl M, Sondergaard HM, Stecher C, Bibby BM, Moller N, Botker HE, Hansen SB, Gjedde A, Rungby J and Brock B. Exenatide alters myocardial glucose transport and uptake depending on insulin resistance and increases

myocardial blood flow in patients with type 2 diabetes. *The Journal of clinical endocrinology and metabolism*. 2012;97:E1165-9.
127. Ossum A, van DU, Engstrom T, Jensen JS and Treiman M. The cardioprotective and inotropic components of the postconditioning effects of GLP-1 and GLP-1(9-36)a in an isolated rat heart. *Pharmacol Res*. 2009;60:411-417.
128. Goodwill A, Casalini E, Conteh A, Noblet J, Sassoon D, Tune J and Mather K. Glucagon like peptide-1 augments cardiac output during regional myocardial ischemia via increases in ventricular preload, independent of changes in cardiac inotropy. *Faseb Journal*. 2014;28.
129. Goodwill AG, Tune JD, Noblet JN, Conteh AM, Sassoon D, Casalini ED and Mather KJ. Glucagon-like peptide-1 (7-36) but not (9-36) augments cardiac output during myocardial ischemia via a Frank-Starling mechanism. *Basic Res Cardiol*. 2014;109:426.
130. Sokos GG, Nikolaidis LA, Mankad S, Elahi D and Shannon RP. Glucagon-like peptide-1 infusion improves left ventricular ejection fraction and functional status in patients with chronic heart failure. *J Card Fail*. 2006;12:694-699.
131. Barragan JM, Eng J, Rodriguez R and Blazquez E. Neural contribution to the effect of glucagon-like peptide-1-(7-36) amide on arterial blood pressure in rats. *Am J Physiol*. 1999;277:E784-E791.
132. Arab S, Gramolini AO, Ping P, Kislinger T, Stanley B, van Eyk J, Ouzounian M, MacLennan DH, Emili A and Liu PP. Cardiovascular Proteomics. *Journal of the American College of Cardiology*. 2006;48:17331741.
133. Cravatt BF, Simon GM and Yates JR, 3rd. The biological impact of mass-spectrometry-based proteomics. *Nature*. 2007;450:991-1000.
134. Pisitkun T, Hoffert JD, Yu MJ and Knepper MA. Tandem Mass Spectrometry in Physiology. *Physiology*. 2007;22:390-400.
135. Gstaiger M and Aebersold R. Applying mass spectrometry-based proteomics to genetics, genomics and network biology. *Nature reviews Genetics*. 2009;10:617-627.
136. Rodriguez-Suarez E and Whetton AD. The application of quantification techniques in proteomics for biomedical research. *Mass spectrometry reviews*. 2012;32:1-26.
137. Hu Q, Noll RJ, Li H, Makarov A, Hardman M and Graham Cooks R. The Orbitrap: a new mass spectrometer. *Journal of mass spectrometry : JMS*. 2005;40:430-443.
138. Kislinger T, Gramolini AO, MacLennan DH and Emili A. Multidimensional protein identification technology (MudPIT): Technical overview of a profiling method optimized for the comprehensive proteomic investigation of normal and diseased heart tissue. *Journal of the American Society for Mass Spectrometry*. 2005;16:12071220.
139. Gramolini AO, Kislinger T, Liu P, MacLennan DH and Emili A. Analyzing the cardiac muscle proteome by liquid chromatography-mass spectrometry-based expression proteomics. *Methods in molecular biology*. 2007;357:15-31.
140. Kessner D, Chambers M, Burke R, Agus D and Mallick P. ProteoWizard: open source software for rapid proteomics tools development. *Bioinformatics (Oxford, England)*. 2008;24:2534-6.

141. Kline KG and Wu CC. MudPIT analysis: application to human heart tissue. *Methods in molecular biology (Clifton, NJ)*. 2009;528:281-293.
142. Lai X, Wang L, Tang H and Witzmann FA. A Novel Alignment Method and Multiple Filters for Exclusion of Unqualified Peptides To Enhance Label-Free Quantification Using Peptide Intensity in LC–MS/MS. *Journal of proteome research*. 2011;10:47994812.
143. Chambers MC, Maclean B, Burke R, Amodei D, Ruderman DL, Neumann S, Gatto L, Fischer B, Pratt B, Egertson J, Hoff K, Kessner D, Tasman N, Shulman N, Frewen B, Baker TA, Brusniak MY, Paulse C, Creasy D, Flashner L, Kani K, Moulding C, Seymour SL, Nuwaysir LM, Lefebvre B, Kuhlmann F, Roark J, Rainer P, Detlev S, Hemenway T, Huhmer A, Langridge J, Connolly B, Chadick T, Holly K, Eckels J, Deutsch EW, Moritz RL, Katz JE, Agus DB, MacCoss M, Tabb DL and Mallick P. A cross-platform toolkit for mass spectrometry and proteomics. *Nat Biotechnol*. 2012;30:918-20.
144. Lindsey ML, Mayr M, Gomes AV, Delles C, Arrell DK, Murphy AM, Lange RA, Costello CE, Jin YF, Laskowitz DT, Sam F, Terzic A, Van Eyk J, Srinivas PR, American Heart Association Council on Functional G, Translational Biology CoCDitYCoCCCoC, Stroke Nursing CoH and Stroke C. Transformative Impact of Proteomics on Cardiovascular Health and Disease: A Scientific Statement From the American Heart Association. *Circulation*. 2015;132:852-72.
145. Wende AR. Post-translational modifications of the cardiac proteome in diabetes and heart failure. *Proteomics Clin Appl*. 2015.
146. de Weger RA, Schipper ME, Siera-de Koning E, van der Weide P, van Oosterhout MF, Quadir R, Steenbergen-Nakken H, Lahpor JR, de Jonge N and Bovenschen N. Proteomic profiling of the human failing heart after left ventricular assist device support. *J Heart Lung Transplant*. 2011;30:497-506.
147. Chugh S, Suen C and Gramolini A. Proteomics and mass spectrometry: what have we learned about the heart? *Curr Cardiol Rev*. 2010;6:124-33.
148. Cieniewski-Bernard C, Mulder P, Henry JP, Drobecq H, Dubois E, Pottiez G, Thuillez C, Amouyel P, Richard V and Pinet F. Proteomic analysis of left ventricular remodeling in an experimental model of heart failure. *J Proteome Res*. 2008;7:5004-16.
149. Barallobre-Barreiro J, Didangelos A, Schoendube FA, Drozdov I, Yin X, Fernandez-Caggiano M, Willeit P, Puntmann VO, Aldama-Lopez G, Shah AM, Domenech N and Mayr M. Proteomics analysis of cardiac extracellular matrix remodeling in a porcine model of ischemia/reperfusion injury. *Circulation*. 2012;125:789-802.
150. Liu T, Chen L, Kim E, Tran D, Phinney BS and Knowlton AA. Mitochondrial proteome remodeling in ischemic heart failure. *Life sciences*. 2014;101:27-36.
151. Littlejohns B, Heesom K, Angelini GD and Suleiman MS. The effect of disease on human cardiac protein expression profiles in paired samples from right and left ventricles. *Clinical proteomics*. 2014;11:34.
152. Mitra A, Basak T, Ahmad S, Datta K, Datta R, Sengupta S and Sarkar S. Comparative Proteome Profiling during Cardiac Hypertrophy and Myocardial Infarction Reveals Altered Glucose Oxidation by Differential Activation of Pyruvate Dehydrogenase E1 Component Subunit beta. *J Mol Biol*. 2015;427:2104-20.

153. Wightman B, Ha I and Ruvkun G. Posttranscriptional regulation of the heterochronic gene lin-14 by lin-4 mediates temporal pattern formation in C. elegans. *Cell*. 1993;75:855-62.
154. Yates LA, Norbury CJ and Gilbert RJ. The long and short of microRNA. *Cell*. 2013;153:516-519.
155. Bartel DP. MicroRNAs: genomics, biogenesis, mechanism, and function. *Cell*. 2004;116:281-97.
156. Doench JG and Sharp PA. Specificity of microRNA target selection in translational repression. *Genes & development*. 2004;18:504-511.
157. Meola N, Gennarino VA and Banfi S. microRNAs and genetic diseases. *PathoGenetics*. 2008;2:7.
158. Latronico MVG and Catalucci D. MicroRNA and cardiac pathologies. *Physiological ….* 2008.
159. D'Alessandra Y, Pompilio G and Capogrossi MC. MicroRNAs and myocardial infarction. *Current opinion in cardiology*. 2012;27:228-35.
160. Bostjancic E and Glavac D. miRNome in myocardial infarction: Future directions and perspective. *World journal of cardiology*. 2014;6:939.
161. Harada M, Luo X, Murohara T, Yang B, Dobrev D and Nattel S. MicroRNA regulation and cardiac calcium signaling: role in cardiac disease and therapeutic potential. *Circulation research*. 2014;114:689-705.
162. Naar AM. MiRs with a sweet tooth. *Cell metabolism*. 2011;14:149-150.
163. McGregor RA and Choi MS. microRNAs in the Regulation of Adipogenesis and Obesity. *Current molecular medicine*. 2011;11:304316.
164. Maarten H, Dieuwke K and Paul H. MicroRNAs regulating oxidative stress and inflammation in relation to obesity and atherosclerosis. *The FASEB Journal*. 2011;25:2515-2527.
165. Heneghan HM, Miller N, McAnena OJ, O'Brien T and Kerin MJ. Differential miRNA expression in omental adipose tissue and in the circulation of obese patients identifies novel metabolic biomarkers. *The Journal of clinical endocrinology and metabolism*. 2011;96:E846-50.
166. Guay C, Roggli E, Nesca V, Jacovetti C and Regazzi R. Diabetes mellitus, a microRNA-related disease? *Translational research : the journal of laboratory and clinical medicine*. 2011;157:253-264.
167. Natarajan R, Putta S and Kato M. MicroRNAs and diabetic complications. *Journal of cardiovascular translational research*. 2012;5:413-422.
168. Williams MD and Mitchell GM. MicroRNAs in insulin resistance and obesity. *Experimental diabetes research*. 2012;2012:484696.
169. Veerle R and Anders MN. MicroRNAs in metabolism and metabolic disorders. *Nature Reviews Molecular Cell Biology*. 2012;13:239-250.
170. Scherr M, Venturini L, Battmer K, Schaller-Schoenitz M, Schaefer D, Dallmann I, Ganser A and Eder M. Lentivirus-mediated antagomir expression for specific inhibition of miRNA function. *Nucleic acids research*. 2007;35:e149.
171. Latronico MVG and Condorelli G. MicroRNAs and cardiac pathology. *Nature Reviews Cardiology*. 2009.

172. Quiat D and Olson EN. MicroRNAs in cardiovascular disease: from pathogenesis to prevention and treatment. *The Journal of clinical investigation*. 2013;123:11-8.
173. Ortega FJ, Mercader JM and Moreno-Navarrete JM. Profiling of circulating microRNAs reveals common microRNAs linked to type 2 diabetes that change with insulin sensitization. *Diabetes ….* 2014.
174. Lee IS, Park KC, Yang KJ, Choi H, Jang YS, Lee JM and Kim HS. Exenatide reverses dysregulated microRNAs in high-fat diet-induced obese mice. *Obesity research & clinical practice*. 2015.
175. Prevention CfDCa. National Diabetes Statistics Report: Estimates of Diabetes and Its Burden in the United States, 2014. 2014.
176. Rana JS, Nieuwdorp M, Jukema JW and Kastelein JJ. Cardiovascular metabolic syndrome - an interplay of, obesity, inflammation, diabetes and coronary heart disease. *Diabetes Obes Metab*. 2007;9:218-32.
177. Hullinger TG, Montgomery RL, Seto AG, Dickinson BA, Semus HM, Lynch JM, Dalby CM, Robinson K, Stack C, Latimer PA, Hare JM, Olson EN and van Rooij E. Inhibition of miR-15 protects against cardiac ischemic injury. *Circulation research*. 2012;110:71-81.
178. Porrello ER, Johnson BA, Aurora AB, Simpson E, Nam YJ, Matkovich SJ, Dorn GW, 2nd, van Rooij E and Olson EN. MiR-15 family regulates postnatal mitotic arrest of cardiomyocytes. *Circulation research*. 2011;109:670-9.
179. Song DW, Ryu JY, Kim JO, Kwon EJ and Kim do H. The miR-19a/b family positively regulates cardiomyocyte hypertrophy by targeting atrogin-1 and MuRF-1. *Biochem J*. 2014;457:151-62.
180. Thum T, Gross C, Fiedler J, Fischer T, Kissler S, Bussen M, Galuppo P, Just S, Rottbauer W, Frantz S, Castoldi M, Soutschek J, Koteliansky V, Rosenwald A, Basson MA, Licht JD, Pena JT, Rouhanifard SH, Muckenthaler MU, Tuschl T, Martin GR, Bauersachs J and Engelhardt S. MicroRNA-21 contributes to myocardial disease by stimulating MAP kinase signalling in fibroblasts. *Nature*. 2008;456:980-4.
181. Zhou Q, Gallagher R, Ufret-Vincenty R, Li X, Olson EN and Wang S. Regulation of angiogenesis and choroidal neovascularization by members of microRNA-23~27~24 clusters. *Proceedings of the National Academy of Sciences of the United States of America*. 2011;108:8287-92.
182. Fiedler J, Jazbutyte V, Kirchmaier BC, Gupta SK, Lorenzen J, Hartmann D, Galuppo P, Kneitz S, Pena JT, Sohn-Lee C, Loyer X, Soutschek J, Brand T, Tuschl T, Heineke J, Martin U, Schulte-Merker S, Ertl G, Engelhardt S, Bauersachs J and Thum T. MicroRNA-24 regulates vascularity after myocardial infarction. *Circulation*. 2011;124:720-30.
183. Marquart TJ, Allen RM, Ory DS and Baldan A. miR-33 links SREBP-2 induction to repression of sterol transporters. *Proceedings of the National Academy of Sciences of the United States of America*. 2010;107:12228-32.
184. Najafi-Shoushtari SH, Kristo F, Li Y, Shioda T, Cohen DE, Gerszten RE and Naar AM. MicroRNA-33 and the SREBP host genes cooperate to control cholesterol homeostasis. *Science*. 2010;328:1566-9.

185. Rayner KJ, Esau CC, Hussain FN, McDaniel AL, Marshall SM, van Gils JM, Ray TD, Sheedy FJ, Goedeke L, Liu X, Khatsenko OG, Kaimal V, Lees CJ, Fernandez-Hernando C, Fisher EA, Temel RE and Moore KJ. Inhibition of miR-33a/b in non-human primates raises plasma HDL and lowers VLDL triglycerides. *Nature*. 2011;478:404-7.
186. Boon RA, Seeger T, Heydt S, Fischer A, Hergenreider E, Horrevoets AJ, Vinciguerra M, Rosenthal N, Sciacca S, Pilato M, van Heijningen P, Essers J, Brandes RP, Zeiher AM and Dimmeler S. MicroRNA-29 in aortic dilation: implications for aneurysm formation. *Circulation research*. 2011;109:1115-9.
187. Maegdefessel L, Azuma J, Toh R, Merk DR, Deng A, Chin JT, Raaz U, Schoelmerich AM, Raiesdana A, Leeper NJ, McConnell MV, Dalman RL, Spin JM and Tsao PS. Inhibition of microRNA-29b reduces murine abdominal aortic aneurysm development. *The Journal of clinical investigation*. 2012;122:497-506.
188. Bonauer A, Carmona G, Iwasaki M, Mione M, Koyanagi M, Fischer A, Burchfield J, Fox H, Doebele C, Ohtani K, Chavakis E, Potente M, Tjwa M, Urbich C, Zeiher AM and Dimmeler S. MicroRNA-92a controls angiogenesis and functional recovery of ischemic tissues in mice. *Science*. 2009;324:1710-3.
189. Hinkel R, Penzkofer D, Zuhlke S, Fischer A, Husada W, Xu QF, Baloch E, van Rooij E, Zeiher AM, Kupatt C and Dimmeler S. Inhibition of microRNA-92a protects against ischemia/reperfusion injury in a large-animal model. *Circulation*. 2013;128:1066-75.
190. Caruso P, Dempsie Y, Stevens HC, McDonald RA, Long L, Lu R, White K, Mair KM, McClure JD, Southwood M, Upton P, Xin M, van Rooij E, Olson EN, Morrell NW, MacLean MR and Baker AH. A role for miR-145 in pulmonary arterial hypertension: evidence from mouse models and patient samples. *Circulation research*. 2012;111:290-300.
191. Corsten MF, Papageorgiou A, Verhesen W, Carai P, Lindow M, Obad S, Summer G, Coort SL, Hazebroek M, van Leeuwen R, Gijbels MJ, Wijnands E, Biessen EA, De Winther MP, Stassen FR, Carmeliet P, Kauppinen S, Schroen B and Heymans S. MicroRNA profiling identifies microRNA-155 as an adverse mediator of cardiac injury and dysfunction during acute viral myocarditis. *Circulation research*. 2012;111:415-25.
192. Rane S, He M, Sayed D, Vashistha H, Malhotra A, Sadoshima J, Vatner DE, Vatner SF and Abdellatif M. Downregulation of miR-199a derepresses hypoxia-inducible factor-1alpha and Sirtuin 1 and recapitulates hypoxia preconditioning in cardiac myocytes. *Circulation research*. 2009;104:879-86.
193. da Costa Martins PA, Salic K, Gladka MM, Armand AS, Leptidis S, el Azzouzi H, Hansen A, Coenen-de Roo CJ, Bierhuizen MF, van der Nagel R, van Kuik J, de Weger R, de Bruin A, Condorelli G, Arbones ML, Eschenhagen T and De Windt LJ. MicroRNA-199b targets the nuclear kinase Dyrk1a in an auto-amplification loop promoting calcineurin/NFAT signalling. *Nat Cell Biol*. 2010;12:1220-7.
194. Montgomery RL, Hullinger TG, Semus HM, Dickinson BA, Seto AG, Lynch JM, Stack C, Latimer PA, Olson EN and van Rooij E. Therapeutic inhibition of miR-208a improves cardiac function and survival during heart failure. *Circulation*. 2011;124:1537-47.

195. Grueter CE, van Rooij E, Johnson BA, DeLeon SM, Sutherland LB, Qi X, Gautron L, Elmquist JK, Bassel-Duby R and Olson EN. A cardiac microRNA governs systemic energy homeostasis by regulation of MED13. *Cell*. 2012;149:671-83.
196. Ren XP, Wu J, Wang X, Sartor MA, Qian J, Jones K, Nicolaou P, Pritchard TJ and Fan GC. MicroRNA-320 is involved in the regulation of cardiac ischemia/reperfusion injury by targeting heat-shock protein 20. *Circulation*. 2009;119:2357-66.
197. van Rooij E and Olson EN. MicroRNA therapeutics for cardiovascular disease: opportunities and obstacles. *Nature reviews Drug discovery*. 2012;11:860-72.
198. Rodriguez RH, Bickta JL, Murawski P and O'Donnell CP. The impact of obesity and hypoxia on left ventricular function and glycolytic metabolism. *Physiol Rep*. 2014;2:e12001.
199. Trask AJ, Katz PS, Kelly AP, Galantowicz ML, Cismowski MJ, West TA, Neeb ZP, Berwick ZC, Goodwill AG, Alloosh M, Tune JD, Sturek M and Lucchesi PA. Dynamic micro- and macrovascular remodeling in coronary circulation of obese Ossabaw pigs with metabolic syndrome. *J Appl Physiol (1985)*. 2012;113:1128-40.
200. Berwick ZC, Dick GM and Tune JD. Heart of the matter: coronary dysfunction in metabolic syndrome. *Journal of molecular and cellular cardiology*. 2012;52:848-56.
201. Adams KF, Schatzkin A, Harris TB, Kipnis V, Mouw T, Ballard-Barbash R, Hollenbeck A and Leitzmann MF. Overweight, obesity, and mortality in a large prospective cohort of persons 50 to 71 years old. *The New England journal of medicine*. 2006;355:763-78.
202. Colombo MG, Meisinger C, Amann U, Heier M, von Scheidt W, Kuch B, Peters A and Kirchberger I. Association of obesity and long-term mortality in patients with acute myocardial infarction with and without diabetes mellitus: results from the MONICA/KORA myocardial infarction registry. *Cardiovascular diabetology*. 2015;14:24.
203. Kragelund C, Hassager C, Hildebrandt P, Torp-Pedersen C, Kober L and group Ts. Impact of obesity on long-term prognosis following acute myocardial infarction. *International journal of cardiology*. 2005;98:123-31.
204. Rana JS, Mukamal KJ, Morgan JP, Muller JE and Mittleman MA. Obesity and the risk of death after acute myocardial infarction. *American heart journal*. 2004;147:841-6.
205. Leopold JA. Obesity-related cardiomyopathy is an adipocyte-mediated paracrine disease. *Trends in cardiovascular medicine*. 2015;25:127-8.
206. Wang Z. miRNA in the regulation of ion channel/transporter expression. *Compr Physiol*. 2013;3:599-653.
207. Greco S, Fasanaro P, Castelvecchio S, D'Alessandra Y, Arcelli D, Di Donato M, Malavazos A, Capogrossi MC, Menicanti L and Martelli F. MicroRNA dysregulation in diabetic ischemic heart failure patients. *Diabetes*. 2012;61:1633-41.

208. Borbouse L, Dick GM, Asano S, Bender SB, Dincer UD, Payne GA, Neeb ZP, Bratz IN, Sturek M and Tune JD. Impaired function of coronary BK(Ca) channels in metabolic syndrome. *Am J Physiol Heart Circ Physiol*. 2009;297:H1629-37.
209. Irizarry RA, Bolstad BM, Collin F, Cope LM, Hobbs B and Speed TP. Summaries of Affymetrix GeneChip probe level data. *Nucleic acids research*. 2003;31:e15.
210. Storey JD and Tibshirani R. Statistical significance for genomewide studies. *Proceedings of the National Academy of Sciences of the United States of America*. 2003;100:9440-5.
211. Martin-Vaquero P, da Costa RC, Allen MJ, Moore SA, Keirsey JK and Green KB. Proteomic analysis of cerebrospinal fluid in canine cervical spondylomyelopathy. *Spine (Phila Pa 1976)*. 2015;40:601-12.
212. Rezaul K, Wu L, Mayya V, Hwang SI and Han D. A systematic characterization of mitochondrial proteome from human T leukemia cells. *Mol Cell Proteomics*. 2005;4:169-81.
213. Burkhoff D, Mirsky I and Suga H. Assessment of systolic and diastolic ventricular properties via pressure-volume analysis: a guide for clinical, translational, and basic researchers. *Am J Physiol Heart Circ Physiol*. 2005;289:H501-12.
214. Suga H. Ventricular energetics. *Physiol Rev*. 1990;70:247-77.
215. Paulino EC, Ferreira JC, Bechara LR, Tsutsui JM, Mathias W, Jr., Lima FB, Casarini DE, Cicogna AC, Brum PC and Negrao CE. Exercise training and caloric restriction prevent reduction in cardiac Ca2+-handling protein profile in obese rats. *Hypertension*. 2010;56:629-35.
216. Pinto TE, Gusso S, Hofman PL, Derraik JG, Hornung TS, Cutfield WS and Baldi JC. Systolic and diastolic abnormalities reduce the cardiac response to exercise in adolescents with type 2 diabetes. *Diabetes care*. 2014;37:1439-46.
217. Yakinci C, Mungen B, Karabiber H, Tayfun M and Evereklioglu C. Autonomic nervous system functions in obese children. *Brain Dev*. 2000;22:151-3.
218. Schulz R, Rose J, Martin C, Brodde OE and Heusch G. Development of short-term myocardial hibernation. Its limitation by the severity of ischemia and inotropic stimulation. *Circulation*. 1993;88:684-95.
219. White WB, Cannon CP, Heller SR, Nissen SE, Bergenstal RM, Bakris GL, Perez AT, Fleck PR, Mehta CR, Kupfer S, Wilson C, Cushman WC, Zannad F and Investigators E. Alogliptin after acute coronary syndrome in patients with type 2 diabetes. *The New England journal of medicine*. 2013;369:1327-35.
220. Zinman B, Gerich J, Buse JB, Lewin A, Schwartz S, Raskin P, Hale PM, Zdravkovic M, Blonde L and Investigators L-S. Efficacy and safety of the human glucagon-like peptide-1 analog liraglutide in combination with metformin and thiazolidinedione in patients with type 2 diabetes (LEAD-4 Met+TZD). *Diabetes care*. 2009;32:1224-30.
221. Panjwani N, Mulvihill EE, Longuet C, Yusta B, Campbell JE, Brown TJ, Streutker C, Holland D, Cao X, Baggio LL and Drucker DJ. GLP-1 receptor activation indirectly reduces hepatic lipid accumulation but does not attenuate

development of atherosclerosis in diabetic male ApoE(-/-) mice. *Endocrinology*. 2013;154:127-39.
222. Zile MR, Baicu CF, Ikonomidis JS, Stroud RE, Nietert PJ, Bradshaw AD, Slater R, Palmer BM, Van Buren P, Meyer M, Redfield MM, Bull DA, Granzier HL and LeWinter MM. Myocardial stiffness in patients with heart failure and a preserved ejection fraction: contributions of collagen and titin. *Circulation*. 2015;131:1247-59.
223. Kruger M and Linke WA. The giant protein titin: a regulatory node that integrates myocyte signaling pathways. *J Biol Chem*. 2011;286:9905-12.
224. ter Keurs HE. The interaction of Ca2+ with sarcomeric proteins: role in function and dysfunction of the heart. *Am J Physiol Heart Circ Physiol*. 2012;302:H38-50.
225. Hamdani N, Franssen C, Lourenco A, Falcao-Pires I, Fontoura D, Leite S, Plettig L, Lopez B, Ottenheijm CA, Becher PM, Gonzalez A, Tschope C, Diez J, Linke WA, Leite-Moreira AF and Paulus WJ. Myocardial titin hypophosphorylation importantly contributes to heart failure with preserved ejection fraction in a rat metabolic risk model. *Circulation Heart failure*. 2013;6:1239-49.
226. Hamdani N, Hervent AS, Vandekerckhove L, Matheeussen V, Demolder M, Baerts L, De Meester I, Linke WA, Paulus WJ and De Keulenaer GW. Left ventricular diastolic dysfunction and myocardial stiffness in diabetic mice is attenuated by inhibition of dipeptidyl peptidase 4. *Cardiovascular research*. 2014;104:423-31.
227. Balderas-Villalobos J, Molina-Munoz T, Mailloux-Salinas P, Bravo G, Carvajal K and Gomez-Viquez NL. Oxidative stress in cardiomyocytes contributes to decreased SERCA2a activity in rats with metabolic syndrome. *Am J Physiol Heart Circ Physiol*. 2013;305:H1344-53.
228. Fredersdorf S, Thumann C, Zimmermann WH, Vetter R, Graf T, Luchner A, Riegger GA, Schunkert H, Eschenhagen T and Weil J. Increased myocardial SERCA expression in early type 2 diabetes mellitus is insulin dependent: In vivo and in vitro data. *Cardiovascular diabetology*. 2012;11:57.
229. Meyer M, Schillinger W, Pieske B, Holubarsch C, Heilmann C, Posival H, Kuwajima G, Mikoshiba K, Just H, Hasenfuss G and et al. Alterations of sarcoplasmic reticulum proteins in failing human dilated cardiomyopathy. *Circulation*. 1995;92:778-84.
230. Dineen SL, McKenney ML, Bell LN, Fullenkamp AM, Schultz KA, Alloosh M, Chalasani N and Sturek M. Metabolic Syndrome Abolishes Glucagon-Like Peptide 1 Receptor Agonist Stimulation of SERCA in Coronary Smooth Muscle. *Diabetes*. 2015;64:3321-7.
231. LeWinter MM and Granzier H. Cardiac titin: a multifunctional giant. *Circulation*. 2010;121:2137-45.
232. Ahmed SH and Lindsey ML. Titin phosphorylation: myocardial passive stiffness regulated by the intracellular giant. *Circulation research*. 2009;105:611-3.
233. Bourajjaj M, Armand AS, da Costa Martins PA, Weijts B, van der Nagel R, Heeneman S, Wehrens XH and De Windt LJ. NFATc2 is a necessary mediator of calcineurin-dependent cardiac hypertrophy and heart failure. *J Biol Chem*. 2008;283:22295-303.

234. Molkentin JD. Calcineurin-NFAT signaling regulates the cardiac hypertrophic response in coordination with the MAPKs. *Cardiovascular research*. 2004;63:467-75.
235. Hogan PG, Chen L, Nardone J and Rao A. Transcriptional regulation by calcium, calcineurin, and NFAT. *Genes Dev*. 2003;17:2205-32.
236. Limpitikul WB, Dick IE, Joshi-Mukherjee R, Overgaard MT, George AL, Jr. and Yue DT. Calmodulin mutations associated with long QT syndrome prevent inactivation of cardiac L-type Ca(2+) currents and promote proarrhythmic behavior in ventricular myocytes. *Journal of molecular and cellular cardiology*. 2014;74:115-24.
237. Liu LF, Liang Z, Lv ZR, Liu XH, Bai J, Chen J, Chen C and Wang Y. MicroRNA-15a/b are up-regulated in response to myocardial ischemia/reperfusion injury. *J Geriatr Cardiol*. 2012;9:28-32.
238. Porrello ER, Mahmoud AI, Simpson E, Johnson BA, Grinsfelder D, Canseco D, Mammen PP, Rothermel BA, Olson EN and Sadek HA. Regulation of neonatal and adult mammalian heart regeneration by the miR-15 family. *Proceedings of the National Academy of Sciences of the United States of America*. 2013;110:187-92.
239. Shen Y, Shen Z, Miao L, Xin X, Lin S, Zhu Y, Guo W and Zhu YZ. miRNA-30 family inhibition protects against cardiac ischemic injury by regulating cystathionine-gamma-lyase expression. *Antioxid Redox Signal*. 2015;22:224-40.
240. Aurora AB, Mahmoud AI, Luo X, Johnson BA, van Rooij E, Matsuzaki S, Humphries KM, Hill JA, Bassel-Duby R, Sadek HA and Olson EN. MicroRNA-214 protects the mouse heart from ischemic injury by controlling Ca(2)(+) overload and cell death. *The Journal of clinical investigation*. 2012;122:1222-32.
241. Wang C, Li Q, Wang W, Guo L, Guo C, Sun Y and Zhang J. GLP-1 contributes to increases in PGC-1alpha expression by downregulating miR-23a to reduce apoptosis. *Biochem Biophys Res Commun*. 2015;466:33-9.
242. Sassoon DJ, Goodwill AG, Noblet JN, Conteh AM, Herring BP, McClintick J, Tune JD and Mather KJ. Obesity Distinctly Influences Cardiac Function and Molecular Responses to Ischemia-Reperfusion and GLP-1 Receptor Agonism. *The FASEB Journal*. 2016;30:770.1-770.1.
243. Pfeffer MA, Claggett B, Diaz R, Dickstein K, Gerstein HC, Kober LV, Lawson FC, Ping L, Wei X, Lewis EF, Maggioni AP, McMurray JJ, Probstfield JL, Riddle MC, Solomon SD, Tardif JC and Investigators E. Lixisenatide in Patients with Type 2 Diabetes and Acute Coronary Syndrome. *The New England journal of medicine*. 2015;373:2247-57.
244. Mogensen UM, Andersson C, Fosbol EL, Schramm TK, Vaag A, Scheller NM, Torp-Pedersen C, Gislason G and Kober L. Cardiovascular safety of combination therapies with incretin-based drugs and metformin compared with a combination of metformin and sulphonylurea in type 2 diabetes mellitus--a retrospective nationwide study. *Diabetes Obes Metab*. 2014;16:1001-8.
245. Kristensen J, Mortensen UM, Schmidt M, Nielsen PH, Nielsen TT and Maeng M. Lack of cardioprotection from subcutaneously and preischemic administered liraglutide in a closed chest porcine ischemia reperfusion model. *BMC cardiovascular disorders*. 2009;9:31.

246. Kristensen J, Mortensen UM, Schmidt M, Nielsen PH, Nielsen TT and Maeng M. Lack of cardioprotection from subcutaneously and preischemic administered liraglutide in a closed chest porcine ischemia reperfusion model. *BMC Cardiovasc Disord*. 2009;9:31.
247. Farris AB, Adams CD, Brousaides N, Della Pelle PA, Collins AB, Moradi E, Smith RN, Grimm PC and Colvin RB. Morphometric and visual evaluation of fibrosis in renal biopsies. *J Am Soc Nephrol*. 2011;22:176-86.
248. Suga H, Hayashi T and Shirahata M. Ventricular systolic pressure-volume area as predictor of cardiac oxygen consumption. *The American journal of physiology*. 1981;240:H39-44.
249. Robinson LE, Holt TA, Rees K, Randeva HS and O'Hare JP. Effects of exenatide and liraglutide on heart rate, blood pressure and body weight: systematic review and meta-analysis. *BMJ Open*. 2013;3.
250. Vilsboll T, Christensen M, Junker AE, Knop FK and Gluud LL. Effects of glucagon-like peptide-1 receptor agonists on weight loss: systematic review and meta-analyses of randomised controlled trials. *BMJ*. 2012;344:d7771.
251. Berwick ZC, Dick GM, O'Leary HA, Bender SB, Goodwill AG, Moberly SP, Owen MK, Miller SJ, Obukhov AG and Tune JD. Contribution of electromechanical coupling between Kv and Ca v1.2 channels to coronary dysfunction in obesity. *Basic Res Cardiol*. 2013;108:370.
252. Dyson MC, Alloosh M, Vuchetich JP, Mokelke EA and Sturek M. Components of metabolic syndrome and coronary artery disease in female Ossabaw swine fed excess atherogenic diet. *Comparative medicine*. 2006;56:35-45.
253. Van Lunen TA. Growth performance of pigs fed diets with and without tylosin phosphate supplementation and reared in a biosecure all-in all-out housing system. *Can Vet J*. 2003;44:571-6.
254. Neeb ZP, Edwards JM, Alloosh M, Long X, Mokelke EA and Sturek M. Metabolic syndrome and coronary artery disease in Ossabaw compared with Yucatan swine. *Comparative medicine*. 2010;60:300-15.
255. Lee L, Alloosh M, Saxena R, Van Alstine W, Watkins BA, Klaunig JE, Sturek M and Chalasani N. Nutritional model of steatohepatitis and metabolic syndrome in the Ossabaw miniature swine. *Hepatology*. 2009;50:56-67.
256. Lonborg J, Kelbaek H, Vejlstrup N, Botker HE, Kim WY, Holmvang L, Jorgensen E, Helqvist S, Saunamaki K, Terkelsen CJ, Schoos MM, Kober L, Clemmensen P, Treiman M and Engstrom T. Exenatide reduces final infarct size in patients with ST-segment-elevation myocardial infarction and short-duration of ischemia. *Circ Cardiovasc Interv*. 2012;5:288-95.
257. Lonborg J, Vejlstrup N, Kelbaek H, Botker HE, Kim WY, Mathiasen AB, Jorgensen E, Helqvist S, Saunamaki K, Clemmensen P, Holmvang L, Thuesen L, Krusell LR, Jensen JS, Kober L, Treiman M, Holst JJ and Engstrom T. Exenatide reduces reperfusion injury in patients with ST-segment elevation myocardial infarction. *Eur Heart J*. 2012;33:1491-9.
258. Woo JS, Kim W, Ha SJ, Kim JB, Kim SJ, Kim WS, Seon HJ and Kim KS. Cardioprotective effects of exenatide in patients with ST-segment-elevation myocardial infarction undergoing primary percutaneous coronary intervention:

results of exenatide myocardial protection in revascularization study. *Arteriosclerosis, thrombosis, and vascular biology*. 2013;33:2252-60.
259. Katout M, Zhu H, Rutsky J, Shah P, Brook RD, Zhong J and Rajagopalan S. Effect of GLP-1 mimetics on blood pressure and relationship to weight loss and glycemia lowering: results of a systematic meta-analysis and meta-regression. *American journal of hypertension*. 2014;27:130-9.
260. Halbirk M, Norrelund H, Moller N, Holst JJ, Schmitz O, Nielsen R, Nielsen-Kudsk JE, Nielsen SS, Nielsen TT, Eiskjaer H, Botker HE and Wiggers H. Cardiovascular and metabolic effects of 48-h glucagon-like peptide-1 infusion in compensated chronic patients with heart failure. *Am J Physiol Heart Circ Physiol*. 2010;298:H1096-102.
261. Ferdinand KC, White WB, Calhoun DA, Lonn EM, Sager PT, Brunelle R, Jiang HH, Threlkeld RJ, Robertson KE and Geiger MJ. Effects of the once-weekly glucagon-like peptide-1 receptor agonist dulaglutide on ambulatory blood pressure and heart rate in patients with type 2 diabetes mellitus. *Hypertension*. 2014;64:731-7.
262. Lovshin JA, Barnie A, DeAlmeida A, Logan A, Zinman B and Drucker DJ. Liraglutide promotes natriuresis but does not increase circulating levels of atrial natriuretic peptide in hypertensive subjects with type 2 diabetes. *Diabetes care*. 2015;38:132-9.
263. Bristow MR. beta-adrenergic receptor blockade in chronic heart failure. *Circulation*. 2000;101:558-69.
264. Esler M, Kaye D, Lambert G, Esler D and Jennings G. Adrenergic nervous system in heart failure. *Am J Cardiol*. 1997;80:7L-14L.
265. Suga H. Total mechanical energy of a ventricle model and cardiac oxygen consumption. *The American journal of physiology*. 1979;236:H498-505.
266. Salling HK, Dohler KD, Engstrom T and Treiman M. Postconditioning with curaglutide, a novel GLP-1 analog, protects against heart ischemia-reperfusion injury in an isolated rat heart. *Regulatory peptides*. 2012;178:51-5.
267. Bose AK, Mocanu MM, Carr RD and Yellon DM. Myocardial ischaemia-reperfusion injury is attenuated by intact glucagon like peptide-1 (GLP-1) in the in vitro rat heart and may involve the p70s6K pathway. *Cardiovasc Drugs Ther*. 2007;21:253-6.
268. O'Gara PT, Kushner FG, Ascheim DD, Casey DE, Jr., Chung MK, de Lemos JA, Ettinger SM, Fang JC, Fesmire FM, Franklin BA, Granger CB, Krumholz HM, Linderbaum JA, Morrow DA, Newby LK, Ornato JP, Ou N, Radford MJ, Tamis-Holland JE, Tommaso CL, Tracy CM, Woo YJ, Zhao DX, Anderson JL, Jacobs AK, Halperin JL, Albert NM, Brindis RG, Creager MA, DeMets D, Guyton RA, Hochman JS, Kovacs RJ, Kushner FG, Ohman EM, Stevenson WG, Yancy CW and American College of Cardiology Foundation/American Heart Association Task Force on Practice G. 2013 ACCF/AHA guideline for the management of ST-elevation myocardial infarction: a report of the American College of Cardiology Foundation/American Heart Association Task Force on Practice Guidelines. *Circulation*. 2013;127:e362-425.

269. Read PA, Khan FZ and Dutka DP. Cardioprotection against ischaemia induced by dobutamine stress using glucagon-like peptide-1 in patients with coronary artery disease. *Heart*. 2012;98:408-13.
270. Chen M, Angeli FS, Shen YT and Shannon RP. GLP-1 (7-36) amide restores myocardial insulin sensitivity and prevents the progression of heart failure in senescent beagles. *Cardiovascular diabetology*. 2014;13:115.
271. Nikolaidis LA, Mankad S, Sokos GG, Miske G, Shah A, Elahi D and Shannon RP. Effects of glucagon-like peptide-1 in patients with acute myocardial infarction and left ventricular dysfunction after successful reperfusion. *Circulation*. 2004;109:962-5.
272. Bose AK, Mocanu MM, Carr RD, Brand CL and Yellon DM. Glucagon-like peptide 1 can directly protect the heart against ischemia/reperfusion injury. *Diabetes*. 2005;54:146-51.
273. Suga H. Cardiac mechanics and energetics--from Emax to PVA. *Frontiers of medical and biological engineering : the international journal of the Japan Society of Medical Electronics and Biological Engineering*. 1990;2:3-22.
274. Madamanchi A. Beta-adrenergic receptor signaling in cardiac function and heart failure. *Mcgill J Med*. 2007;10:99-104.
275. Wu AH, Pitt B, Anker SD, Vincent J, Mujib M and Ahmed A. Association of obesity and survival in systolic heart failure after acute myocardial infarction: potential confounding by age. *Eur J Heart Fail*. 2010;12:566-73.
276. Dick GM and Sturek M. Effects of a physiological insulin concentration on the endothelin-sensitive Ca2+ store in porcine coronary artery smooth muscle. *Diabetes*. 1996;45:876-80.
277. Chen S, Chen J, Huang P, Meng XL, Clayton S, Shen JS and Grayburn PA. Myocardial regeneration in adriamycin cardiomyopathy by nuclear expression of GLP1 using ultrasound targeted microbubble destruction. *Biochem Biophys Res Commun*. 2015;458:823-9.
278. Patching SG. Surface plasmon resonance spectroscopy for characterisation of membrane protein-ligand interactions and its potential for drug discovery. *Biochimica et biophysica acta*. 2014;1838:43-55.

Curriculum Vitae

Daniel Jay Sassoon

Education:

- Doctor of Philosophy - Indiana University, Indianapolis, IN. Department of Cellular and Integrative Physiology. Primary Mentor Johnathan Tune, PhD. 2016
- Bachelor of Science - University of the Pacific, Stockton, CA. 2009 Magna Cum Laude

Honors, Awards, Fellowships:

- Indiana Physiological Society Poster Presentation, Award. 2016
- NIH/NCATS. Indiana Clinical and Translational Sciences Institute. TL1 Program (A. Shekhar, PI) July 1, 2013 – June 30, 2015
- Moenkhaus Physiology Fellowship. Awarded for academic excellence. August 2014-June 2015
- Indiana Physiological Society Oral Presentation, Award. 2015
- IUSM Travel Grant. December 13,2013. Support awarded for technical and lay abstract. Funds used to attend 2014 Experimental Biology Conference in San Diego, CA
- Phi Beta Kappa . May 2009

Publications:

1. **Sassoon DJ**, Goodwill AG, Noblet JN, Conteh AM, Herring BP, McClintick JN, Tune JD and Mather KJ. Obesity alters molecular and functional cardiac

responses to ischemia/reperfusion and glucagon-like peptide-1 receptor agonism. Basic Res Cardiol. 2016;111:43.

2. Noblet JN, Goodwill AG, **Sassoon DJ**, Kiel AM and Tune JD. Leptin augments coronary vasoconstriction and smooth muscle proliferation via a Rho-kinase-dependent pathway. Basic Res Cardiol. 2016;111:25.
3. Goodwill AG, Fu L, Noblet JN, Casalini ED, **Sassoon D**, Berwick ZC, Kassab GS, Tune JD and Dick GM. KV7 channels contribute to paracrine, but not metabolic or ischemic, regulation of coronary vascular reactivity in swine. Am J Physiol Heart Circ Physiol. 2016;310:H693-704.
4. Noblet JN, Owen MK, Goodwill AG, **Sassoon DJ** and Tune JD. Lean and Obese Coronary Perivascular Adipose Tissue Impairs Vasodilation via Differential Inhibition of Vascular Smooth Muscle K+ Channels. Arteriosclerosis, thrombosis, and vascular biology. 2015;35:1393-400.
5. Owen MK, Noblet JN, **Sassoon DJ**, Conteh AM, Goodwill AG and Tune JD. Perivascular adipose tissue and coronary vascular disease. Arteriosclerosis, thrombosis, and vascular biology. 2014;34:1643-9.
6. Goodwill AG, Tune JD, Noblet JN, Conteh AM, **Sassoon D**, Casalini ED and Mather KJ. Glucagon-like peptide-1 (7-36) but not (9-36) augments cardiac output during myocardial ischemia via a Frank-Starling mechanism. Basic Res Cardiol. 2014;109:426.
7. Goodwill AG, Mather KJ, Conteh AM, **Sassoon DJ**, Noblet JN and Tune JD. Cardiovascular and hemodynamic effects of glucagon-like peptide-1. Rev Endocr Metab Disord. 2014;15:209-17.

8. Sharif-Kashani P, Hubschman JP, **Sassoon D** and Kavehpour HP. Rheology of the vitreous gel: effects of macromolecule organization on the viscoelastic properties. J Biomech. 2011;44:419-23.
9. Bennett DB, Taylor ZD, Tewari P, Singh RS, Culjat MO, Grundfest WS, **Sassoon DJ**, Johnson RD, Hubschman JP and Brown ER. Terahertz sensing in corneal tissues. J Biomed Opt. 2011;16:057003.

- **Sassoon DJ**, Tune JD, Mather KJ, Noblet JN, Conteh AM, Goodwill AG. Glucagon like peptide-1 receptor activation augments sympathetic mediated increases in cardiac function and improves efficiency in obese swine following myocardial infarction. In preparation.

Selected Conference Presentations:

Oral Presentations:

- Experimental Biology (EB), San Diego, CA. April 2016
  - Obesity Distinctly Influences Cardiac Function and Molecular Responses to Ischemia-Reperfusion and GLP-1 Receptor Agonism.
- Indiana Physiological Society, Indianapolis Indiana, February 2015.
  - Obesity Alters Global Cardiac Response to Exendin-4 in the Setting of Ischemia Reperfusion.
- Translational Science, Washington, D.C. April 2015
  - Micro-RNA Regulation Responses to Cardiac Ischemia/Reperfusion Injury Differ Between Lean and Obese Swine.

Poster Presentations:

- Experimental Biology (EB), San Diego, CA. April 2016 and Indiana Physiological Society, Greencastle, Indiana, February 2016.
    - Obesity Distinctly Influences Cardiac Function and Molecular Responses to Ischemia-Reperfusion and GLP-1 Receptor Agonism. **Daniel J. Sassoon**, Adam G. Goodwill, Jillian N. Noblet, Abass M. Conteh, . Paul Herring, Jeanette McClintick, Johnathan D. Tune, Kieren J. Mather
    - The Long Acting GLP1 Receptor Agonist, Liraglutide, Augments Myocardial Contractile Responses and Cardiac Efficiency Under Sympathetic Stimulation in Obesity and Myocardial Infarction. Adam Glenn Goodwill, **Daniel J Sassoon**, Jillian N Noblet, Abass M Conteh, Kieren J Mather, Johnathan D Tune. 4757-P
- United States and Canadian Academy of Pathology, Seattle, WA. March 2016.
    - Discrepancy Between Local and Central Pathological Review of Radical Orchiectomy Specimens. Saul E Harari, **Daniel J Sassoon**, John Eble, Thomas M Ulbright, David J Grignon, Mohammed Idrees, Costantine Albany, Timothy A Masterson, Nasser H Hanna, Richard S Foster, Lawrence H Einhorn, Liang Cheng. Vol. 96, pp. 237A-237A
    - Needle Biopsy of Renal Masses: Analysis of 121 Matched Biopsy and Resection Cases. Saul E Harari, **Daniel J Sassoon**, John Eble, Liang

Cheng, Mohammed Idrees, Helen E Michael, David J Grignon. Vol. 96, pp. 237A-237A

- American Diabetes Association, Boston, MA, June 2015
  - Micro-RNA Regulation Responses to Cardiac Ischemia/Reperfusion Injury Differ Between Lean and Obese Swine. **Sassoon DJ**, Tune JD, Goodwill AG, Noblet JN, Herring BP, McClintick JN, Mather KJ. 2162-P
- Translational Science, Washington, D.C. April 2014
  - Differential Physiologic, and Molecular Cardiac Responses to Exendin-4 in Lean vs. Obese Ossabaw Swine in the Setting of Ischemia/Reperfusion Injury. **Sassoon DJ**, Mather KJ, Goodwill AG, Herring BP, McClintick JN, Conteh AM, Noblet JN, Tune JD
- Experimental Biology (EB) San Diego, CA. April 2014
  - Characterization of cardiovascular performance during ischemia-reperfusion injury in obese vs. lean Ossabaw swine. **D. Sassoon**, A. Goodwill, A. Conteh, J. Noblet, K. Mather and J. Tune. Experimental Biology Poster. San Diego, CA 1050.4 –April 30, 2014

Professional and Teaching Experience:

- Guest Lecturer for N217; Indiana University-Purdue University Indianapolis · Department of Biology, April 2014
- Genetics Laboratory Teaching Assistant, University of the Pacific: Fall 2009, Spring 2010
- Eagle Sight Ophthalmology. R&D, Beverly Hills, CA 2009-2010

- Research Assistant, Jean-Pierre Hubschman, UCLA Jules Stein Eye Institute, Los Angeles, CA 2008-2010